

**UCLA**

**UCLA Electronic Theses and Dissertations**

**Title**

Impacts of Anthropogenic Activities on Wild Species: An Evaluation of Environmental Stressors Associated with Urban and Agricultural Land Use on Bobcats, Mule Deer and Bats in Southern California

**Permalink**

<https://escholarship.org/uc/item/7k38s0kq>

**Author**

Fraser, Devaughn Lee

**Publication Date**

2017

Peer reviewed|Thesis/dissertation

UNIVERSITY OF CALIFORNIA

Los Angeles

Impacts of Anthropogenic Activities on Wild Species:

An Evaluation of Environmental Stressors Associated with Urban and Agricultural Land Use on  
Bobcats, Mule Deer and Bats in Southern California

A dissertation submitted in partial satisfaction of the  
requirements for the degree Doctor of Philosophy

in Biology

by

Devaughn Lee Fraser

2017

© Copyright by

Devaughn Lee Fraser

2017

## ABSTRACT OF THE DISSERTATION

Impacts of Anthropogenic Activities on Wild Species:

An Evaluation of Environmental Stressors Associated with Urban and Agricultural Land Use on  
Bobcats, Mule Deer, and Bats in California

by

Devaughn Lee Fraser

Doctor of Philosophy in Biology

University of California, Los Angeles, 2017

Professor Robert Wayne, Chair

Human land use is responsible for global declines in biodiversity, primarily through the loss, fragmentation and degradation of natural habitat. Urban development and agriculture are the two most important forms of land use change causing species imperilment in the US, both of which are strongly associated with additional environmental stressors such as pesticides and movement barriers. Socially, economically and ecologically important species are often affected negatively, and thus, priority should be placed on evaluating how land use affects natural populations. This research focuses on three distinct systems to identify the effects of habitat fragmentation and chemical pollutants on wildlife, including 1) the physiological effects of persistent anticoagulant rodenticide exposure on bobcats in the Santa Monica Mountains and Simi Hills near Los Angeles, CA; 2) the effect of highways on geneflow in mule deer occupying various open spaces

separated by intervening highways and characterized by varying degrees of urban development;  
and 3) the influence of pesticide use on resource selection and dietary diversity in big brown bats  
in an intensively managed agricultural landscape.

The dissertation of Devaughn Lee Fraser is approved.

Winifred Frick

James Lloyd-Smith

Walter Metzner

Robert Wayne, Committee Chair

University of California, Los Angeles

2017

## DEDICATION

To my amazing family who have always inspired me with the confidence to pursue my passion. You have supported me every step along this journey, and without you, I would never have found my way here. I love you.

TABLE OF CONTENTS

List of Tables ..... vii

List of Figures ..... ix

Acknowledgements ..... xiii

Vita ..... xvii

Introduction ..... 1

References ..... 5

Chapter 1. Genome-wide expression reveals multiple systemic effects associated with detection  
of anticoagulant poisons in bobcats (*Lynx rufus*) ..... 8

Tables and Figures ..... 32

References ..... 47

Chapter 2. Connectivity of mule deer (*Odocoileus hemionus*) populations in southern California:  
A genetic survey of a mobile ungulate in a highly fragmented landscape ..... 57

Tables and Figures ..... 78

References ..... 89

Chapter 3. Dietary diversity and resource selection by big brown bats (*Eptesicus fuscus*) in  
agricultural landscapes of California ..... 94

Tables and Figures ..... 110

References ..... 116



## LIST OF TABLES

<b>Table 1.1.</b> Summary of the variance on the first 12 Principal Components. F-statistics and p-values are reported for four significantly correlated variables (AR-detection, age class, PLV detection, and <i>Bartonella</i> spp. seropositivity).	32
<b>Table 1.2</b> Differential expressed genes listed as related to warfarin in the Comparative Toxicogenomic Database.	33
<b>Table 1.3.</b> Figure code, functional category, GO term ID, GO term description, and p-value for the downregulated genes.	34
<b>Table 1.4.</b> Figure code, functional category, GO term ID, GO term description, and p-value for the upregulated genes.	35
<b>Table 1.5.</b> List of differentially expressed interleukin cytokines and interleukin cytokine receptors from the linear model analysis.	36
<b>Table 1.6.</b> Transcript Origin Analysis for leukocytes and leukocyte subsets.	37
<b>Table 1.7.</b> Summary of physiological pathways and processes affected, analytical support, relevant genes of interest and the implications for fitness in AR exposed bobcats.	38
<b>Table 2.1.</b> Annual Average Daily Traffic volumes (cars per day) in 1993 and 2014 for 5 major highways intersecting subregions of natural habitat in the study area.	78
<b>Table 2.2.</b> Logistic regression model structure for estimating mule deer habitat quality. The inverse of this model was used to create a cost surface for comparing pair-wise least cost paths	

and accumulated cost paths to pairwise genetic distance.	78
<b>Table 2.3.</b> Competing model results using Akaike Information Criterion (AIC) and two model fit statistics, adjusted $R^2$ , and Area under the Receiver Operating Curve (AUC).	79
<b>Table 2.4.</b> Effective population size, observed heterozygosity and expected heterozygosity across 14 loci for each subregion.	80
<b>Table 2.5.</b> Pairwise and average genetic distances ( $D_{est}$ ) between 7 mountainous subregions separated by major highways in Southern California.	80
<b>Table 2.6.</b> Average proportional assignment of individuals to K clusters and relative evenness across clusters by subregion for both STRUCTURE (A) and DAPC (B).	81
<b>Table 2.7.</b> Generalized linear models for predictors of individual pairwise relatedness ( $1/r$ ) between deer sampled in adjacent subregions.	82
<b>Table 3.1.</b> Telemetry location numbers, observed foraging extent (OFE), mean foraging distance from roost locations (Avg. Dist) and the furthest location from roost locations (Max Dist.) for each radio-tracked bat ( $n = 10$ ).	110
<b>Table 3.2.</b> Mixed effects model components, $\Delta AIC$ (calculated against null model), and significantly ( $p < 0.05$ ) selected (S) and avoided (A) land features with and without the interaction of pesticide inputs (lbs).	110

## LIST OF FIGURES

- Figure 1.1.** Map of the study area depicting sample locations for all 52 bobcats, whether or not the animal tested positive (+) or not positive (⊙) for ARs, and the general land use categories (urban, altered open, and natural). 39
- Figure 1.2.** Workflow summary of genome wide analysis of anticoagulant rodenticide impacts on gene expression in bobcats. 40
- Figure 1.3.** Linear regression of biological and technical factors on the principal components (PC) of the normalized read counts after regressing out technical factors significant on the first PC (sequencing platform, RIN, library preparation 5). 41
- Figure 1.4.** False discovery rate distribution after 1000 permutations compared to the p-value distribution of the linear modeling analyses. 42
- Figure 1.5.** (A) Volcano plot depicting the  $-\log_{10}$  of the Q value against the  $\beta$  fold change for all 12,332 genes. Significant gene ( $Q < 0.05$ ) are highlighted in tan. Labeled genes are color coded by associated physiological process (depicted in B-C). Mean normalized counts of upregulated genes (B) and downregulated genes (C) shown for AR-negative (light color) and AR-positive (dark color) bobcats. 43
- Figure 1.6.** Treemap of the GO Biological Processes for the down (A) and up (B) regulated genes ( $Q < 0.05$ ). Box size correlates to the  $-\log_{10}$  p-value of the GO-term enrichment. Boxes with the same color represent higher level categories of processes. Main Abbreviations: (+): positive regulation, (-) : negative regulation, macroph: macrophage. See Table 1.3, 1.4 for GO term details. 44

**Figure 1.7.** INCA index for each k-value after resampling. The number of clusters directly preceding the greatest negative slope (11) is assigned as the most probable number of clusters in the data. 45

**Figure 1.8.** (A) Number of significant genes (from linear model) assigned to one of six functional categories (from WGCNA) as a proportion of total module size. (B) Correlation between AR exposure and WGCNA module eigengenes. (C) Heat maps displaying the expression profiles and dendrograms of AR-negative (light color) and AR-positive (dark color) bobcats for the “T cell signaling” and “inflammatory response” modules. Columns are individual bobcats and rows are individual genes. 46

**Figure 2.1.** Study area map showing the location of genetic samples gathered across the subregions and the other occurrence records used to estimate selection of habitat features by mule deer for the whole study area (A), and sample locations for the LA (B) and OC regions (C). We used a paired random sampling approach to sample the range of conditions found in the areas where samples and occurrence data were collected. 83

**Figure 2.2.** Posterior assignments for individual deer to each of 5 genetic clusters identified in STRUCTURE. Subregions are arranged and grouped according to the pairwise genetic distance matrix as shown by the dendrogram. 85

**Figure 2.3.** Mean pairwise genetic distance as a function of the accumulated cost along the least cost path divided by the Euclidean distance between samples collected within all subregions (squares) and between adjacent subregions (circles). The correlation was significant (adj.  $R^2 = 0.24$ ,  $F_{\text{stat}} = 5$ ,  $p\text{-value} = 0.045$ ). 86

**Figure 2.4.** Response curves for mule deer occurrence data versus an equal number of randomly

stratified locations. Factors exhibiting direct responses (quadratic and linear) include terrain unevenness and openness, and 4 LANDFIRE attributes (A). Factors modified by an interaction term include site exposure index (SEI) x slope, and 2 LANDFIRE attributes (red and green) x road density (B). 87

**Figure 2.5.** Cost surface used to estimate mule deer habitat connectivity for the study area (A.). Using a resource selection function (RSF) approach, we estimated high quality habitat would have little cost for movement for mule deer in the region and landscape features where mule deer were not observed to use, as having a high cost of movement on a scale of 0-1 (the inverse probability of mule deer presence). To explore whether or not high traffic volume freeways may pose a movement barrier, we added additional costs to the locations of freeway systems based on the Ahead Annual Average Daily Traffic (AADT) volume rescaled to values between 0-1 and added it to the habitat based cost surface. These areas of increased cost to transverse are shown for a portion of the US-101 (B.), the I-405 (C.), and the CA-91 and CA-71 intersection (D.). 88

**Figure 3.1.** Study area map with relative position of both sites (A), as well as observed foraging extents (OFE), distribution of crop types and pesticide inputs for SH (B) and AV (C). 111

**Figure 3.2.** Relative abundance of prey types detected in guano from 17 brown bats captured in a low pesticide-use area (ARVIN- left) and high pesticide-use area (SHAFTER- right). For readability, only the first 20 most abundant prey types are listed in the legend. 113

**Figure 3.3.** Average accumulation of prey sequences across sampling intervals ranging from 1000 – 10,000. Rarefaction results are presented as the average accumulation across 10 replicate runs. Error bars are shown for brown bats captured at the Arvin site (blue) and the Shafter site

(purple). Other bat species include Yuma myotis (green), pallid bat (red), and free-tailed bat (orange).

114

**Figure 3.4.** Comparison of alpha (top panels) and beta (bottom panels) diversity of prey types detected in guano of 17 brown bats captured in a low (ARVIN) and high (SHAFTER) pesticide-use area. Alpha diversity did not differ significantly between sites whether measured by the relative abundance of observed prey sequences (A;  $t = 0.99$ ;  $p = 0.38$ ) or Shannon Entropy (B;  $t = 1.34$ ,  $p = 0.21$ ). Beta diversity of prey types as calculated using the Bray-Curtis dissimilarity measure implemented in a PERMANOVA test was significantly different between the two sites (C;  $F = 2.54$ ;  $R^2 = 0.145$ ;  $p = 0.007$ ); and by a nonmetric multidimensional scaling analysis (D;  $k = 3$ ; stress = 0.074;  $p = 0.005$ ). The figure shows a two-dimensional representation of dietary similarity between the bats captured at ARVIN (green closed circles) and SHAFTER (blue open diamonds).

115

## ACKNOWLEDGEMENTS

This dissertation is by no means an isolated effort and there are so many people to thank. I wish to emphatically thank **Dr. Robert K. Wayne** for being an exceptional mentor and advisor. When I first started this journey, you encouraged me to develop myself as a scholar and a scientist first and foremost. You supported me when I came to you with my passion for bats, and saved me from the trenches when my sample sizes were too low. It's because of you that I have developed into a diverse scientist and you have always given me the right guidance at the right time in order to help me finish what I started.

I next wish to thank all the individuals that played pivotal roles in the production of manuscripts, either already accepted or in the process of being submitted, and resulting in this dissertation. Chapter 1 is a reformatted version of a manuscript entitled "Genome-wide expression reveals multiple systemic effects associated with detection of anticoagulant poisons in bobcats (*Lynx rufus*)" by Devaughn Fraser, Alice Mouton, Laurel E.K. Serieys, Steve Cole, Scott Carver, Sue Vandouwoude, Michael Lappin, Seth P.D. Riley, and Robert K. Wayne, which is accepted for publication in *Molecular Ecology*. I give special acknowledgement to **Alice Mouton**, equal first co-author of this paper. You put up with me in my many moody moments and you did so with absolute poise and grace. You're an amazing collaborator and I hope to work with you many more times in the future. Thank you to **Laurel E.K. Serieys** for bringing me into the bobcat world with open arms and offering a crash course in carnivore trapping. Also for always setting the bar high. You're an amazing scientist and truly a pioneer. Your foresight and fortitude in trapping and developing immunological assays for bobcats made this paper possible. Thank you to **Seth P.D. Riley** for all the work you do to conserve wildlife in the Santa Monica Mountains by recognizing the link between anticoagulant rodenticides and wildlife health. And

to all other co-authors, **Steve Cole** for dropping serious immunological knowledge in this paper, **Scott Carver, Sue Vandewoude, and Michael Lappin** for generating such a thorough disease dataset. Also, thank you to **Dr. Michael Kohn** for your invaluable editorial feedback.

I thank my co-authors of Chapter 2 which is being prepared for submission. **Dr. Erin Boydston**, thank you for making me a part of this mule deer project. Through your ingenuity and commitment to wildlife research, you recognized a disparity in the literature and worked your magic to facilitate funding and bring agencies together in collaboration. You've been a great mentor and principle investigator for this project. **Dr. Kirsten Ironside**, co-author and mapper extraordinaire, thank you for all the time and energy you spent generating resistance surfaces and calculating movement costs for mule deer.

Chapter 3 is a collaboration between several people and is also in preparation for submission. I especially thank **Dr. Emily Curd** for being a metagenomics mastermind and running the sequence data through the Anacapa pipeline. I will be proud to share my name on a paper with you when this chapter gets published. I also thank **Rochelle Kelley** for aiding in the study design.

To **Joseph Nikko Curti, Lester Fox-Rosales, Tony Nguyen** thank you for being rock-star level field techs. Keeping track of bats is tricky business and you all shined. **Mary-Beth Bourne, Colin Shew** and all the undergraduate volunteers who spent time in the field and lab with me to make these analyses possible, I thank you.

I thank **Tiffany Armenta** for seriously helping me keep my soul and my sanity through all this. And to both **Tiffany Armenta** and **Laurel Serieys** you for being totally down to turn Ladies Night into a mad science support group.



I thank **Dr. Jacqueline Robinson** and **Dr. Rachel Johnston** for their constant guidance and incredible patience. I've looked up to the both of you as scientists and as people, and I truly would not have made it through graduate school without the two of you. I also thank **John Pollinger** for being the keystone of the Wayne Lab, even from across the country. You have imparted so much knowledge to myself and many others and you are truly a treasure.

I thank my doctoral committee members **Dr. Jamie Lloyd-Smith**, **Dr. Thomas B. Smith**, **Dr. Winifred Frick**, and **Dr. Walter Metzner**. I put you all through the ringer with my constant requests for letters of recommendation and you never let me down. Your guidance and feedback throughout this process have been invaluable.

I thank all the growers that let me sample bats in their orchards: **Laura Cattani**, **Ed Kuykendall**, and **Glenn Anderson**.

I thank all the enterprising graduate students and Post-docs who have come and gone from the Wayne Lab over the years. It's been a pleasure and an inspiration working with each of you. I also wish to thank all the PhD students that I worked for before starting my own doctorate. You gave me the skills and confidence to go out on my own and do science.

As for all the people that have helped make this dissertation possible in other ways, I start by thanking **Margaret Nelson** and **Arianne Fraser**. Where do I even begin? None of this was possible without you. You have stood by me always, even at my worst, and always encouraged me to follow my dreams and do my best. You two form the foundation for everything I am and have accomplished, and I thank you. Thank you to **John C. Fraser** for being a continual source of wisdom and comfort when things got too unbearable. Thank you to **Henry Winterstern** for constantly reminding me not to be ABD. To **Scott J. Losi**, thank you for continuing to believe in

me when I doubted myself and for being eternally patient as I made my way to this point. I'm so grateful for you in my life.

Finally, I wish to thank my dogs **Jerome** and **Guinness** who always provided me with a laugh when I didn't think laughing was possible, and my beloved cat **Cymmi** whom I miss every day. You were simply the best.

This dissertation was made possible by multiple funding sources: Bats Conservation International, the Environmental Protection Agency, the Summerlee Foundation, the Switzer Foundation, and the Department of Ecology and Evolution at the University of California, Los Angeles.

## VITAE

### EDUCATION

Doctor of Philosophy in Biology at the University of California, Los Angeles, September 2010-Present. Expected 2017. Dissertation Title: **Impacts of Anthropogenic Activities on Wild Species: An Evaluation of Environmental Stressors Associated with Urban and Agricultural Land Use on Bobcats, Mule Deer and Bats in Southern California.**

Bachelor of Science at the University of California, Berkeley 2003.

### PUBLICATIONS

Fraser D., Mouton A., Serieys L., Cole S., Carver S., Vanwouden S., Lappin M., Riley S.P.D., Wayne R. Genome-wide expression reveals multiple systemic effects associated with detection of anticoagulant poisons in bobcats (*Lynx rufus*). *Molecular Ecology* (in press).

Sastre N., Francino O., Curti J. N., Armenta T. C., Fraser D. L., Kelly R. M., ... & Ferrer L. (2016). Detection, Prevalence and Phylogenetic Relationships of Demodex spp. and further Skin Prostigmata Mites (Acari, Arachnida) in Wild and Domestic Mammals. *PloS one*, 11(11), e0165765.

### PRESENTATIONS

June 2017 International Urban Wildlife Conference. Oral Presentation Title: "Population structure in mule deer (*Odocoileus hemionus*) across major highways in Southern California"

June 2017 International Urban Wildlife Conference. Poster Presentation Title: “Global gene expression reveals immune and systemic dissonance in bobcats (*Lynx rufus*) exposed to anticoagulant poisons”

October 2015 45<sup>th</sup> Annual North American Symposium for Bat Research. Poster Presentation Title: “Do Pesticides Influence Bat Foraging Decisions?”

October 2016 UCLA Genomics Consortium. Presenter. “RNA-Seq: From benchwork to differential gene expression”

February 2016 UCLA/LaKretz Center Conservation Genomics Workshop. Instructor. “RNA-Seq: From benchwork to differential gene expression”

## **GRANTS AWARDED**

NSF Bioinformatics Workshop (2011)

GAANN Fellowship (2011-2012, 2013-2014)

UCLA Dept. EEB (2011, 2013, 2017)

BCI Student Scholarship Grant (2012, 2014)

Bob Berry Research Grant (2013)

LaKretz Conservation Center Student Grant (2013)

Switzer Environmental Fellowship (2013)

UCLA Bartholomew Fellowship (2014)

EPA STARS Fellowship (2014-2016)

Summerlee Foundation Grant (2015)

## **APPOINTMENTS**

Teaching Assistant, Department of Ecology and Evolutionary Biology, University of California, Los Angeles. 2011-2017

## INTRODUCTION

Human activities are causing a precipitous decline in biodiversity worldwide. While altered habitat availability- via degradation, loss, and fragmentation- presents the most immediate threat to species (Brooks et al., 2002; Groom et al., 2006; Hanski 2011), secondary stressors such as pollution often operate in tandem to exacerbate local effects of changing landscapes (McNeely 1992; Crain et al., 2008; Serieys et al., 2015). Understanding the scope and magnitude of these interactions is critical to maintaining biodiversity and managing populations of ecologically and economically important species in highly altered urban and agricultural environments.

Habitat fragmentation reduces both resource availability and population connectivity, and thus carries both demographic and genetic consequences for wild species. Populations may decline in response to limited resources necessary for reproduction and survival (Herkert 1994, Newman et al. 2013), while decreased gene flow between remaining patches can lead to reduced genetic diversity (Sato et al. 2014, Barr et al. 2015) and inbreeding depression (Bouzat et al., 1998; Johnson et al., 2010) thus limiting the evolutionary-response capabilities of populations to environmental change (Hughes et al., 2003; Schaberg et al., 2008). Such isolation can also lead to transiently high local population densities or “crowding effects”, with implications for habitat quality, disease transmission and survival (Lindsey et al., 2009, Gabriel et al., 2017). Further, other stressors associated with human land-use, such as pollutants, can have profoundly negative effects on natural populations inhabiting areas along an urban- or agricultural-wild interface. Cumulatively, such impacts can reduce population fitness and contribute to population declines over time. The two most common forms of habitat degradation that contribute to species imperilment include urbanization and agriculture, both highly associated with habitat

fragmentation and chemical contaminants such as pesticides (Ricketts & Imhoff, 2003; McPherson et al., 2013).

I and my co-authors have selected three distinct systems through which to evaluate direct and indirect consequences of human land-use change on natural populations. In **Chapter 1** of this dissertation entitled “**Genome-wide expression reveals multiple systemic effects associated with detection of anticoagulant poisons in bobcats (*Lynx rufus*),**” We evaluated the effects of sublethal anticoagulant rodenticide exposure on genome wide expression patterns in peripheral whole blood from an urban-associated population of bobcats (*Lynx rufus*). Rodenticide exposure is pervasive in this population and is potentially linked to an epizootic of notoedric mange that lasted from 2002-2011 (Riley et al. 2007, Serieys., et al 2015). We used three analytical approaches to identify multiple physiologic systems that are impacted by exposure to rat poisons. We then extended our findings to hypothesize about potential mechanisms leading to increased susceptibility to notoedric mange in this bobcat population. We found that AR exposure in bobcats results in differential expression of genes related to endoplasmic reticulum stress, epithelial formation and maintenance and both innate and adaptive immunity. We hypothesized that the combination of simultaneous immune activation and immune suppression paired with compromised epithelial integrity predisposes AR-exposed bobcats to opportunistic infection by an ectoparasite.

In **Chapter 2** entitled “**Connectivity of mule deer (*Odocoileus hemionus*) populations in southern California: A genetic survey of a mobile ungulate in a highly fragmented landscape**” we examined the direct effects of major highways and urban development on the distribution of genetic diversity in mule deer across two highly urbanized regions in southern California. Urbanization is a substantial force shaping the genetic and demographic structure of

natural populations. As urban areas expand, so too do transportation corridors that facilitate human movement, such as highways. As such, genetic continuity in wild species is increasingly compromised and should be assessed for a multitude of highly mobile species that exhibit varying responses to human activity. While carnivores are well studied in general, common species such as mule deer are often overlooked. However, as the only wide-ranging ungulate species in Southern California, genetic and demographic impacts of urban development on mule deer is an important area of research. Here, we present the first assessment of genetic connectivity for mule deer focused explicitly at understanding mule deer response to habitat fragmentation in an increasingly urbanized landscape. We use a combination of genetic analyses and resource selection modeling to show that deer movement is limited by major highways and the associated urban development. Therefore, deer should be an important consideration during wildlife connectivity planning in urban landscapes.

Finally, in **Chapter 3** entitled “**Dietary diversity and resource selection by big brown bats (*Eptesicus fuscus*) in agricultural landscapes exhibiting different levels of pesticide-use in California**” we examined patterns of dietary diversity and resource use in big brown bat populations in an agricultural landscape in central California. Bats provide invaluable economic and environmental services in agricultural landscapes by consuming insects that damage crops and are otherwise controlled through the use of chemical pesticides. Quantifying these services is a major research focus, yet little is known about the dietary diversity or foraging behavior of bats in such landscapes. Further, few data are available for understanding the influence of pesticide-use on bat foraging, concomitantly negating our understanding of exposure risks for bats. We have implemented an RSF modeling approach to analyze telemetry data on ten female foraging big brown bats, in order to determine if bats exhibit a preference for certain crop types over

others and to test whether bats tend to avoid or select for areas with high pesticide use. We additionally have analyzed guano from 18 wild bats captured in two locations which vary in landscape levels of insecticides applied. We demonstrate that bats show consistent selection and avoidance for specific crop and land-use types and that pesticides do exhibit a significant influence on bat foraging decisions. We further show that dietary diversity is reduced in high-pesticide use areas, likely due to reduced prey availability. Collectively, our results highlight the importance of understanding foraging strategies for economically valuable species and may provide a management framework for agricultural producers to promote bat predation on their lands.



## REFERENCES

1. Barr, K. R., Kus, B. E., Preston, K. L., Howell, S., Perkins, E., & Vandergast, A. G. (2015). Habitat fragmentation in coastal southern California disrupts genetic connectivity in the cactus wren (*Campylorhynchus brunneicapillus*). *Molecular ecology*, *24*(10), 2349-2363.
2. Brooks, T. M., Mittermeier, R. A., Mittermeier, C. G., Da Fonseca, G. A., Rylands, A. B., Konstant, W. R., ... & Hilton-Taylor, C. (2002). Habitat loss and extinction in the hotspots of biodiversity. *Conservation biology*, *16*(4), 909-923.
3. Bouzat, J. L., Cheng, H. H., Lewin, H. A., Westemeier, R. L., Brawn, J. D., & Paige, K. N. (1998). Genetic evaluation of a demographic bottleneck in the greater prairie chicken. *Conservation Biology*, *12*(4), 836-843.
4. Crain, C. M., Kroeker, K., & Halpern, B. S. (2008). Interactive and cumulative effects of multiple human stressors in marine systems. *Ecology letters*, *11*(12), 1304-1315.
5. Czech, B.; Krausman, P.R.; Devers, P.K. 2000. Economic associations among causes of species endangerment in the United States. *BioScience*. 50(July): 593-601.
6. Didham, R. K. (2010). Ecological consequences of habitat fragmentation. *eLS*.
7. Gabriel, D. N., Gould, L., & Cook, S. (2017). Crowding as a primary source of stress in an endangered fragment-dwelling strepsirrhine primate. *Animal Conservation*.
8. Groom, M. J., Meffe, G. K., & Carroll, C. R. (2006). *Principles of conservation biology* (No. Sirsi) i9780878935185). Sunderland: Sinauer Associates.
9. Hanski, I. (2011). Habitat loss, the dynamics of biodiversity, and a perspective on conservation. *AMBIO: A Journal of the Human Environment*, *40*(3), 248-255.
10. Herkert, J. R. (1994). The effects of habitat fragmentation on midwestern grassland bird communities. *Ecological applications*, *4*(3), 461-471.
11. Hughes, T. P., Baird, A. H., Bellwood, D. R., Card, M., Connolly, S. R., Folke, C., ... & Lough, J. M. (2003). Climate change, human impacts, and the resilience of coral reefs. *science*, *301*(5635), 929-933.

12. Johnson, W. E., Onorato, D. P., Roelke, M. E., Land, E. D., Cunningham, M., Belden, R. C., ... & Howard, J. (2010). Genetic restoration of the Florida panther. *Science*, 329(5999), 1641-1645.
13. Lindsey, E., Mehta, M., Dhulipala, V., Oberhauser, K., & Altizer, S. (2009). Crowding and disease: effects of host density on response to infection in a butterfly–parasite interaction. *Ecological Entomology*, 34(5), 551-561.
14. McNeely, J. A. (1992). The sinking ark: pollution and the worldwide loss of biodiversity. *Biodiversity and Conservation*, 1(1), 2-18.
15. McPhearson, T., Auch, R., & Alberti, M. (2013). Regional Assessment of North America: Urbanization trends, biodiversity patterns, and ecosystem services. In *Urbanization, biodiversity and ecosystem services: Challenges and opportunities* (pp. 279-286). Springer Netherlands.
16. Newman, B. J., Ladd, P., Brundrett, M., & Dixon, K. W. (2013). Effects of habitat fragmentation on plant reproductive success and population viability at the landscape and habitat scale. *Biological Conservation*, 159, 16-23.
17. Sato, J. J., Kawakami, T., Tasaka, Y., Tamenishi, M., & Yamaguchi, Y. (2014). A few decades of habitat fragmentation has reduced population genetic diversity: A case study of landscape genetics of the large Japanese field mouse, *Apodemus speciosus*. *Mammal study*, 39(1), 1-10.
18. Schaberg, P. G., DeHayes, D. H., Hawley, G. J., & Nijensohn, S. E. (2008). Anthropogenic alterations of genetic diversity within tree populations: Implications for forest ecosystem resilience. *Forest Ecology and Management*, 256(5), 855-862.
19. Serieys, L. E., Lea, A., Pollinger, J. P., Riley, S. P., & Wayne, R. K. (2015). Disease and freeways drive genetic change in urban bobcat populations. *Evolutionary applications*, 8(1), 75-92.
20. Wear, D.N.; Greis, J.G. 2002. Southern forest resource assessment. Gen. Tech. Rep. SRS-53. Asheville, NC: U.S. Department of Agriculture, Forest Service, Southern Research Station. [Available online: <http://www.srs.fs.fed.us/sustain/>]

21. Wilcove, D. S., Rothstein, D., Dubow, J., Phillips, A., & Losos, E. (1998). Quantifying threats to imperiled species in the United States. *BioScience*, 48(8), 607-615.

## CHAPTER 1

### Genome-wide expression reveals multiple systemic effects associated with detection of anticoagulant poisons in bobcats (*Lynx rufus*)

#### INTRODUCTION

Poisons aimed at controlling specific pest species may threaten populations of non-target species. For toxicants that bioaccumulate in the food chain, these threats are greatest to predatory and scavenging species. Although some mortality in non-target animals occurs via the same molecular pathways that the toxicant are designed to disrupt, sublethal exposure can also have cryptic physiological effects that nonetheless impact individual fitness (Baldwin et al., 2009; Santadino et al., 2014; Gill & Raine, 2014), and hence, may decrease population viability (Thompson et al., 2014; Rattner et al., 2014; Serieys et al., 2015a).

Anticoagulant rodenticides (ARs) are toxicants used globally to eliminate rodent pests and have been implicated as an important source of mortality in many non-target species that consume poisoned rodents (Eason et al., 2001; Fournier-Chambrillon et al., 2004; Sánchez-Barbudo et al., 2012; Rattner et al., 2014; Dennis et al., 2015; Gabriel et al., 2015; Huang et al., 2016). For example, 81% of tested stone martens (*Martes foina*) and 77% of polecat (*Mustela putorius*) were exposed in Belgium, and between 84% and 100% of birds and other animals tested were exposed in Denmark (Baert et al., 2015; Elmeros et al., 2011; Christensen et al., 2012). In California, exposure to ARs is a statewide problem with over 70% (368/492) of birds and mammals testing positive for ARs between 1995 and 2011 ([California Department of Pesticide Regulation 2013](#)). AR toxicity was a leading cause of mortality in predatory and scavenging birds (Kelly et al., 2014) and in coyotes (*Canis latrans*) (Riley et al., 2003), and it is increasingly recognized as a major

threat to the Pacific fisher (*Pekania pennanti*) (Gabriel et al., 2012; Thompson et al., 2014) and to the endangered San Joaquin kit fox (*Vulpes macrotis mutica*) (Nogeire et al., 2015). In Southern California over 90% of bobcats and mountain lions (*Puma concolor*) tested positive for ARs (Riley et al., 2007). Further, AR exposure occurs in a wide variety of environments, from pristine areas such as the Sierra Nevada Mountains, to agricultural areas with low human densities such as cattle and horse ranches and grain storage facilities, to urban areas with both high and low-density housing, as well as highly modified areas such as golf courses and natural areas which abut human habitation (Gabriel et al., 2012; Gabriel et al., 2015; Nogeire et al., 2015; Serieys et al., 2015).

Several formulations of ARs are available and are grouped into first- and second generation ARs (FGARs and SGARs); the latter are more acutely toxic and persistent in tissue as they were developed as a countermeasure to heritable resistance in rodent populations to FGARs. The most commonly deployed FGARs are warfarin, chlorophacinone, and diphacinone and the most commonly used SGARs are brodifacoum, bromadiolone, difenacoum, and difethialone (US EPA-<https://www.epa.gov/rodenticides/restrictions-rodenticide-products>). In the Santa Monica Mountains near Los Angeles, CA (USA), bromadiolone and brodifacoum (SGARs) had the highest prevalence of detection in bobcats, whereas diphacinone (FGAR) was detected at the highest concentrations in animal tissues (Serieys et al. 2015a).

ARs are vitamin K antagonists that reduce vitamin K availability for a variety of critical processes including hemostasis, bone metabolism, angiogenesis, apoptosis, oxidative protein folding, and immune function (Opal & Esmon, 2002; Li et al., 2003; Shearer & Newman, 2008; Esmon, 2005; Suttie, 2009; Ferland, 2012; Rutkevich & Williams, 2012; El Asmar et al., 2014; Danziger, 2008). While secondary exposure to ARs frequently leads directly to death from

hemorrhaging ([California Department of Pesticide Regulation 2013](#)), persistent sublethal exposure appears to be common in non-target species (Fournier-Chambrillon et al., 2004; Riley et al., 2007; Gabriel et al., 2015; Nogeire et al., 2015). Known side effects of sublethal exposure to vitamin K antagonists in humans and rats include pathologies such as arterial calcification (Danziger et al., 2008), severe skin irritation (Ozcan et al., 2012; Pourdeyhimi et al., 2014) and both immune activation and suppression (Kater et al., 2002; Popov et al., 2013). Given these potential effects, it is likely that sublethal AR exposure in natural populations disrupts important biological pathways necessary for survival from injury and pathogens.

Here, we analyze global gene expression patterns to evaluate the systemic effects of sublethal AR exposure in wild bobcats living near Los Angeles, California, USA. Bobcats are a highly mobile, widely distributed North American felid and are obligate carnivores that utilize a variety of habitats across their range and have been found even in some urban landscapes (Riley et al., 2010). They are highly territorial and solitary, with average home range sizes in our study area of approximately 2.5 km<sup>2</sup> for females and 5.0 km for males (Riley et al., 2010). In the study area, their diets consist primarily of lagomorph and rodent species including cottontail and brush rabbits, pocket gophers, ground squirrels, and voles; all of which are primary targets of ARs (Fedriani et al., 2000; Riley et al. 2010; Bartos et al., 2011). Additionally, some non-target rodents are exposed to ARs, such as woodrats, that are also bobcat prey (Moriarty et al., 2012).

Despite high exposure prevalence in our study area, few bobcat mortalities have been attributed directly to AR toxicity (Riley et al., 2007). However, previous research repeatedly found mortality from notoedric mange (caused by the mite *Notoedris cati*) to be associated with the level of ARs (Riley et al., 2007; Serieys et al., 2015a), suggesting the potential for sublethal effects of ARs on the ability of bobcats to resist mange mite infection. Mange was the primary source of

mortality in the bobcat population from 2002-20008 (Riley et al. 2010, Riley et al. 2015), which resulted in a genetic bottleneck (Serieys et al., 2015 b). Notoedric mange had never previously been known to have such severe demographic impacts on any wild felid population, and typically only affected a few individuals that were likely already unhealthy (e.g., Penner and Parke 1954; Pence et al. 1982; Pence et al. 1995). The emergence of this epizootic prompted NPS biologists to submit bobcat carcasses to the California Animal Health and Food Safety Laboratory (CAFHS) for necropsy and full evaluation to assess cause of death and any associated factors. Carcass examination and testing for a panel of eight environmental contaminants (lead, manganese, iron, mercury, arsenic, zinc, copper and cadmium) in addition to ARs suggested ARs as the only consistent underlying complication in bobcats that succumbed to death from mange infection (Riley et al., *personal communication*). However, the mechanism underlying this potential link between mange and AR exposure remains unknown.

By comparing AR-positive cases to those without detectable AR levels, we demonstrate the use of RNA-seq on whole blood to investigate genes and cellular processes that are affected by sublethal AR exposure in bobcats. Based on genes known to interact with vitamin K antagonists (<http://ctdbase.org/>) (Davis et al., 2017), we expected differential expression of genes involved in hemostasis, xenobiotic metabolism, and the immune system. We further sought to identify potential links between altered gene expression and disease susceptibility in bobcats and potentially, other wildlife. To our knowledge, this is the first genome-wide assessment of transcriptional responses to secondary AR exposure in a wild vertebrate population.

## MATERIAL AND METHODS

### *SAMPLING*

We conducted our analyses on 52 RNA preserved whole blood samples from bobcats captured as part of an ongoing research project directed by the National Park Service. We selected our samples to include 26 bobcats for which ARs were detected and 26 samples for which ARs were not detected in whole blood at the time of capture (Serieys et al., 2015a). Additionally, we balanced our samples across sex and age. These bobcats were captured across the Santa Monica Mountains, Simi Hills and Hollywood Hills between 2008-2012 (Figure 1). The study area was comprised of large natural areas within the Santa Monica Mountains, relatively large fragments of natural habitat surrounded by roads and development in the Simi Hills, and intensely urbanized areas in the Hollywood Hills. The dominant natural vegetation types were coastal sage scrub and chaparral. Each animal was captured, processed and sampled in accordance with the Office of Animal Research Oversight of the University of California Los Angeles (Protocol ARC#2007-167-12) and under authorization through California Department of Fish and Wildlife (SC-9791), assessed for AR exposure as described in (Serieys et al., 2015) and released at the capture site. Briefly, AR exposure was assessed using high performance liquid chromatography for the presence, and liquid chromatography- mass spectrometry for the quantity of warfarin, coumachlor, bromadiolone, brodifacoum, diphacinone, chlorophacinone, and difethialone from tissue, serum or whole blood. Detection of AR exposure in blood can greatly underestimate true exposure prevalence as paired liver samples from necropsied animals frequently tested positive for ARs even in the absence of detection in blood (Serieys et al., 2015a). Several factors may determine the detectability of ARs in blood: time since exposure; the magnitude of exposure; and the metabolic half-life of the AR which is both species and compound specific. Thus, although detection in blood most likely indicates a relatively recent exposure event, we cannot distinguish among all these effector variables. Further, many samples fell below the limit of quantitation but



above the level of detection. Hence, we considered AR exposure status as a binary variable (see Serieys et al., 2015a), and conservatively considered individuals showing detectable levels of at least one and up to five of the seven screened compounds (i.e., > 1 ppb) as positive for AR exposure (AR-positive).

All animals in this study were apparently healthy at the time of capture (i.e. no sign of disease). Disease screening was performed at the Center for Companion Animals Studies or in the Feline Retrovirus Research Laboratory in the Microbiology, Immunology, and Pathology Department at Colorado State University. Serum samples were analyzed separately for Feline Immunodeficiency Virus (FIV) and Puma Lentivirus (PLV) using western blot. Serum from blood samples was also assayed for Feline Calicivirus (FCV), Feline Herpesvirus (FHV), *Bartonella* sp. and *Toxoplasmosis gondii* specific IgG by enzyme linked immunosorbant assay (ELISA). To test for *Mycoplasma haemofelis*, *M. haemominutum*, *B. henselae* and *B. clarridgeae* infection, PCR assays were performed on whole blood.

## *METHOD DETAILS*

### *RNA processing*

Total RNA was extracted from 0.5 mL whole blood using the Ambion Mouse RiboPure Blood extraction kit, followed by globin removal using the Ambion GlobinClear Mouse kit (Life Technologies, Inc). RNA was quantified on the Agilent bioanalyzer (Agilent Technologies, USA). RIN scores from globin-depleted RNA samples ranged from 5.5 to 9.3. A minimum of 100 ng was used as input for cDNA library preparation using the Kapa Biosystems stranded mRNA kit (Kapa Biosystems, LTD). Each sample was uniquely tagged with custom index sequences developed at UCLA (Faircloth et al., 2014) comparable to Illumina TruSeq tags. Individual sample libraries

were then pooled in equimolar ratios, with 13 or 14 samples per pool and each pool sequenced on two lanes of an Illumina HiSeq 2500 or HiSeq 4000 sequencer. Sequencing was performed for 150 bp single end reads. Library quantification, pooling and sequencing were performed at the Vincent Coates Sequencing Facility at UC Berkeley.

#### *Quality control, mapping and trimming and read quantification*

Raw sequences were processed using Trim Galore! 0.3.1 (Krueger, 2015) to remove Illumina adapters and filter out sequences that did not meet the quality thresholds ( $q > 20$ , length  $> 25$  bp). Alignment of reads was performed on TOPHAT2 2.1.0 (Kim et al., 2013) using the domestic cat (*Felis catus*) as a reference genome (Ensembl release 85.62) (Yates et al., 2015). To maximize the number of unique reads mapped to the reference genome, we used the following parameters: read mismatches 10, max-insertion-length 12, read-edit-dist 22. On average, 70% of reads mapped uniquely, leaving an average of 13,232,179 mapped reads per individual (3,405,189-22,898,827).

#### *Gene expression quantification*

Aligned reads were converted to raw counts using HTSEQ (Anders et al., 2014) with the “union” mode, resulting in alignment to 21,890 genes. After removal of three globin-related genes (ENSFCAG00000030531, ENSFCAG00000031043, ENSFCAG00000022139) with high expression levels prior to normalization, values for the remaining 21,887 genes were normalized using the trimmed mean of M-values (TMM) method in the edgeR package (Robinson & Oshlack, 2010) in R and adjusted for gene length and GC content using custom Python scripts and the package CQN in R (Hansen et al., 2012). The number of genes remaining after filtering for protein-coding genes and sufficient coverage ( $> 10$  reads in 75% of cDNA libraries) was 12,332. We used

hierarchical clustering of the gene expression adjacency matrix to identify outlier samples (defined as having a z-score greater than 3) with the R package WGCNA (Langfelder & Horvath, 2008).

## STATISTICAL ANALYSIS

A summary of the analyses used in the present paper is available in Figure 1.2.

### *LIMMA*

We performed principal components analysis to identify and remove technical factors from the expression data (Figure 1.3). Gene by gene linear mixed models were used to identify differentially expressed genes in AR-positive bobcats using the limma package in R (Ritchie et al., 2015). We adjusted our significance values to account for multiple hypothesis testing using the false discovery rate (FDR) method as implemented in the qvalue package in R (Storey et al., 2015) and selected genes falling below  $Q < 0.05$ . We selected the genes falling under a Q-value threshold of 0.05 and then performed Gene Ontology (GO) analysis on the up and downregulated genes that passed this threshold using g:Profiler (Reimand et al., 2016). In g:Profiler (version 1682), we used the 12,332 genes as a statistical background and aligned our significant Ensembl gene ID specifically to the *Felis catus* genome. We required a minimum of 2 for the query intersection and applied the Benjamini-Hochberg FDR correction for the significance threshold. The remaining parameters were set using the defaults.

### *WGCNA (Weighted Gene Correlation Network Analysis)*

We assigned all 12,332 genes to functional categories based on coordinated expression patterns using the WGCNA package in R (Langfelder & Horvath, 2008). Briefly, WGCNA searches for genes with similar expression profiles and transforms this correlation matrix into an adjacency matrix via a power function  $\beta$  (Zhang & Horvath, 2005). The adjacency matrix is used

to define a measure of node dissimilarity. In conjunction with a clustering method (average hierarchical clustering) and the node dissimilarity measure, the user can identify modules containing highly interconnected genes which can then be related to a trait of interest (Langfelder & Horvath, 2008).

We first ran a k-means clustering optimization to determine the most likely number of clusters in our expression dataset using the ICGE package in R (Irigoiien et al., 2012). In WGCNA, we then followed the automatic, one-step network construction and module detection implemented with the function “blockwiseModules” with an unsigned network algorithm, a power  $\beta= 6$ , corType= bicor, maximum block size = 13000, min module size = 40, mergeCutHeight =0.5, mergingThresh = 0.5. The remaining parameters were kept at the default setting. This cutoff value yielded the “correct” number of modules, including the “grey” module, which contains genes that are not part of any modules. Subsequently, we performed a hub gene analyses (genes with the highest intramodular connectivity) on each resulting module, and submitted the top hub genes (up to 100) for GO analysis using g:Profiler (Reimand et al., 2016). We used these functional categories based on gene enrichment of biological processes to aid in the interpretation of our linear model results at a systemic level.

In order to assess the stability of the modules and therefore the biological interpretation of the hub gene analyses, we performed a module stability analysis (Langfelder & Horvath, 2012). We conducted 50 full module construction and module detection runs on resampled expression data, where each iteration randomly sampled 52 animals from the original dataset, with replacement. Module assignment for each gene was then compared to the original module assignment and overall stability of the hub genes was calculated as the mean proportional assignment of each hub gene to the original module. In addition, we repeated our module detection

analysis after changing the correlation type to the default (Pearson) and subsequently calculated module preservation statistics to evaluate whether a given module defined in one dataset (reference network) can also be found in another dataset (test network) across 200 permutations. Each permutation will report the observed value and the permutation Z score to measure significance, which is then summarized in a composite measure called Z.summary.

### *Transcript Origin Analysis (TOA) & Transcriptome Representation Analysis (TRA)*

Transcript Origin Analysis (TOA) was applied as in Cole et al. (2011) to identify the specific cell types giving rise to observed AR-related differences in whole blood gene expression. Transcriptome Representation Analysis (TRA) was performed as in Powell et al. (2013) to quantify differences in the prevalence of specific cell types based on coordinated shifts in cell type-specific RNA profiles in AR-positive bobcats. Both analyses utilize publicly available leukocyte subset-specific expression profiles as reference distributions to generate cell diagnosticity scores for each gene analyzed. The cell diagnosticity scores for AR-associated genes (defined either by fold expression difference ( $> 1.5$ ) or significance ( $q < 0.05$ )) are then tested for significant over-representation relative to the basal prevalence of diagnosticity scores across all genes present in the data set (TOA), or the most cell type-diagnostic transcripts are tested for differential expression as a function of AR exposure (TRA). Cell type-specific reference profiles used in the present analyses included major leukocyte subsets (i.e., monocytes, dendritic cells, natural killer cells, B lymphocytes, CD4+ T lymphocytes, CD8+ T lymphocytes, from GEO data set GSE1133), immature/classical (CD16-) vs mature/non-classical (CD16+) monocytes (GSE25913), M1 vs M2 macrophages (GSE51446), and two data sets comparing naïve B lymphocytes with progressively more differentiated B cell subpopulations (GSE64028 and GSE13411).

## RESULTS

### *Principal Components of Expression Data*

To evaluate the influence of technical (i.e. batch effects) and biological variables on data structure, we performed linear regression on the principal components (PC) of the normalized read counts. We regressed out technical factors that were significantly correlated with the first PC, including the sequencing platform (HiSeq 2500 or HiSeq 4000), RNA integrity number (RIN) and library preparation. After correcting for technical effects, we found that exposure status was highly significant on PC 1, which explained 19.4 % of the total variance (Figure S2). Importantly, none of the pathogens for which each bobcat was currently infected (*Mycoplasma haemominutum*, *M. haemofelis/turricensis*, *Bartonella clarridgeie*, *B. henselae*) were significantly correlated with the first 12 PCs, and although evidence of exposure (seropositivity) to Puma Lentivirus (PLV) and *Bartonella* spp. was significant on PC 9 (PLV) and PC 12 (*Bartonella*), these principal components explained only 2.6% and 1.9% of the total variation in expression (Figure S2, Table 1.1). Therefore, differential expression profiles in AR-positive bobcats are not likely due to current infection status for the 10 common feline pathogens (Bevins et al., 2012; Carver et al., 2016) examined. Additionally, age classification (juvenile or adult) was significant on PC 6, which explained only 3.5 % of the variance in the data.

### *AR exposure as a linear predictor of differentially expressed genes*

To identify genes influenced by AR exposure, we used linear regression to measure fold-change ( $\beta$ ) and statistical significance (Q). Our dataset included read counts for 12,332 genes that were retained after normalization and low coverage filtering. After applying a false discovery rate (FDR) corrected for multiple testing (Figure S3), a total of 1,783 genes were significantly ( $Q < 0.05$ ) predicted by exposure status, of which 530 were downregulated and 1,253 were upregulated (Figure 2). Eighteen of these genes identified in our model overlap with genes listed in the

Comparative Toxicogenomics Database (Davis et al., 2017) as interacting with warfarin, although the direction of dysregulation was not consistent for all genes with responses observed in rats or humans (Table 1.2).

Downregulated genes were enriched for several gene ontology (GO) terms related to immune function, including response to IL-12 and IL-6; positive regulation of acute inflammatory response; complement-mediated cytotoxicity; myeloid differentiation; monocyte activation; FC-epsilon receptor signaling; and positive regulation of macrophage chemotaxis. Downregulated genes were also enriched for terms related to epithelium including keratinocyte proliferation, glomerulus development, and intestinal epithelial differentiation; and for terms related to vascular processes including Tie-signaling, negative regulation of vasoconstriction, regulation of angiotensin levels in blood, negative regulation of blood circulation, and platelet aggregation. Additional terms related to cell cycle, biosynthetic processes, metabolism, reproductive processes, and transport (Figure 3A; Table 1.3).

We observed downregulation of several genes related directly to wound healing and epithelial integrity, including matrix metalloproteinase 1 (*MMP1*:  $\beta = -0.99$ ;  $Q = 0.038$ ) and matrix metalloproteinase 10 (*MMP10*:  $\beta = -1.26$ ;  $Q = 0.01$ ); as well as two important transcription factors involved in white blood cell production and differentiation, GATA binding protein 2 (*GATA2*:  $\beta = -0.54$ ;  $Q = 0.047$ ) and kruppel-like factor 5 (*KLF5*:  $\beta = -0.67$ ;  $Q = 0.016$ ). Further several genes involved in the allergic response were downregulated. These included membrane spanning 4-domains A2 (*MS4A2*:  $\beta = -0.79$ ;  $Q = 0.03$ ) and Fc Fragment of IgE Receptor 1a (*FCER1A*:  $\beta = -0.88$ ;  $Q = 0.025$ ), encoding for the high affinity IgE beta and alpha receptors, and carboxypeptidase A3 (*CPA3*:  $\beta = -1.29$ ;  $Q = 0.019$ ) which is involved in granulocytic mediated inflammation. Bobcats exposed to ARs thus may experience a depressed inflammatory response coupled with

diminished epithelial integrity and wound healing response.

There were 2.36 times as many upregulated genes, which were enriched for GO terms related predominantly to immune function, specifically to T lymphocytes, as well as terms for gene expression and RNA processing. Immune related terms included positive regulation of immune response, T cell differentiation, thymocyte aggregation, and T cell receptor signaling (Figure 3B; Table 1.4). Notably, we also observed upregulation of UbiA prenyltransferase domain containing 1 *UBIADI* ( $\beta = 0.38$ ;  $Q = 0.032$ ), a mammalian gene involved in the biosynthesis of vitamin K2 (Nakagawa et al., 2010; Meehan & Beckwith, 2017), as well as several genes involved in xenobiotic metabolism including Cytochrome P450 Family 2 Subfamily U Member 1 (*CYP2U1*:  $\beta = 0.35$ ;  $Q = 0.016$ ), ATP Binding Cassette Subfamily B Member 1 (*ABCB1*:  $\beta = 0.52$ ;  $Q = 0.015$ ), Carbohydrate Sulfotransferase 2 (*CHST2*:  $\beta = 0.65$ ;  $Q = 0.013$ ), and Heparan Sulfate-Glucosamine 3-Sulfotransferase 1 (*HS3ST1*:  $\beta = 0.64$ ;  $Q = 0.039$ ). These results suggest that ARs may activate the adaptive immune system as well as processes associated with xenobiotic metabolism and, potentially, responses to vitamin K deficiency. Other GO terms included gene expression, RNA metabolic process, translation, positive regulation of RNA splicing, response to dsRNA, and ribonucleoprotein complex biogenesis (Figure 3B; Table 1.4). Several of the genes in these terms relate specifically to immune and cellular stress-responses, likely reflecting increased transcriptional activity due to immune activation and toxicant metabolism.

Further, we observed differential expression of several interleukin cytokines (ILs) in AR-positive bobcats (Table 1.5). Downregulated IL genes were generally regulators of inflammation including *IL13* ( $\beta = -0.9$ ;  $Q = 0.016$ ) and *IL36B* ( $\beta = -0.8$ ;  $Q = 0.013$ ); whereas upregulated IL genes were generally indicators of B and T cell activity, including *ILF2* ( $\beta = 0.24$ ;  $Q = 0.044$ ), *ILF3* ( $\beta = 0.25$ ;  $Q = 0.033$ ) and *IL7R* ( $\beta = 0.6$ ;  $Q = 0.017$ ). Overall, the up- and downregulation of



numerous cytokines demonstrate a pronounced dysregulation of critical mediators of immune function, implying both immunosuppressive and stimulating effects of AR exposure.

### *Transcript Origin Analysis & Transcriptome Representation Analysis*

To identify and quantify cellular subsets that contribute to differential gene expression in AR-positive bobcats, we applied a Transcript Origin Analysis (TOA) and Transcriptome Representation Analysis (TRA). The TOA analyses of major leukocyte subsets showed that AR-downregulated genes originated disproportionately from monocytes (CD14+ cells) whereas upregulated genes originated primarily from helper (CD4+CD8-) and cytotoxic (CD4-CD8+) T cells and CD19+ B cells (Table 1.6). Further, TRA analyses indicated an average 6.4% reduction in total monocyte prevalence within circulating blood of AR-positive bobcats (mean TRA log2 prevalence ratio for monocyte-diagnostic genes =  $-0.102 \pm \text{SE } 0.047$ ,  $p = 0.039$ ). These results were consistent regardless of whether the differential expression analysis was assessed by effect size (0.917 fold-change) or as a function of the significance threshold ( $Q < 0.05$ ; 0.952-fold change).

Subsequent TOA analysis focusing on specific monocyte subsets showed that AR-downregulated genes derived predominantly from CD16- (immature “classical”) monocytes whereas AR-upregulated genes derived predominantly from CD16+ (mature, “non-classical”) monocytes. Again, these results were consistent regardless of whether differential expression was defined by effect size or statistical significance. In terms of patterns for B cells, TOA analyses of distinct B cell differentiation states linked AR exposure to a shift toward immature, naive B-cells; whereas downregulated genes derived predominantly from more mature/memory B cell phenotypes, including plasma cells whose primary role is the secretion of antibodies, indicating that these cells were less common or less active or both (Table 1.6). In general, these results

indicate that AR exposure may affect immune function by impacting the relative abundance of circulating immune effector cells and cell-subsets.

### *Weighted Gene Co-Expression Network Analysis (WGCNA)*

We implemented a WGCNA to assign all 12,332 genes to modules based on patterns of coordinated expression, resulting in 11 modules, including a non-specific module which was consistent with the k-means clustering results (Figure S4). We subsequently assigned each module to functional categories based on GO enrichment analysis of modular hub genes and assessed how many significantly differentially expressed genes (based on the linear model) were assigned to each module (Figure 4A). The dominant expression profile (eigengene) for two of the ten modules were significantly correlated ( $p < 0.05$ ) with exposure after FDR correction (Figure 4B; Figure 4C). Functionally, these modules related to T-cell activation and signaling (Pearson's  $r = 0.46$ ,  $p_{\text{adjusted}} = 0.006$ ; light blue module), and the inflammatory response (Pearson's  $r = -0.39$ ,  $p_{\text{adjusted}} = 0.025$ ; blue module). In addition, 4 of the remaining 8 modules had an overlap of 10 or more genes that were significant in the linear model. These modules were enriched functionally for transferase activity (green module), wound healing/coagulation (red module), endoplasmic reticulum stress response (purple module), and heme metabolic process (yellow module). Module stability for these 6 modules ranged from 27% - 98%. The hub genes were re-assigned at 98% for the light blue module, at 88% for the green module, at 96% for the red module, at 78% for the yellow module, at 57% for the blue module, at 27% for the purple module. Similarly, all our modules showed high preservation, with Z.summary scores ranging from 19 to 56.

## DISCUSSION

The analysis of genome-wide transcriptional changes is a potent but largely underutilized

method to assess organismal response to sublethal toxicant exposure in the wild, especially when controlled exposure experiments are logistically or ethically unfeasible, as is often the case with wild carnivores. Bobcats in the Santa Monica Mountains persistently exposed to ARs do not exhibit canonical signs of coagulation disruption, such as hemorrhaging, despite the fact that this was the second-leading cause of mortality in a long-term coyote study (Gehrt and Riley 2010). However, bobcats do appear more susceptible to notoedric mange (Riley et al. 2007; Serieys et al., 2015a), consistent with sublethal effects of AR-exposure.

Other environmental toxicants or stressors that potentially influence gene expression may be common in areas in AR-use areas. Consequently, ARs may not be the ultimate cause of the pattern we observe or may be one of several contributing factors. However, we argue that ARs are the most likely cause of gene expression dysregulation for the following reasons: 1) ARs are known to accumulate in food chains and are targeted at prey species which bobcats frequently consume (Riley et al., 2010), so there is a specific and well-understood pathway of exposure for bobcats; 2) AR exposure is correlated generally with more intensive human land use, however AR exposure has also been documented in pristine environments (Gabriel et al., 2012), and particularly near modified open space areas such as landscaped parks, cemeteries, equestrian facilities, and golf courses (Nogieres et al., 2015, Serieys et al., 2015a) which are less degraded than more intensively urbanized settings; 3) the most urban-associated bobcats in our study area were nonetheless largely using natural areas, with commonly more than 75% or more of their radio telemetry (Riley et al., 2010); 4) necropsies performed on bobcats throughout the course of the 20+ year study of carnivores in SMMNRA have not shown any other toxicants consistently linked to disease or mortality other than ARs in bobcats or in other carnivores such as coyotes or mountain lions (Gehrt and Riley 2010, Beier et al. 2010); and 5) many of the pathways we have found

differentially expressed are known to be affected by ARs as discussed below. For these reasons, we suggest that sublethal AR-exposure in bobcats is the best candidate for gene dysregulation and physiologic perturbation.

In addition to impacts related to hemostasis and vitamin K availability, we observed substantial effects on multiple biological processes including xenobiotic metabolism and ER stress response, inflammatory and allergic immune response, adaptive immunity, and skin integrity (Figure 2; Table 1.7). For each process discussed below, these effects have important implications for bobcat health, and taken together, also constitute strong plausible links between AR exposure and mange susceptibility in bobcats.

#### *Blood Hemostasis and Vitamin K*

Bobcats, like domestic cats, appear less sensitive than other species to the common effects of ARs (Petterino & Paolo, 2001; Beusekom, 2015). Specifically, clotting times do not differ significantly between AR-positive and AR-negative bobcats (Serieys et al. *unpublished data*). Importantly, however, one bobcat and three mountain lions (Riley et al., 2007) have died from coagulopathy in the study area. Our gene expression results also suggest that there are some direct effects of ARs on hemostasis, potentially related to the vitamin K cycle. We observed GO enrichment for hemostasis-related terms in downregulated genes, and several downregulated genes overlapped with the coagulation module from WGCNA, including genes involved in platelet activation (i.e. thromboxane A synthase 1; *TBXAS1*) and fibrin-clot formation (i.e. serpin family E member 2; *SERPINE2*). Notably, upregulation of *UBIADI* in AR-positive animals may reflect a possible compensatory mechanism in bobcats. Vitamin K2 has been shown to offset effects of vitamin K antagonists on arterial calcification (Kawashima et al., 1997) and is supportive for hematopoietic and bone metabolism (Tabb et al., 2003; Miyazawa & Aizawa, 2004).

## *Xenobiotic Metabolism and Endoplasmic Reticulum stress*

Xenobiotic metabolism is a primary function of the liver that occurs over three phases—cellular uptake, transformation and excretion (Ioannides, 2001; Filser, 2008; Lee et al., 2011). During the second phase, reactive intermediates can be formed that directly target enzymes in the ER, thereby triggering oxidative and ER stress responses (Foufelle & Fromenty, 2016; Cribb, 2005). In bobcats, evidence that AR exposure activates the ER stress response is, as shown by the differential expression of genes such as Lysosomal Associated Membrane Protein 3 (*LAMP3*), Heat Shock Proteins (*HSP90B1*), Hypoxia Up-Regulated 1 (*HYOU1*), X Box Binding Protein 1 (*XBPI*) and Protein Disulfide Isomerase (*PDI6*), all of which were clustered in the WGCNA module related to ER stress (Figure 4A; Figure 4B).

In model organisms, ARs are processed through canonical xenobiotic pathways and are recognized inducers of oxidative stress (Ware et al., 2015; Miller, 2009). However, in felids, mechanisms of xenobiotic metabolism are poorly understood (Beusekom, 2015). For instance, cats are deficient in several enzymes identified as necessary for drug elimination in rats and humans (Beusekom, 2015; Court, 2013). Similarly, the mammalian gene encoding for UGT1A6, specifically involved in warfarin metabolism, is a pseudogene in the felid family and is therefore not expressed as a functional protein (Shresta et al., 2012). High tolerance for ARs suggest that felids have possibly developed alternate and perhaps more efficient mechanisms for metabolizing these toxicants. We observed upregulation of *CYP2U1*, a member of the CYP450 gene family whose products are the primary mediators of xenobiotic metabolism (Zanger & Schwab, 2013; Lynch & Price, 2007; Karlgren et al., 2005). In humans, variants in certain CYP enzymes are associated with differential warfarin sensitivity (Freeman et al., 2000). Given the high variability of CYP function across species (Zanger & Schwab, 2013), it is plausible that *CYP2U1* plays an

active role in the metabolism of ARs in felids. Additionally, we observed upregulation of *CHST2* and *HS3ST1*, two genes involved in the xenobiotic metabolism pathway (Zhu et al., 2016), as well as *ABCB1*, essential for elimination of AR metabolites (Miller, 2009; Beusekom, 2015) and also associated with differential warfarin sensitivity (Wadelius et al., 2004).

### *Immunomodulation by ARs*

Controlled experiments on herbicides and pesticides document exposure-related changes in circulating leukocyte composition in a variety of species (Malik & Chughtai, 2003; Cimino-Reale et al., 2008). For ARs specifically, rats exhibited reduced monocytes and increased lymphocyte numbers (Mikhail & Abdel-Hamid, 2007). We found evidence of similar patterns of AR-induced changes in circulating leukocytes in bobcats, likely resulting in both immune suppression (of myeloid lineage immune cell function) and stimulation (of lymphoid lineage cell functions).

With respect to immune suppression, we observed downregulation of several genes involved in the allergic immune response including *FCERIA*, *HDC*, *MS4A2*, and *CPA3*, each primarily associated with the function of mast cells and monocytes. Evidence of reduced total monocytes in AR-exposed bobcats, with a higher relative abundance of activated or mature to naive monocytes suggests a decrease in the production of immature myeloid lineage cells. In mammals, white blood cell production (hematopoiesis) occurs in bone marrow, where transcriptional regulation, cytokine signaling and properties of the stromal niche operate in tandem to determine lineage commitment of hematopoietic stem cells (Dorshkind, 1990; Schoeters et al., 1995; Orkin & Zon, 2008). We observed downregulation of several transcription factors involved in hematopoiesis in bone marrow. GATA-2 is critical for the production and maintenance of early hematopoietic progenitors (Tsai et al., 1997). Mutations in this gene are associated with myeloid

cell abnormalities in humans (Hsu et al., 2011; Pasquet et al., 2013). Transcription factors *KLF4* and *KLF5* share co-regulatory roles during hematopoiesis (Ishikawa et al., 2013) including monocyte production and development (Park et al., 2016; Shahrin et al., 2016). Further, vitamin K has been shown to improve the supportive function of bone marrow stromal cells for hematopoiesis (Miyazawa & Aiwazawa, 2004) and directly promotes survival and differentiation of myeloid progenitor cells (Sada et al., 2010). Therefore, AR exposure may impact the number of circulating monocytes through effects of vitamin K availability on bone marrow integrity as well as through deregulation of transcription factors necessary for monocyte differentiation.

With respect to immune stimulation, we observed an increase in gene expression by B- and T-lymphocytes in AR-positive bobcats. In B-cells, upregulation stemmed specifically from increased activity of naive relative to mature or differentiated B-cells. There was also a strong signal for a reduction in the proportion of plasma cells. As above, this may indicate altered output of early lymphocyte progenitor cells, hence inflating the number of naive B-cells in peripheral leukocytes. Conversely, it may indicate an increased elimination of standing activated and memory B-cells, with a responding increase in lymphopoiesis. In this respect, *KLF5* emerges as an important candidate gene. In heterozygote deficient mice (*KLF* +/-) this gene has been linked experimentally to the manifestation of systemic sclerosis (SSc) symptoms, a disease characterized by B-cell dysregulation, skin lesions and vasculopathy (Noda et al., 2014). Total and relative naive B-cells were elevated in SSc patients, whereas proportions of memory B and plasma cells were decreased, which was attributable to increased spontaneous death of these cells (Sato et al., 2004). Our results imply that although total B cells are elevated in exposed bobcats, the animal's ability to maintain sufficient memory B-cells capable of recognizing specific pathogens upon secondary challenge may be compromised. This could limit the immunologic capacity of exposed bobcats to

mount a rapid response to a previously encountered pathogen such as notoedric mange.

Our results also indicate that AR-exposure is associated with upregulation of T-cell activity. Indeed, all three of the mature T-cell coreceptor molecules (*CD3G*, *CD3D*, and *CD3E*) are highly upregulated in exposed bobcats. Previous work demonstrated that T-cells can be activated directly by anticoagulants through MHC presentation (Naisbitt et al., 2005). Phenindione, for instance, is a vitamin K antagonist anticoagulant that is known to cause hypersensitivity in some human patients. It is also one of the most commonly detected AR compounds (in the form of diphacinone) in our study population (Serieys et al., 2015a). Manifestation of hypersensitivity occurs primarily in the skin and is correlated with rapid proliferation of drug-specific CD4<sup>+</sup> T cell clones (Naisbitt et al., 2005). In the latter study, it was shown that warfarin (a coumarin compound) can also adopt a phenindione-like structure and similarly elicit T cell proliferation. Hence, AR exposure may directly induce T cell proliferation through the antigen presentation, potentially leading to immune exhaustion or expansion of dichotomous (i.e. Th1 and Th2) T cell subpopulations.

#### *Keratinocyte Regulation*

Genes downregulated in AR-positive bobcats indicated that ARs may interact with epithelial maintenance and formation. Considerable evidence suggests that the skin may be a target tissue of warfarin. Some warfarin treated patients experienced skin necrosis (Chan et al., 2000; Pourdeyhimi et al., 2014), while endothelial cell injury has been observed in experimental warfarin treated rats (Ozcan et al., 2012). In bobcats, three differentially expressed genes are consistent with these observations. Transglutaminase 1 (*TGMI*) is a key enzyme in keratinocyte differentiation (Elias et al., 2002, Thacher & Rice, 1985; Russel et al., 1995) and was downregulated in AR-exposed bobcats. Mutations in this gene result in deficient epidermal cornification (Herman et al.,



2009) and inhibited skin cell maturation (Jiang et al., 2010). Second, stratifin (*SNF*) is also downregulated in AR-positive bobcats. This gene been demonstrated to affect the expression levels of matrix metalloproteinases (MMPs) which are integral to the wound healing process (Dong, 2008; Medina et al., 2007; Nuutila et al., 2012). Interestingly, two metalloproteinases *MMP1* and *MMP10* were some of the most downregulated genes in AR-positive bobcats. Finally, previously discussed transcription factors *KFL4* and *KLF5* are involved in epidermal differentiation when expressed in keratinocytes (McConnell et al., 2007; Segre et al., 1999; Tetreault et al., 2016).

#### *Potential links between AR exposure and susceptibility to mange*

The immune response to mange-causing parasites is highly variable among species (Walton, 2010). With limited understanding of the immunological responses to mange in felids, it is difficult to link mange-susceptibility mechanistically to AR-exposure in bobcats. One hypothesis based on our results is that simultaneous immune dysregulation and disruption of epithelial integrity specifically predisposes bobcats to opportunistic infection by an ectoparasite pathogen.

Studies of *Sarcoptes scabiei*, a close relative of *Notoedris cati*, indicates that both innate and adaptive immune pathways are activated in response to infestation. In some mammals, an initial localized inflammatory response of the skin, characterized by infiltrates of mast cells, neutrophils and mononuclear cells, is typically followed by a pronounced humoral response, which subsides over time in resistant hosts upon secondary challenge (Rahman et al., 2010; Arlian et al., 1996). We found that AR-positive bobcats exhibit a substantial reduction in the expression of genes involved in allergic immune response, as well as from both monocytes and late stage B lymphocytes including plasma cells. Reduction of these cell types in AR-positive bobcats suggests that the basic immune machinery, specifically proinflammatory monocytes, mast cells, and

antibody producing B-cells/plasma cells, necessary to protect against severe mange infestation is compromised by ARs. Further, downregulation of proinflammatory cytokines known to operate directly on keratinocytes (e.g. *IL36*) (Foster et al., 2014), in addition to downregulation of several genes involved in epithelial formation and maintenance, suggest that ARs directly affect skin integrity and immunity.

We hypothesize that the cumulative effects of these cellular responses to AR exposure increases the susceptibility of individuals to opportunistic parasitism of the skin and inhibits wound healing, allowing for the mange lesions to expand and leading to death. Future research should focus on assessing transcriptional changes in skin following AR exposure, as well as determining the impacts on bone marrow integrity and leukocyte production. Further, antibody production against a range of pathogens potentially threatening to bobcats (e.g., Feline Leukaemia virus, Canine Distemper virus, plague, gastrointestinal parasites) should be tested in AR exposed animals, perhaps in captivity, to assess other secondary effects of AR exposure. In general, experimental models to understand responses to simultaneous toxicant and pathogen exposure need to be developed and tested.

## CONCLUSION

We investigated the effects of anticoagulant rodenticides using RNA-seq and provide convincing evidence that sublethal exposure to ARs has substantial and dramatic gene regulatory consequences in a wild carnivore population. We demonstrate that surveying genome wide expression from whole blood is an effective method to analyze the effects of toxicants in natural populations. Our analyses provided a system wide perspective on the physiological effects of these toxicants and enabled us to detect subtle stage-specific changes in circulating leukocyte populations, which has critical implications for the biological function of these cell types. With

the increasing accessibility and reduced cost of genome sequencing, this method could be translated to other systems and identify sensitive diagnostic biomarkers for AR exposure in felids and other species. Overall, our results show that the focus on the lethal effects of toxicants developed for pest control which cause a failure of blood to clot in target species, may be misplaced. Individual fitness and population persistence may be critically impacted without signs of the target effects of ARs. This result may apply to other toxicants in the natural environment. Given the worldwide application of anticoagulants in a wide variety of settings from residential to rural environments and even pristine environments, research on the sublethal effects may be a new, previously unacknowledged priority for future research.

TABLES AND FIGURES

**Table 1.1.** Summary of the variance on the first 12 Principal Components. F-statistics and p-values are reported for four significantly correlated variables (AR-detection, age class, PLV detection, and *Bartonella* spp. seropositivity).

	PCA1	PCA2	PCA3	PCA4	PCA5	PCA6
Standard deviation	24.81	17.2	13.7336	11.8603	11.41883	10.6628
Proportion of variance	0.194	0.932	0.05941	0.04431	0.04107	0.03581
Cumulative proportion	0.194	0.287	0.34648	0.39079	0.43186	0.46768
Variable	AR-detection					age
F-statistic	11.97					9.214
p-value	0.001					0.0038
	PCA7	PCA8	PCA9	PCA10	PCA11	PCA12
Standard deviation	9.588	9.26402	9.10637	8.65275	8.43	7.82635
Proportion of variance	0.029	0.02703	0.02612	0.02358	0.0224	0.01929
Cumulative proportion	0.497	0.52367	0.5498	0.57338	0.596	0.61508
Variable			PLV <sup>1</sup>			<i>Bartonella</i> spp.
F-statistic			12.25			9.063
p-value			0.001			0.004

<sup>1</sup> PLV = puma lentivirus

**Table 1.2** Differential expressed genes listed as related to warfarin in the Comparative Toxicogenomic Database<sup>1</sup>

Gene name	Gene symbol	Known interactions with warfarin	Present study (bobcats)	Beta fold change ( $\beta$ )
ATP binding cassette subfamily B member 1	<i>ABCB1</i>	ABCB1 polymorphism affects the susceptibility to Warfarin	↑	0.52266
		ABCB1 protein affects the metabolism of warfarin		
adenosylhomocysteinase	<i>AHCY</i>	↓	↑	0.18268
BCL2, apoptosis regulator	<i>BCL2</i>	↓ (Vitamin K2 inhibit the interaction and increase expression)	↑	0.49731
chaperonin containing TCP1 subunit 5	<i>CCT5</i>	↑	↑	0.3042
Eukaryotic Translation Initiation Factor 3 Subunit I	<i>EIF3I</i>	↓	↑	0.24019
Ectonucleotide Phosphodiesterase 1	<i>ENPP1</i>	↑	↑	0.835109
G3BP Stress Granule Assembly Factor 1	<i>G3BP1</i>	↑	↑	0.224469
Heat Shock Protein 90 Alpha Family Class B Member 1	<i>HSP90AB1</i>	↓	↑	0.34457
Heat Shock Protein Family A (Hsp70) Member 8	<i>HSPA8</i>	↑	↑	0.34054
Keratin 18	<i>KRT18</i>	↓	↑	0.38046
NmrA like redox sensor 1	<i>NMRAL1</i>	↑	↑	0.38422
Nucleobindin 1	<i>NUCB1</i>	↑	↑	0.25164
Proliferation-Associated 2G4	<i>PA2G4</i>	↑	↑	0.321884
Protein Disulfide Isomerase Family A Member 3	<i>PDIA3</i>	↑	↑	0.227104
		↓		
Ribosomal Protein L27	<i>RPL27</i>	↑	↑	0.31455
Selenophosphate Synthetase 1	<i>SEPHS1</i>	↑	↑	0.31914
Tumor Protein P53	<i>TP53</i>	Affect the expression	↑	0.33625
		Increase degradation of TP53 protein		
U2 Small Nuclear RNA Auxiliary Factor 2	<i>U2AF2</i>	↑	↑	0.18791

<sup>1</sup> symbol: ↑ = upregulated, ↓=downregulated

**Table 1.3.** Figure code, functional category, GO term ID, GO term description, and p-value for the downregulated genes.

Code	Functional category	GO_terms ID	Description	Pvalue
1	Vascular process	GO:0003018	Vascular process in circulatory system	0.015
2	Vascular process	GO:0090331	Negative regulation of platelet aggregation	0.05
3	Vascular process	GO:0048014	Tie signaling pathway	0.005
4	Vascular process	GO:0045906	Negative regulation of vasoconstriction	0.016
5	Vascular process	GO:0002002	Regulation of angiotensin levels in blood	0.031
6	Immune	GO:0038095	Fc-epsilon receptor signaling pathway	0.016
7	Immune	GO:1903307	Positive regulation of regulated secretory pathway	0.045
8	Immune	GO:0010759	Positive regulation of macrophage chemotaxis	0.05
9	Immune	GO:0002675	Positive regulation of acute inflammatory response	0.041
10	Immune	GO:0030222	Eosinophil differentiation	0.016
11	Immune	GO:0032506	Cytokinetic process	0.018
12	Immune	GO:0090383	Phagosome acidification	0.031
13	Immune	GO:0002762	Negative regulation of myeloid leukocyte differentiation	0.014
14	Immune	GO:0032675	Regulation of interleukin-6 production	0.015
15	Immune	GO:0042117	Monocyte activation	0.016
16	Immune	GO:0070671	Response to interleukin-12	0.002
17	Immune	GO:0097278	Complement-dependent cytotoxicity	0.005
18	Epithelium	GO:0032835	Glomerulus development	0.038
19	Epithelium	GO:0010839	Negative regulation of keratinocyte proliferation	0.05
20	Epithelium	GO:0060575	Intestinal epithelial cell differentiation	0.008
21	Membrane	GO:0051088	PMA-inducible membrane protein ectodomain proteolysis	0.016
22	Membrane	GO:0001508	Action potential	0.032
23	HGF	GO:0032905	Transforming growth factor beta1 production	0.031
24	HGF	GO:0060396	Growth hormone receptor signaling pathway	0.008
25	Reproductive	GO:2000243	Positive regulation of reproductive process	0.018
26	Biosynthetic process	GO:0046504	Glycerol ether biosynthetic process	0.05
27	Biosynthetic process	GO:0008611	Ether lipid biosynthetic process	0.016
28	Biosynthetic process	GO:0045714	Regulation of low-density lipoprotein particle receptor biosynthetic process	0.05
29	Biosynthetic process	GO:0036092	Phosphatidylinositol-3-phosphate biosynthetic process	0.05
30	Transport	GO:0015711	Organic anion transport	0.038
31	Transport	GO:0046942	Carboxylic acid transport	0.045
32	Transport	GO:0071985	Multivesicular body sorting pathway	0.002
33	Metabolic process	GO:0006195	Purine nucleotide catabolic process	0.038
34	Metabolic process	GO:0006734	NADH metabolic process	0.05
35	Metabolic process	GO:0019720	Mo-molybdopterin cofactor metabolic process	0.05
36	Metabolic process	GO:0006007	Glucose catabolic process	0.031

37	Metabolic process	GO:0009109	Coenzyme catabolic process	0.031
38	Cell process	GO:0045598	Regulation of fat cell differentiation	0.029
39	Cell process	GO:0072423	Response to DNA damage checkpoint signaling	0.05
40	Cell process	GO:0040020	Regulation of meiotic nuclear division	0.006
41	Cell process	GO:0006390	Transcription from mitochondrial promoter	0.024

**Table 1.4.** Figure code, functional category, GO term ID, GO term description, and p-value for the upregulated genes.

<b>Code</b>	<b>Cluster</b>	<b>GO_terms</b>	<b>Description</b>	<b>Pvalue</b>
1	Immune	GO:0071594	Thymocyte aggregation	0.006
2	Immune	GO:0030217	T cell differentiation	0.003
3	Immune	GO:0050778	Positive regulation of immune response	0.009
4	Immune	GO:0050852	T cell receptor signaling pathway	0.007
5	RNA	GO:0033120	Positive regulation of RNA splicing	0.006
6	RNA	GO:0022613	Ribonucleoprotein complex biogenesis	0.011
7	RNA	GO:0016070	RNA metabolic process	0.0003
8	RNA	GO:0043331	Response to dsRNA	0.009
9	Gene expression	GO:0006412	Translation	0.001
10	Gene expression	GO:0010467	Gene expression	0.000016

**Table 1.5.** List of differentially expressed interleukin cytokines and interleukin cytokine receptors from the linear model analysis.

Gene Symbol	Coefficient	Q-value	Description
IL13	-0.909	0.0010	Anti-inflammatory; Th2 mediating
IL36B	-0.803	0.0003	Role in local inflammatory response at epithelial barriers
IL1R2	-0.770	0.0113	Decoy receptor for IL1B (proinflammatory) ligand
IL36RN	-0.642	0.0051	IL36 antagonist
IL36G	-0.627	0.0042	Role in local inflammatory response at epithelial barriers
IL27	-0.543	0.0108	Promotes Th1 response; expansion of naïve CD4+ T-cells
IL4I1	-0.421	0.0082	Induced by IL4 in B-cells; possible role in lysosomal antigen processing
ILF2	0.242	0.0111	Regulation of IL2 expression during T-cell activation
IL2RG	0.247	0.0004	Signaling component for IL2, -4, -7 and -21
ILF3	0.257	0.0062	Regulation of IL2 expression during T-cell activation
IL12RB1	0.408	0.0055	IL12 signal transduction
IL2RB	0.503	0.0025	IL2 receptor involved in T cell mediated immune response
IL21R	0.507	0.0018	Promotes proliferation of B and T lymphocytes and NK cells
IL27RA	0.527	0.0006	Regulation of Th1 immune response and innate immune response
IL7R	0.602	0.0011	Role in V(D)J recombination of lymphocytes



**Table 1.6.** Transcript Origin Analysis for leukocytes and leukocyte subsets<sup>1</sup>

CELL TYPE	<i>P</i> value	
	FD > 1.5	FD < 0.67
<b>PBMC</b>	<i>N</i> = 108	<i>N</i> = 149
<b>CD14 Monocytes</b>	0.998	0.004*
<b>BDCA4 Dendritic Cells</b>	0.999	0.999
<b>CD56 NK Cells</b>	< 0.0001*	0.018*
<b>CD4 T cells</b>	0.002	0.556
<b>CD8 T cells</b>	< 0.0001*	0.038*
<b>CD19 B cells</b>	< 0.0001*	0.038*
<b>Monocytes</b>	<i>N</i> = 76	<i>N</i> = 105
<b>CD14+16-</b>	0.992	0.0008*
<b>CD14+16+</b>	0.0072*	0.999
<b>B cells- naïve vs memory</b>	<i>N</i> = 194	<i>N</i> = 252
<b>Human_IgM+IgD+CD27+</b>	0.0254*	0.070
<b>Human_class switched</b>	0.999	0.655
<b>Human_IgM+IgD-CD27+</b>	0.058	< 0.0001*
<b>Human_IgM+IgD+CD27-</b>	0.006	0.998
<b>B cells- class switched</b>	<i>N</i> = 117	<i>N</i> = 151
<b>naïve</b>	0.427	0.738
<b>IgM</b>	0.339	0.819
<b>switched mem. B cells</b>	0.964	1
<b>plasma cells</b>	0.889	0.0006*

<sup>1</sup> FD = Fold Change; PBMC = peripheral blood mononuclear cell, N = Number of genes, \* = significant

**Table 1.7.** Summary of physiological pathways and processes affected, analytical support, relevant genes of interest and the implications for fitness in AR exposed bobcats.

Pathway/ process affected	Pattern	Methods			Candidate Genes	Implication for fitness
		Linear Model	TOA/TRA	WGCNA		
Innate Immunity	↓	↓ Inflammation	↓ total and naïve monocytes	↓ Inflammation	FCER1A, KLF5, KLF 4, GATA2, CPA3, HDC, MS4A2	Decreased defense against extracellular pathogens and allergens
Adaptive Immunity	↑↓	↑ T cell activation	↑ T & B cell activation; ↓ mature/ plasma B cells	↑ T cell signaling	CD3D, CD3G, CD3E	Immune activation leading to exhaustion; reduced specific antibody
Xenobiotic Metabolism and ER stress	↑	↑ drug metabolism genes	-	↑ ER stress	HYOU1, LAMP3, HSP90B1, XBP1, PDIA6	Increased cell death
Epithelial Integrity and wound healing	↓	↓ keratinocyte proliferation	-	↓ wound healing	SFN, IL36B, TGM1, MMP1, MMP10	Reduced epithelial integrity; Increased vulnerability to ectoparasites
Hemostasis and vitamin K	↓	↓ platelet aggregation	-	↓ coagulation	SERPINE2, TBXAS1	Coagulopathy; hemorrhaging

**Figure 1.1.** Map of the study area depicting sample locations for all 52 bobcats, whether or not the animal tested positive (+) or not positive (⊙) for ARs, and the general land use categories (urban, altered open, and natural).

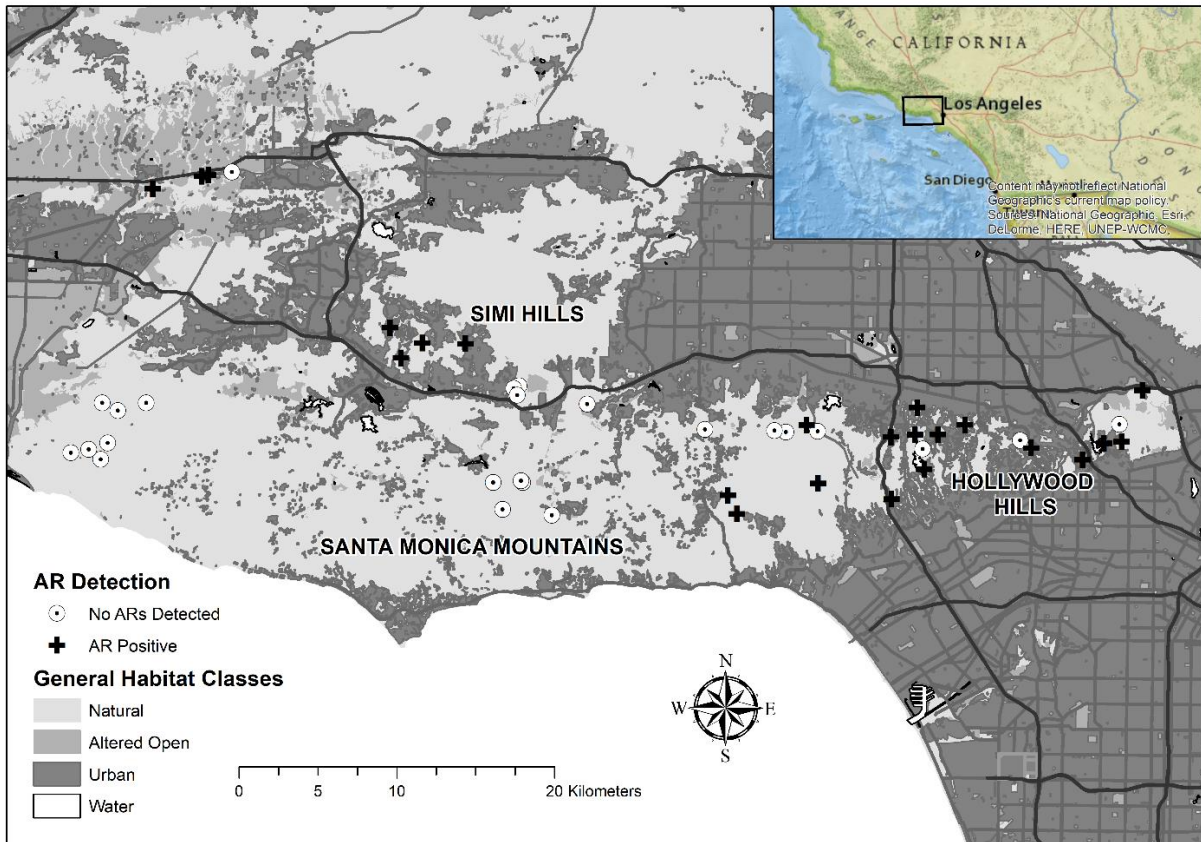


**Figure 1.2.** Workflow summary of genome wide analysis of anticoagulant rodenticide impacts on gene expression in bobcats.

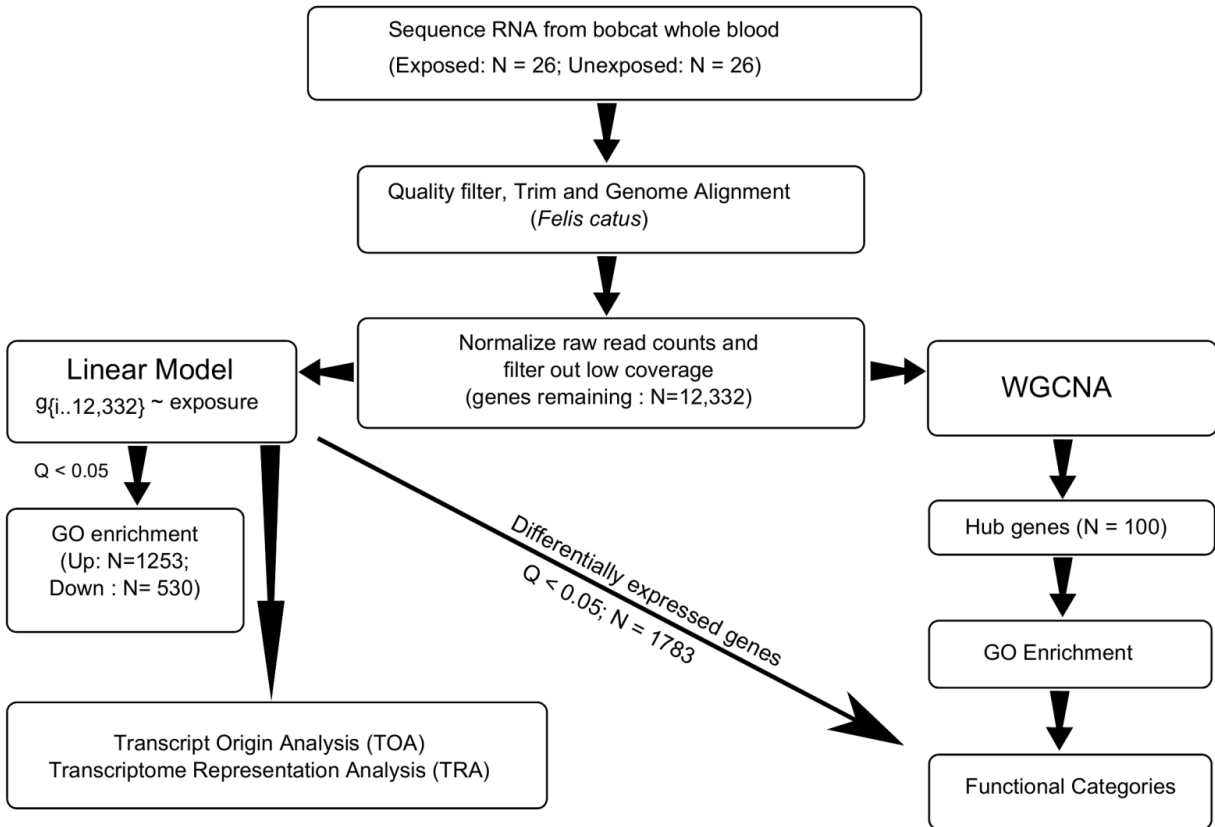


**Figure 1.3.** Linear regression of biological and technical factors on the principal components (PC) of the normalized read counts after regressing out technical factors significant on the first PC (sequencing platform, RIN, library preparation 5).

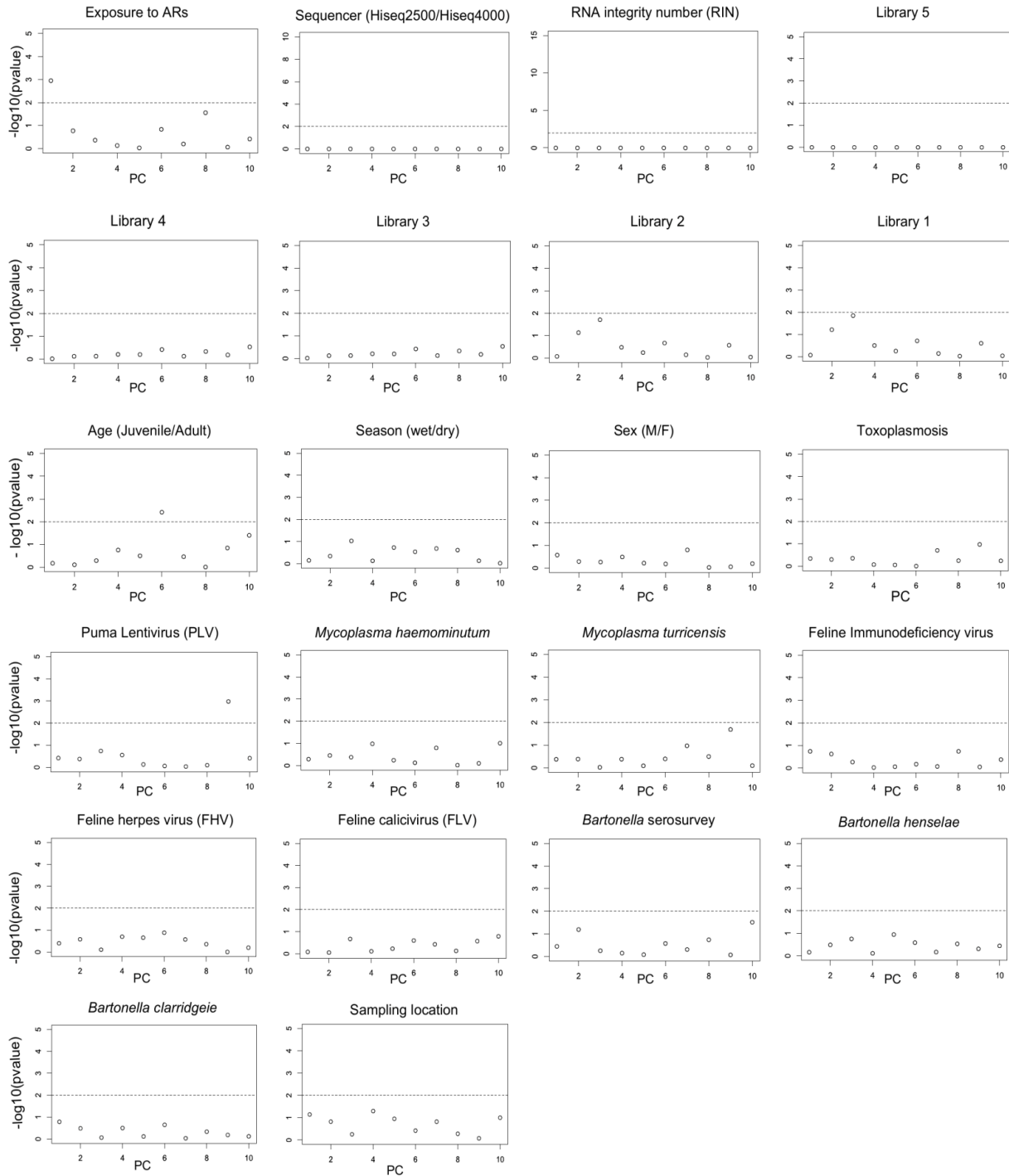


**Figure 1.4.** False discovery rate distribution after 1000 permutations compared to the p-value distribution of the linear modeling analyses.

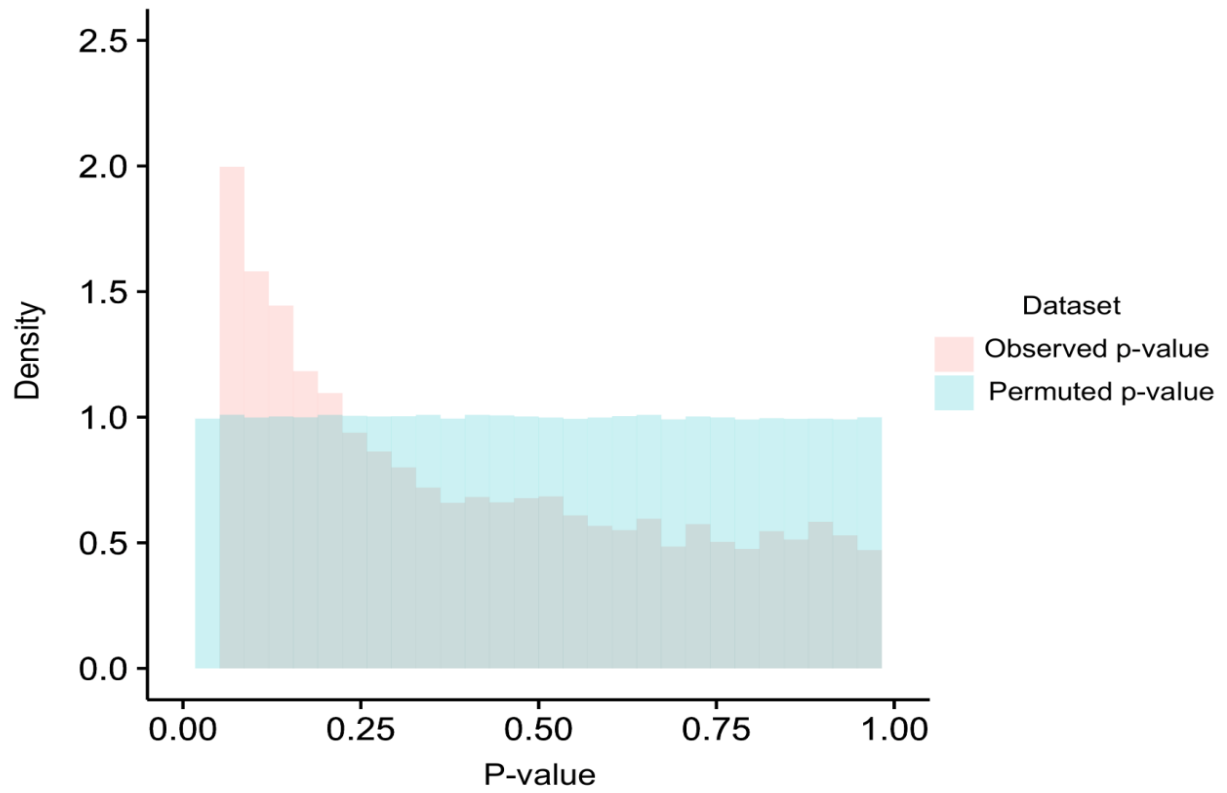


**Figure 1.5.** (A) Volcano plot depicting the  $-\log_{10}$  of the Q value against the  $\beta$  fold change for all 12,332 genes. Significant gene ( $Q < 0.05$ ) are highlighted in tan. Labeled genes are color coded by associated physiological process (depicted in B-C). Mean normalized counts of upregulated genes (B) and downregulated genes (C) shown for AR-negative (light color) and AR-positive (dark color) bobcats.

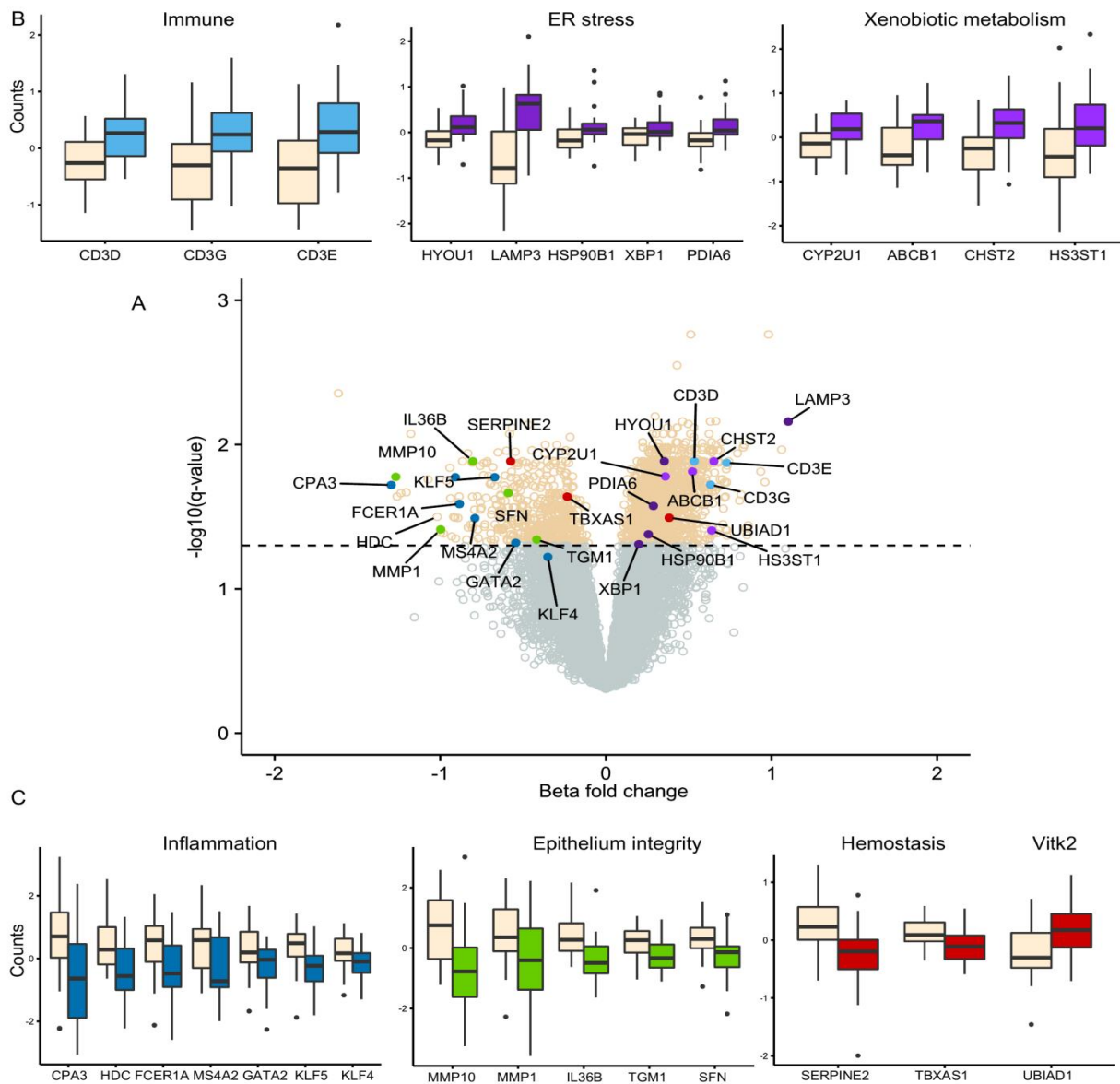


**Figure 1.6.** Treemap of the GO Biological Processes for the down (A) and up (B) regulated genes ( $Q < 0.05$ ). Box size correlates to the  $-\log_{10}$  p-value of the GO-term enrichment. Boxes with the same color represent higher level categories of processes. Main Abbreviations: (+) : positive regulation, (-) : negative regulation, macroph: macrophage. See Table S4, S5 for GO term details.

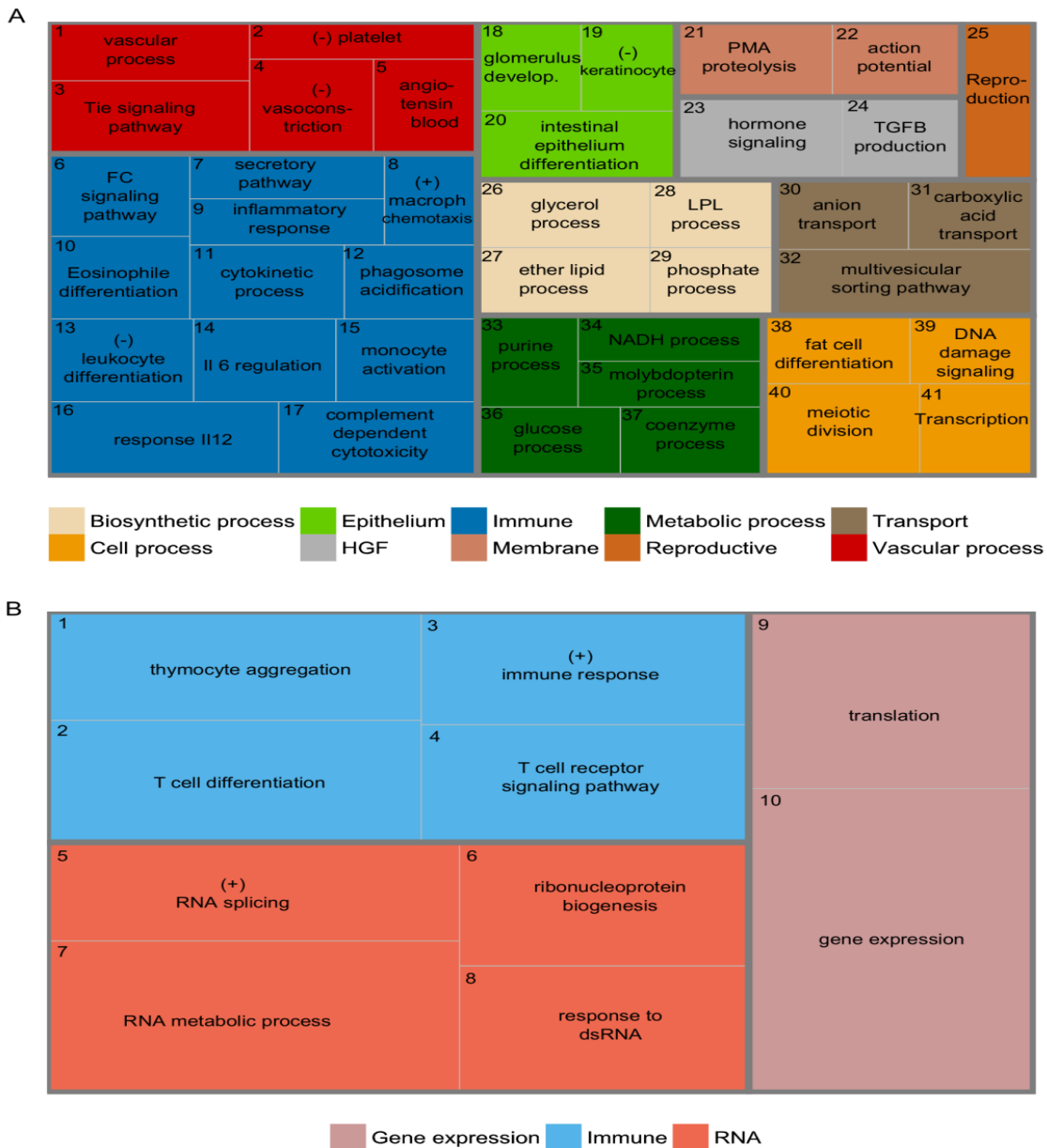




**Figure 1.7.** INCA index for each k-value after resampling. The number of clusters directly preceding the greatest negative slope (11) is assigned as the most probable number of clusters in the data.

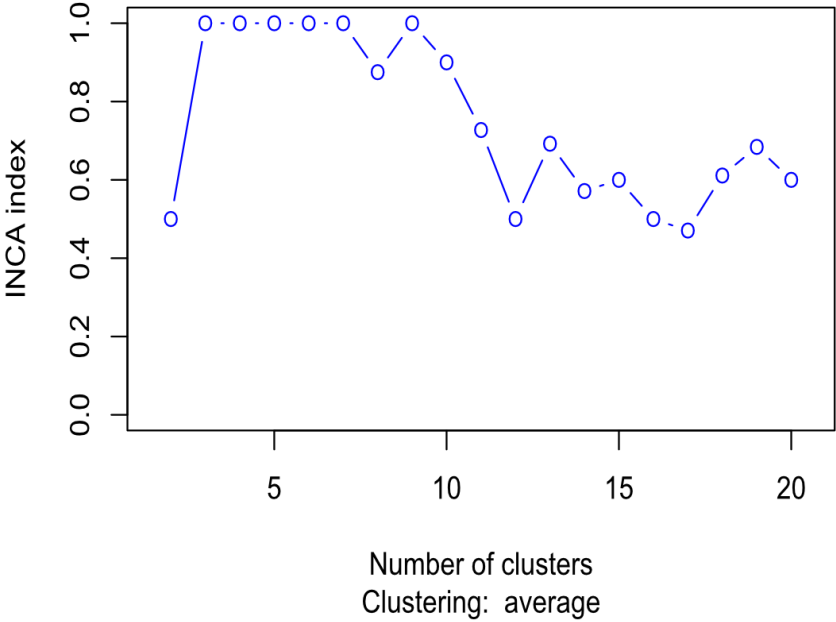
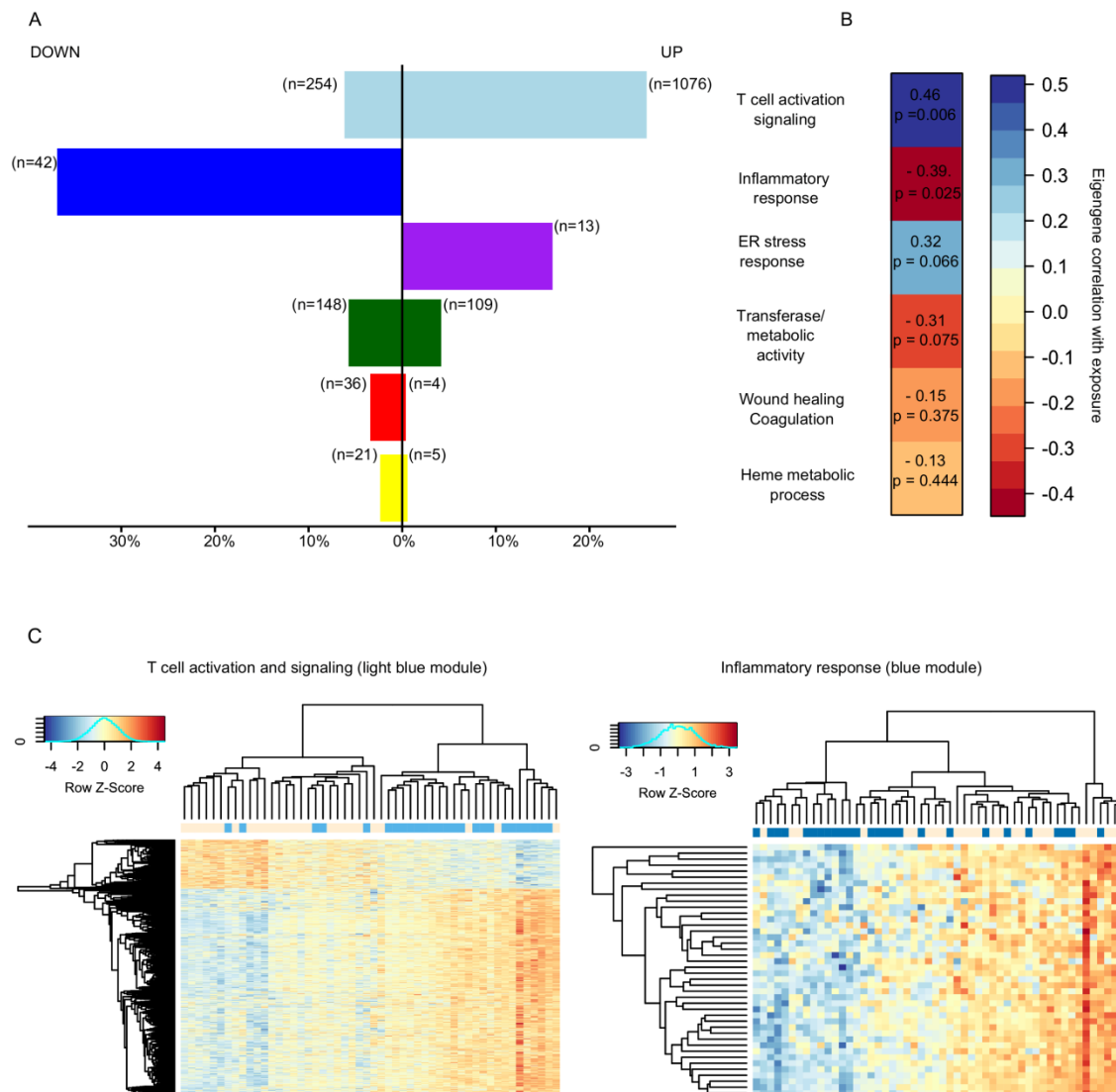


**Figure 1.8.** (A) Number of significant genes (from linear model) assigned to one of six functional categories (from WGCNA) as a proportion of total module size. (B) Correlation between AR exposure and WGCNA module eigengenes. (C) Heat maps displaying the expression profiles and dendrograms of AR-negative (light color) and AR-positive (dark color) bobcats for the “T cell signaling” and “inflammatory response” modules. Columns are individual bobcats and rows are individual genes.



## REFERENCES

1. Anders, S., Pyl, P.T. & Huber, W. (2014). HTSeq—a Python framework to work with high-throughput sequencing data. *Bioinformatics* p.btu638
2. Arlian, L.G., Morgan, M.S., Rapp, C.M. & Vyszynski-Moher, D.L. (1996). The development of protective immunity in canine scabies. *Vet. parasitol.* 62(1-2):133-142
3. Baert, K., Van Den Berge, K., Jansen, I., Gouwy, J., Croubels, S., Casaer, J. (2015). Secundaire intoxicatie bij het gebruik van rodenticiden - Analyse van leverresiduen bij bunzing en steenmarter. Brussels, Rapporten van het Instituut voor Natuur- en Bosonderzoek, INBO.R.2015.9435187.
4. Baldwin, D. H., Spromberg, J. A., Collier, T. K. & Scholz, N. L. (2009). A fish of many scales: extrapolating sublethal pesticide exposures to the productivity of wild salmon populations. *Ecol. Appl.* 19: 2004–2015
5. Bartos, M., Dao, S., Douk, D., Falzone, S., Gumerlock, E., Hoekstra, S., ... & Ward, J. (2011). Use of anticoagulant rodenticides in single-family neighborhoods along an urban-wildland interface in California. *Cities and the Environment (CATE)*, 4(1), 12.
6. Beier, P., Riley, S. P. D., & Sauvajot, R. M. (2010). Mountain lions (*Puma concolor*). *Urban carnivores: Ecology, conflict, and conservation*, 141-156.
7. Bevins, S.N., Carver, S., Boydston, E.E., Lyren, L.M., Alldredge, M., Logan, K.A., Riley, S.P., ... Salman, M. (2012). Three pathogens in sympatric populations of pumas, bobcats, and domestic cats: implications for infectious disease transmission. *PLoS One* 7(2): p.e31403
8. California Department of Pesticide Regulation (2013). Second generation anticoagulant rodenticide assessment Memorandum. [http://www.cdpr.ca.gov/docs/registration/reevaluation/chemicals/brodifacoum\\_final\\_assess.pdf](http://www.cdpr.ca.gov/docs/registration/reevaluation/chemicals/brodifacoum_final_assess.pdf)
9. Carver, S., Bevins, S.N., Lappin, M.R., Boydston, E.E., Lyren, L.M., Alldredge, M., Logan, ... Fisher, R.N. (2016). Pathogen exposure varies widely among sympatric populations of wild and domestic felids across the United States. *Ecol. App.* 26(2): 367-381
10. Chan, Y.C., Valenti, D., Mansfield, A.O. & Stansby, G. (2000). Warfarin induced skin necrosis. *Brit. J. Surg.* 87(3): 266-272
11. Christensen, T. K., Lassen, P., & Elmeros, M. (2012). High exposure rates of anticoagulant rodenticides in predatory bird species in intensively managed landscapes in Denmark. *Archives of environmental contamination and toxicology*, 63(3), 437-444.
12. Cimino-Reale, G., Ferrario, D., Casati, B., Brustio, R., Diodovich, C., Collotta, A., Vahter, M. & Gribaldo, L. (2008). Combined in utero and juvenile exposure of mice to arsenate

and atrazine in drinking water modulates gene expression and clonogenicity of myeloid progenitors. *Toxicol lett.* 180(1): 59-66

13. Cole, S.W., Hawkey, L.C., Arevalo, J.M. & Cacioppo, J.T. (2011). Transcript origin analysis identifies antigen-presenting cells as primary targets of socially regulated gene expression in leukocytes. *P. Natl. Acad. Sci. USA* 108(7):3080-3085
14. Court, M.H. (2013). Feline drug metabolism and disposition: pharmacokinetic evidence for species differences and molecular mechanisms. *Vet. Clin. North. Am. Small. Anim. Pract.* 43(5): 1039-1054
15. Cribb, A.E., Peyrou, M., Muruganandan, S. & Schneider, L. (2005). The endoplasmic reticulum in xenobiotic toxicity. *Drug metab. rev.* 37(3):405-442
16. Danziger, J. (2008). Vitamin K-dependent proteins, warfarin, and vascular calcification. *Clin. J. Am. Soc. Nephrol.* 3(5):1504-1510
17. Davis, A.P., Grondin, C.J., Johnson, R.J., Sciaky, D., King, B.L., McMorran, R., Wieggers, J., ... Mattingly, C.J. (2017). The Comparative Toxicogenomics Database: update 2017. *Nucleic Acids Res.* 45(D1):972-978
18. Dennis, Gillian C., and Brett D. Gartrell. "Nontarget mortality of New Zealand lesser short-tailed bats (*Mystacina tuberculata*) caused by diphacinone." *Journal of wildlife diseases* 51.1 (2015): 177-186.
19. Dong, K.K., Damaghi, N., Picart, S.D., Markova, N.G., Obayashi, K., Okano, Y., Masaki, H., ... Yarosh, D.B. (2008). UV-induced DNA damage initiates release of MMP-1 in human skin. *Exper. dermatol.* 17(12):1037-1044
20. Dorshkind, K. (1990). Regulation of hemopoiesis by bone marrow stromal cells and their products. *Annu. rev. immuno.* 8(1): 111-137
21. Eason, C.T., Murphy, E.C., Wright, G.R. & Spurr, E.B.( 2001). Assessment of risks of brodifacoum to non-target birds and mammals in New Zealand. *Ecotox* 11(1): 35-48
22. El Asmar, M.S., Naoum, J.J. & Arbid, E.J.(2014). Vitamin k dependent proteins and the role of vitamin k2 in the modulation of vascular calcification: a review. *Oman Med J.* 29(3): 172-177
23. Elias, P.M., Schmuth, M., Uchida, Y., Rice, R.H., Behne, M., Crumrine, D., Feingold, K.R., & Holleran, W.M.(2002) Basis for the permeability barrier abnormality in lamellar ichthyosis. *Exp Dermatol.* 11:258–256
24. Elmeros, M., Christensen, T.K., Lassen, P. (2011). Concentrations of anticoagulant rodenticides in stoats *Mustela erminea* and weasels *Mustela nivalis* from Denmark. *Sci. Total Environ.* 409, 2373–2378.

25. Esmon, C.T. (2005). The interactions between inflammation and coagulation. *Brit. j.haematol.* 131(4): 417-430
26. Faircloth, B.C., Glenn, T.C., & White, N.D. (2014). Fairclothlab Illumina library prep protocol.
27. Fedriani, J. M., Fuller, T. K., Sauvajot, R. M., & York, E. C. (2000). Competition and intraguild predation among three sympatric carnivores. *Oecologia*, 125(2), 258-270.
28. Ferland, G. (2012). Vitamin K and the nervous system: an overview of its actions. *Adv. Nutr.: An International Review Journal* 3(2): 204-212
29. Filser, J. (2008). Ecotoxicology and ecosystems: Relevance, restrictions, research needs. *Basic App. Ecol.* 9(4):333-336
30. Foster, A.M., Baliwag, J., Chen, C.S., Guzman, A.M., Stoll, S.W., Gudjonsson, J.E., Ward, N.L. & Johnston, A. (2014). IL-36 promotes myeloid cell infiltration, activation, and inflammatory activity in skin. *J. immunol.*, 192(12): 6053-6061
31. Fougere, F. & Fromenty, B. (2016). Role of endoplasmic reticulum stress in drug-induced toxicity. *Pharmacology res. persp.* 4(1)
32. Fournier-Chambrillon, C., Berny, P.J., Coiffier, O., Barbedienne, P., Dassé, B., Delas, G., Galineau, H., ... Fournier, P. (2004). Evidence of secondary poisoning of free-ranging riparian mustelids by anticoagulant rodenticides in France: implications for conservation of European mink (*Mustela lutreola*). *J. Wildlife Dis.* 40(4): 688-695
33. Freeman, B. D., Zehnbauser, B. A., McGrath, S., Borecki, I., & Buchman, T. G. (2000). Cytochrome P450 polymorphisms are associated with reduced warfarin dose. *Surgery* 128(2): 281-285
34. Gabriel MW, Woods LW, Poppenga R, Sweitzer RA, Thompson C, et al. (2012) Anticoagulant Rodenticides on our Public and Community Lands: Spatial Distribution of Exposure and Poisoning of a Rare Forest Carnivore. *PLoS ONE* 7(7): e40163. doi:10.1371/journal.pone.0040163
35. Gabriel, Mourad W., et al. (2015) "Patterns of natural and human-caused mortality factors of a rare forest carnivore, the fisher (*Pekania pennanti*) in California." *PloS one* 10.11 (2015): e0140640.
36. Gehrt, S. D., Riley, S. P., & Cypher, B. L. (Eds.). (2010). *Urban carnivores: ecology, conflict, and conservation*. JHU Press.

37. Gill, R.J. & Raine, N.E., (2014). Chronic impairment of bumblebee natural foraging behaviour induced by sublethal pesticide exposure. *Funct. Ecol.* 28(6):1459-1471
38. Hansen, K.D, Irizarry, R.A, & Wu, Z. (2012). Removing technical variability in RNA-seq data using conditional quantile normalization. *Biostatistics* 13(2): 204–216
39. Herman, M.L., Farasat, S., Steinbach, P.J., Wei, M.H., Toure, O., Fleckman, P., Blake, P., ... Toro, J.R. (2009). Transglutaminase-1 gene mutations in autosomal recessive congenital ichthyosis: Summary of mutations (including 23 novel) and modeling of TGase-1. *Hum. mut.* 30(4): 537-547
40. Hsu, A.P., Sampaio, E.P., Khan, J., Calvo, K.R., Lemieux, J.E., Patel, S.Y., Frucht, D.M., ... Olivier, K.N. (2011). Mutations in GATA2 are associated with the autosomal dominant and sporadic monocytopenia and mycobacterial infection (MonoMAC) syndrome. *Blood* 2653-2655
41. Huang, A.C., Elliott, J.E., Hindmarch, S., Lee, S.L., Maisonneuve, F., Bowes, V., Cheng, K.M. & Martin, K. (2016). Increased rodenticide exposure rate and risk of toxicosis in barn owls (*Tyto alba*). *Ecotox.* 25(6): 1061-1071
42. Ioannides, C. (2001) Xenobiotic Metabolism: An Overview, in *Enzyme Systems that Metabolise Drugs and Other Xenobiotics* (ed C. Ioannides), Wiley, Chichester: 1–32
43. Irigoien, I., Sierra, B., & Arenas, C. (2012). ICGE: an R package for detecting relevant clusters and atypical units in gene expression. *BMC bioinformatics*, 13(1), 30.
44. Ishikawa, E.T., Chang, K.H., Nayak, R., Olsson, H.A., Ficker, A.M., Dunn, S.K., Madhu, M.N., ... Cancelas, J.A. (2013). Klf5 controls bone marrow homing of stem cells and progenitors through Rab5-mediated  $\beta$ 1/ $\beta$ 2-integrin trafficking. *Nature Comm.* 4: 1660
45. Jiang, H., Jans, R., Xu, W., Rorke, E.A., Lin, C.Y., Chen, Y.W., Fang, S., ... Eckert, R.L. (2010). Type I transglutaminase accumulation in the endoplasmic reticulum may be an underlying cause of autosomal recessive congenital ichthyosis. *J. Biol. Chem.* 285(41):31634-31646
46. Karlgren M, Miura S, Ingelman-Sundberg M (2005). *Toxicol. Appl. Pharmacol.* 207(2):57-61
47. Kater, A.P., Peppelenbosch, M.P., Brandjes, D.P. & Lumbantobing, M. (2002). Dichotomal effect of the coumadin derivative warfarin on inflammatory signal transduction. *Clin. Diagn. Lab. Immunol.* 9(6): 1396-1397
48. Kawashima, H., Nakajima, Y., Matubara, Y., Nakanowatari, J., Fukuta, T., Mizuno, S., Takahashi, S., ... Nakamura, T. (1997). Effects of vitamin K2 (menatetrenone) on atherosclerosis and blood coagulation in hypercholesterolemic rabbits. *Jap. Journ.*

49. Kelly TR, Poppenga RH, Woods LA, et al (2014). Causes of mortality and unintentional poisoning in predatory and scavenging birds in California. *Veterinary Record Open*.1(1):e000028. doi:10.1136/vropen-2014-000028.
50. Kim, D., Perteau, G., Trapnell, C., Pimentel, H., Kelley, R. & Salzberg, S.L. (2013). TopHat2: accurate alignment of transcriptomes in the presence of insertions, deletions and gene fusions. *Genome Biol.* 14(4): R36
51. Krueger, F. (2015). Trim Galore!: A wrapper tool around Cutadapt and FastQC to consistently apply quality and adapter trimming to FastQ files
52. Langfelder, P. & Horvath, S. (2008). WGCNA: an R package for weighted correlation network analysis. *BMC bioinformatics* 9(1): 559
53. Langfelder P & Horvath S. (2012) Fast R Functions for Robust Correlations and Hierarchical Clustering. *J. statistic. soft*;46(11):i11.
54. Lee, J.S., Ward, W.O., Liu, J., Ren, H., Vallanat, B., Delker, D. & Corton, J.C. (2011). Hepatic xenobiotic metabolizing enzyme and transporter gene expression through the life stages of the mouse. *PloS one* 6(9): p.e24381
55. Li, J., Lin, J.C., Wang, H., Peterson, J.W., Furie, B.C., Furie, B., Booth, S.L., ... Rosenberg, P.A. (2003). Novel role of vitamin k in preventing oxidative injury to developing oligodendrocytes and neurons. *J. Neurosci.* 23(13): 5816-5826
56. Lynch, T. & Price, A. (2007). The effect of cytochrome P450 metabolism on drug response, interactions, and adverse effects. *Am Fam Physician* 76: 391-6
57. Malik, N.A. & Chughtai, A.S. (2003). The Effects of Lindane on Rabbit Hemopoietic System: An Experimental Study. *Int. J. Pathology* 1:39-41
58. McConnell, B.B., Ghaleb, A.M., Nandan, M.O. & Yang, V.W. (2007). The diverse functions of Krüppel-like factors 4 and 5 in epithelial biology and pathobiology. *Bioessays* 29(6):549-557
59. Medina, A., Ghaffari, A., Kilani, R.T. & Ghahary, A. (2007). The role of stratifin in fibroblast-keratinocyte interaction. *Mol. cell. biochem.* 305(1-2): 255-264
60. Meehan, B.M. & Beckwith, J. (2017). From Protein Folding to Blood Coagulation: Menaquinone as a Metabolic Link between Bacteria and Mammals. In *Vitamin K2-Vital for Health and Wellbeing*. InTech.
61. Mikhail, M.W. & Abdel-Hamid, Y.M. (2007). Effect of warfarin anticoagulant rodenticide on the blood cell counts of *Rattus norvegicus* and *Rattus rattus*. *J. Egypt. Soc. Paras.*

37(3):853-861

62. Miller, G.P., Jones, D.R., Sullivan, S.Z., Mazur, A., Owen, S.N., Mitchell, N.C., Radominska-Pandya, A. & Moran, J.H. (2009). Assessing cytochrome P450 and UDP-glucuronosyltransferase contributions to warfarin metabolism in humans. *Chem. res. toxicol.* 22(7): 1239-1245
63. Miyazawa, K. & Aizawa, S. (2004). Vitamin K2 improves the hematopoietic supportive functions of bone marrow stromal cells in vitro: a possible mechanism of improvement of cytopenia for refractory anemia in response to vitamin K2 therapy. *Stem cells dev.* 13(5): 449-451
64. Moriarty, J. G., Riley, S. P., Serieys, L. E., Sikich, J. A., Schoonmaker, C. M., & Poppenga, R. H. (2012). Exposure of wildlife to anticoagulant rodenticides at Santa Monica Mountains National Recreation Area: From mountain lions to rodents. In *25th Vertebrate Pest Conference (March 5-8 2012), Monterey, California, USA.*
65. Naisbitt, D.J., Farrell, J., Chamberlain, P.J., Hopkins, J.E., Berry, N.G., Pirmohamed, M. & Park, B.K. (2005). Characterization of the T-cell response in a patient with phenindione hypersensitivity. *J. Pharmacol. Exp. Ther.* 313(3): 1058-1065
66. Nakagawa, K., Hirota, Y., Sawada, N., Yuge, N., Watanabe, M., Uchino, Y., Okuda, N., ... Okano, T. (2010). Identification of UBIAD1 as a novel human menaquinone-4 biosynthetic enzyme. *Nature* 468(7320): 117-121
67. Noda, S., Asano, Y., Nishimura, S., Taniguchi, T., Fujiu, K., Manabe, I., Nakamura, K., ... Takahashi, T. (2014). Simultaneous downregulation of KLF5 and Fli1 is a key feature underlying systemic sclerosis. *Nat. Commun.* 5
68. Nogeire, T. M., Lawler, J. J., Schumaker, N. H., Cypher, B. L., & Phillips, S. E. (2015). Land Use as a driver of patterns of rodenticide exposure in modeled kit fox populations. *PLoS one*, 10(8), e0133351.
69. Nuutila, K., Siltanen, A., Peura, M., Bizik, J., Kaartinen, I., Kuokkanen, H., Nieminen, T., ... Kankuri, E. (2012). Human skin transcriptome during superficial cutaneous wound healing. *Wound Rep.Regen.* 20(6): 830-839
70. Opal, S.M. & Esmon, C.T. (2002). Bench-to-bedside review: functional relationships between coagulation and the innate immune response and their respective roles in the pathogenesis of sepsis. *Crit. Care* 7(1): 23
71. Orkin, S.H. & Zon, L.I. (2008). Hematopoiesis: an evolving paradigm for stem cell biology. *Cell* 132(4): 631-644
72. Ozcan, A., Ware, K., Calomeni, E., Nadasdy, T., Forbes, R., Satoskar, A.A., Nadasdy, G., ... Brodsky, S.V. (2012). 5/6 Nephrectomy as a Validated Rat Model Mimicking Human



Warfarin-Related Nephropathy. *American J.Nephrol* 35(4): 356–364

73. Park, C.S., Shen, Y., Lewis, A. & Lacorazza, H.D. (2016). Role of the reprogramming factor KLF4 in blood formation. *J. of Leukocyte Biol.* 99(5): 673-685
74. Pasquet, M., Bellanné-Chantelot, C., Tavitian, S., Prade, N., Beaupain, B., LaRochelle, O., Petit, A., ... Poirel, H.A. (2013). High frequency of GATA2 mutations in patients with mild chronic neutropenia evolving to MonoMac syndrome, myelodysplasia, and acute myeloid leukemia. *Blood* 121(5): 822-829.
75. Pence, D. B., Matthews III, F. D., & Windberg, L. A. (1982). Notoedric mange in the bobcat, *Felis rufus*, from south Texas. *Journal of Wildlife Diseases*, 18(1), 47-50.
76. Pence, D. B., Tewes, M. E., Shindle, D. B., & Dunn, D. M. (1995). Notoedric mange in an ocelot (*Felis pardalis*) from southern Texas. *Journal of Wildlife Diseases*, 31(4), 558-561.
77. Penner, L. R., & Parke, W. N. (1954). Notoedric mange in the bobcat, *Lynx rufus*. *Journal of Mammalogy*, 35(3), 458-458.
78. Petterino, C. & Paolo, B. (2001) Toxicology of various anticoagulant rodenticides in animals. *Vet. Hum. Toxicol.* 43(6):353–360
79. Popov, A., Belij, S., Subota, V., Zolotarevski, L., Mirkov, I., Kataranovski, D. & Kataranovski, M. (2013) Oral warfarin affects peripheral blood leukocyte IL-6 and TNF  $\alpha$  production in rats. *J. Immunotoxicol* 10(1): 17-24
80. Pourdeyhimi, N. & Bullard, Z. (2014). Warfarin-Induced Skin Necrosis. *Hosp. pharm.* 49(11): 1044-1048
81. Powell, N.D., Sloan, E.K., Bailey, M.T., Arevalo, J.M., Miller, G.E., Chen, E., Kobor, M.S., ... Cole, S.W. (2013). Social stress up-regulates inflammatory gene expression in the leukocyte transcriptome via  $\beta$ -adrenergic induction of myelopoiesis. *P. Natl. Acad. Sci. USA* 110(41):16574-16579
82. Rahman, M.M., Lecchi, C., Fraquelli, C., Sartorelli, P. & Ceciliani, F. (2010). Acute phase protein response in Alpine ibex with sarcoptic mange. *Vet. parasitol.* 168(3) : 293-298
83. Rattner, B.A., Lazarus, R.S., Elliott, J.E., Shore, R.F. & van den Brink, N.(2014). Adverse outcome pathway and risks of anticoagulant rodenticides to predatory wildlife. *Environ.l Sci Technol.* 48(15):.8433-8445
84. Reimand, J., Arak, T., Adler, P., Kolberg, L., Reisberg, S., Peterson, H. & Vilo, J. (2016). g: Profiler—a web server for functional interpretation of gene lists (2016 update). *Nucleic acids research*:gkw199
85. Riley, S. P.D., Sauvajot, R. M., Fuller, T. K., York, E. C., Kamradt, D. A., Bromley, C., &

Wayne, R. K. (2003). Effects of urbanization and habitat fragmentation on bobcats and coyotes in southern California. *Conservation Biology*; 17(2): 566-576.

86. Riley, S.P.D., Bromley, C., Poppenga, R.H., Uzal, F.A., Whited, L. & Sauvajot, R.M. (2007). Anticoagulant exposure and notoedric mange in bobcats and mountain lions in urban southern California. *J.Wildlife Manage* 71(6): 1874-1884
87. Riley, S. P. D., E. E. Boydston, K. R. Crooks, and L. M. Lyren. (2010). Bobcats (*Lynx rufus*). Pp 120-138 in S. D. Gehrt, S. P. D. Riley, and B. Cypher, editors, *Urban Carnivores: Ecology, Conflict, and Conservation*. Johns Hopkins University Press.
88. Riley, S. P. D., L. E. K. Serieys, and J. G. Moriarty. (2015). Infectious disease and contaminants in urban wildlife: unseen and often overlooked threats. In B. McCleery, C. Moorman, and N. Peterson, editors, *Urban Wildlife Science: Theory and Practice*. Elsevier Press.
89. Ritchie, M.E., Phipson, B., Wu, D., Hu, Y., Law, C.W., Shi, W. & Smyth, G.K. (2015). limma powers differential expression analyses for RNA-sequencing and microarray studies. *Nuc. acids res.* :gkv007
90. Robinson, MD, & Oshlack, A (2010). A scaling normalization method for differential expression analysis of RNA-seq data. *Genome Biol* 11: R25.
91. Russell, L.J., DiGiovanna, J.J., Rogers, G.R., Steinert, P.M., Hashem, N., Compton, J.G & Bale, S.J. (1995) Mutations in the gene for transglutaminase 1 in autosomal recessive lamellar ichthyosis. *Nat Genet* 9:279–83
92. Rutkevich, L.A. & Williams, D.B. (2012). Vitamin K epoxide reductase contributes to protein disulfide formation and redox homeostasis within the endoplasmic reticulum. *Mol. biol.cell* 23(11): 2017-2027
93. Sada, E., Abe, Y., Ohba, R., Tachikawa, Y., Nagasawa, E., Shiratsuchi, M. & Takayanagi, R. (2010). Vitamin K2 modulates differentiation and apoptosis of both myeloid and erythroid lineages. *Eur. j. haematol.* 85(6): 538-548
94. Sánchez-Barbudo, I.S., Camarero, P.R. & Mateo, R. (2012). Primary and secondary poisoning by anticoagulant rodenticides of non-target animals in Spain. *Sci Total Environ.* 420: 280-288
95. Santadino, M., Coviella, C. & Momo, F. (2014). Glyphosate sublethal effects on the population dynamics of the earthworm *Eisenia fetida* (Savigny, 1826). *Water Air Soil Poll.* 225(12): 2207
96. Sato, S., Fujimoto, M., Hasegawa, M. & Takehara, K. (2004). Altered blood B lymphocyte homeostasis in systemic sclerosis: expanded naive B cells and diminished but activated memory B cells. *Arthritis Rheum.* 50(6): 1918-1927

97. Schoeters, G.E.R., Vander Plaetse, F., Leppens, H. & Van Den Heuvel, R. (1995). Haemopoietic and osteogenic toxicity testing in vitro using murine bone marrow cultures. *Toxicol. in vitro* 9(4): 421-428
98. Segre, J.A., Bauer, C. & Fuchs, E. (1999). Klf4 is a transcription factor required for establishing the barrier function of the skin. *Nature genet.* 22(4) : 356-360
99. Serieys, L.E., Armenta, T.C., Moriarty, J.G., Boydston, E.E., Lyren, L.M., Poppenga, R.H., Crooks, K.R., ... Riley, S.P. (2015a). Anticoagulant rodenticides in urban bobcats: exposure, risk factors and potential effects based on a 16-year study. *Ecotoxicology* 24(4): 844-862
100. Serieys, L. E.K., A. Lea, J. P. Pollinger, S. P. D. Riley, and R. K. Wayne. (2015b). Disease and urbanization drive temporal and spatial genetic changes among bobcat populations in an urban, fragmented landscape. *Evolutionary Applications* 8:75-92.
101. Shahrin, N.H., Diakiw, S., Dent, L.A., Brown, A.L. & D'Andrea, R.J. (2016). Conditional knockout mice demonstrate function of Klf5 as a myeloid transcription factor. *Blood* 128(1): 55-59
102. Shearer, M.J. & Newman, P. (2008). Metabolism and cell biology of vitamin K. *Thromb Haemost* 100(4): 530-547
103. Shrestha, B., Reed, J.M., Starks, P.T., Kaufman, G.E., Goldstone, J.V., Roelke, M.E., O'Brien, S.J., ... Frank, L.G. (2011). Evolution of a major drug metabolizing enzyme defect in the domestic cat and other felidae: phylogenetic timing and the role of hypercarnivory. *PLoS One* 6(3): p.e18046
104. Suttie, J.W. (2009). Vitamin K in health and disease. CRC Press
105. Storey, J., Bass, A., Dabney, A. & Robinson, D. (2015). qvalue: Q-value estimation for false discovery rate control. R package version 2.6.0
106. Tabb, M.M., Sun, A., Zhou, C., Grün, F., Errandi, J., Romero, K., Pham, H., ... Forman, B.M. (2003). Vitamin K2 regulation of bone homeostasis is mediated by the steroid and xenobiotic receptor SXR. *Journ. Biolo. Chem.* 278(45): 43919-43927
107. Tetreault, M.P., Weinblatt, D., Shaverdashvili, K., Yang, Y. & Katz, J.P. (2016). KLF4 transcriptionally activates non-canonical WNT5A to control epithelial stratification. *Sci. Rep.* 6
108. van Beusekom, C.D. van (2015). Feline hepatic biotransformation and transport mechanisms. (Doctoral dissertation, Utrecht University)

109. Thacher, S.M & Rice, R.H (1985). Keratinocyte-specific transglutaminase of cultured human epidermal cells: relation to cross-linked envelope formation and terminal differentiation. *Cell*. 40:685–695
110. Tsai, F.Y. & Orkin, S.H. (1997). Transcription factor GATA-2 is required for proliferation/survival of early hematopoietic cells and mast cell formation, but not for erythroid and myeloid terminal differentiation. *Blood* 89(10): 3636-3643
111. Thompson, C., Sweitzer, R., Gabriel, M., Purcell, K., Barrett, R., & Poppenga, R. (2014). Impacts of rodenticide and insecticide toxicants from marijuana cultivation sites on fisher survival rates in the Sierra National Forest, California. *Conservation Letters*, 7(2), 91-102
112. Wadelius, M., Sörlin, K., Wallerman, O., Karlsson, J., Yue, Q.Y., Magnusson, P.K.E., Wadelius, C. & Melhus, H. (2004). Warfarin sensitivity related to CYP2C9, CYP3A5, ABCB1 (MDR1) and other factors. *Pharmacogenomics J.* 4(1): 40-48
113. Walton, S.F. (2010). The immunology of susceptibility and resistance to scabies. *Paras. immunol.* 32(8): 532-540
114. Ware, K.M., Feinstein, D.L., Rubinstein, I., Weinberg, G., Rovin, B.H., Hebert, L., Muni, N., ... Brodsky, S.V. (2015). Brodifacoum induces early hemoglobinuria and late hematuria in rats: novel rapid biomarkers of poisoning. *Am. j. nephrol.* 41(4-5): 392-399
115. Yates, A., Akanni, W., Amode, M.R., Barrell, D., Billis, K., Carvalho-Silva, D., Cummins, C., ... Girón, C.G. (2015). Ensembl 2016. *Nucl. acids res.:* gkv1157
116. Zanger, U.M. & Schwab, M. (2013). Cytochrome P450 enzymes in drug metabolism: regulation of gene expression, enzyme activities, and impact of genetic variation. *Pharmacol. therapeut.* 138(1):103-141
117. Zhang, B. & Horvath, S. (2005). A General Framework for Weighted Gene Co-Expression Network Analysis. *Stat. App. Gen. Mol. Biol.* 4(1)
118. Zhu, L., Qu, K., Xia, B., Sun, X. & Chen, B., (2016) Transcriptomic response to water accommodated fraction of crude oil exposure in the gill of Japanese flounder, *Paralichthys olivaceus*. *Marine pollution bulletin*, 106(1): 283-291

## CHAPTER 2

### Connectivity of mule deer (*Odocoileus hemionus*) populations in southern California: A genetic survey of a mobile ungulate in a highly fragmented landscape

#### ABSTRACT

Urbanization is a substantial force shaping the genetic and demographic structure of natural populations. As urban areas expand, so too do transportation corridors that facilitate human movement, such as highways. As such, genetic continuity in wild species is increasingly compromised and should be assessed for a multitude of highly mobile species that exhibit varying responses to human activity. While carnivores are well studied in general, common species such as mule deer are often overlooked. However, as the only wide-ranging ungulate species in Southern California, genetic and demographic impacts of urban development on mule deer is an important area of research. Here, we present the first assessment of genetic connectivity for mule deer focused explicitly at understanding mule deer response to habitat fragmentation in an increasingly urbanized landscape. We use a combination of genetic analyses and resource selection modeling to show that deer movement is limited by major highways and the associated urban development. Therefore, deer should be an important consideration during wildlife connectivity planning in urban landscapes.

#### INTRODUCTION

Habitat fragmentation is a primary threat to biodiversity worldwide (Brook et al 2008, Mora et al. 2011) that can have demographic and genetic consequences for natural populations. Populations may decline due to resource limitation alone (Herkert 1994, Newman et al. 2013).

However, genetic factors that reduce diversity such as impeded movement between habitat patches (Sato et al. 2014, Barr et al. 2015) and inbreeding (Bouzat et al. 1998, Johnson et al. 2010), can limit the adaptive potential for environmental change and have direct fitness effects through inbreeding depression (Eldridge et al. 1999, Reviewed in Keller and Waller 2002). Major roadways, in particular, can be a significant impediment to gene flow for a variety of species (Riley et al. 2004, Keller et al. 2003, Holderegger and Di Giulio 2010, Munshi-South and Karchenko 2010, Frantz et al. 2012), as well an important source of mortality for dispersing individuals. Cumulatively, such impacts can reduce population viability over time.

The genetic impacts of fragmentation on large mammalian carnivores have been of particular conservation focus (Riley et al., 2006; Benson et al., 2016; McClure et al. 2017) as these species are typified by life history traits that intersect poorly with human development (i.e. large home ranges, territorial, low population densities, high maternal investment for few offspring, human conflict, etc.). Comparatively fewer studies exist which examine the effects of habitat fragmentation on the genetics of large ungulates, especially in the context of urban development. Large ungulates possess intrinsically different life history traits than carnivores and so their genetic response to habitat fragmentation is potentially also different. Although multiple studies suggest that deer and other ungulates are highly sensitive to fragmentation and anthropogenic barriers (Wang and Schreiber 2001; Coulon 2004; Epp et al. 2005; Frantz et al. 2012; Ito et al., 2013); other studies show that deer can adapt to urban settings (Harveson et al. 2007; Blanchong et al. 2013) and that their social structure, specifically male biased dispersal and non-random mating across matrilineal groups, may buffer them from genetic impacts of fragmentation observed in other wide ranging species (Blanchong et al. 2013). Understanding factors influencing the genetic responses of large, highly mobile species is essential for the

maintenance of genetic variability in rapidly expanding urban landscapes, especially where large wild spaces are intersected by major highways.

Southern California serves as a unique model for assessing the effects of expanding urban development and highway infrastructure on wild populations. California is among the most heavily human populated of 25 biodiversity hot spot across the globe (Cincotta et al. 2000). The juxtaposition of dense human populations and large undeveloped natural areas is common across the state, particularly in the Los Angeles Basin. Vast networks of major highways are a defining characteristic of southern California landscapes, and studies demonstrate the genetic impacts of fragmentation due to roads on medium and large carnivores (Riley et al. 2006, Benson et al 2016; Ernest et al., 2014). For example, mountain lion (*Puma concolor*) populations in both the Santa Monica Mountains (Los Angeles and Ventura Counties) and the Santa Ana Mountains (Orange, San Bernadino and Riverside Counties) exhibited extremely low genetic diversity and high levels of inbreeding, attributable to the isolation imposed by major highways (Riley et al. 2014, Ernest et al. 2014). The long-term viability for both these mountain lion populations was predicted to be highly contingent on maintaining immigration from surrounding populations (Ernest et al. 2014, Benson et al. 2016). Similarly, definitive population structure was observed among both bobcats (*Lynx rufus*) and coyotes (*Canis latrans*) sampled across two major highways dividing the Santa Monica Mountains, which developed despite movement across highways by radio-collared individuals (Riley et al. 2006). For territorial species, highways may impose social barriers to reproduction for dispersing individuals because territory boundaries may coincide with freeways, thus limiting gene flow despite physical movement across them. High genetic differentiation was also observed between bobcats sampled in the Santa Ana Mountains and the San Joaquin Hills (Lee et. al. 2012).

Although carnivores have been studied extensively in Southern California (Riley et al. 2006; Ernest et al. 2014; Serieys et al. 2015), relatively little is known about the effects of habitat fragmentation on the movement, demography and population genetic structure of the only common native ungulate, the mule deer (*Odocoileus hemionus*). Camera trapping studies suggest that deer movement may be more restricted by highways than other species, as highway underpasses were used less frequently by deer than bobcats, coyotes, and raccoons (Ng et al. 2004; Alonso et al. 2014; Brown et al. *unpublished data*). Deer appear to have highly specific requirements, such as adequate height and suitable adjacent habitat, for utilizing underpasses (Ng et al. 2004) and thus may have fewer opportunities to cross highways. Therefore, deer may be more highly impacted by the isolating effects of highways, especially for populations that migrate seasonally (Nicholson et al. 1997). In contrast, deer are less restricted by territoriality than carnivores, and so may have more opportunities for reproduction, and hence gene flow, if they successfully traverse roadway barriers. Given the role large herbivores play in structuring ecosystems (Rooney et al. 2003, Hobbs 1993) and their importance as prey for large carnivores such as mountain lions (Benson et al. 2016), understanding factors that influence local population dynamics is important in conservation planning.

In this study, we conducted the first assessment of mule deer genetic connectivity in two major mountain regions in southern California. We considered a large geographic region with multiple areas of appropriate deer habitat bordering highways potentially enabling genetic continuity if deer can cross freeways. We predicted that if highways are an important barrier to gene flow, then population structure would align with highways and associated urban development that prevented or inhibited deer from successfully crossing. Finally, we expected lower pairwise relatedness between individuals in different subregions (8 in total in LA and



Orange County) than between individuals in the same subregion and differentiation habitat resistance when controlling for distance.

## MATERIALS AND METHODS

### *STUDY AREA*

The study area consisted of two main regions, LA (including areas in both Los Angeles and Ventura Counties) and OC (including areas in San Bernadino, Riverside and Orange Counties), that were further divided into eight subregions based on hills and mountains and major highways separating them (Figure 1a). Sampling locations (subregions) in the LA Region were Santa Monica Mountains (SMM), Santa Susana Mountains and Simi Hills (SIMI), Hollywood Hills including Griffith Park (HH) which are the eastern end of the Santa Monica Mountains Ecoregion, and Verdugo Mountains (VM) further east in Los Angeles County (Figure 1b). Major highways in this area were: I-405 separating HH from SMM; and CA-101 separating SMM and SIMI and running through the eastern part of HH. The Verdugo Mountains are separated from HH by I-5 and CA-134 and a highly developed urban matrix, and from the adjacent San Gabriel Mountains by I-210. The OC Region included the Santa Ana Mountains (SAM), Chino Hills and the Puente-Chino Hills Corridor (CH), Prado Basin (Prado), and San Joaquin Hills (SJH) (Figure 1c). Major highways between OC subregions were CA-91 separating SAM from CH and PB; CA-7 running between CH and PB; and I-5, separating SAM from SJH. In addition, there is a large urban matrix separating SAM from SJH, which was bordered to the other side by the Pacific Ocean. VM and HH were the closest parts of the LA Region to the OC Region, but were separated from CH by continuous urban matrix interspersed with small natural fragments and multiple highways, including I-10 and CA-60. The size and landscape context

varied across each of these subregions, as did the size, traffic volume and degree of associated urban development for each of the major highways (Figure 1; Table S3).

### *SAMPLE COLLECTION*

Scat and opportunistic tissue samples from animals found dead were collected from November 2014 –June 2015, by researchers, project partners, and volunteers. Collectors followed a protocol to prioritize collection from deer pellet piles that appeared fresh and consolidated, and hence most likely from a single individual. Site information, GPS coordinates, date, time, and initials of the collector were recorded for each sample. Samples were collected and placed in paper envelopes or suspended in 95% ethanol and transported to UCLA for processing. Scat samples were assigned a quality score based on appearance and received further processing, or were archived and stored in the lab. A total of 648 samples were collected, rated on a quality scale of 1-5 (Supplementary Info), stored, and catalogued. DNA extractions were performed on 538 of these samples. Those omitted did not meet the minimum quality requirements for DNA extraction ( $\geq 3$ ) based on suspected age of the samples or degradation due to prolonged environmental exposure. Here and throughout, the term ‘sample’ refers to the scat or tissue from which DNA was extracted whereas genotypes refer to the samples for which PCR amplifications were successful across a minimum of 10/15 loci. Finally, we refer to the genotypes included in the final analyses as individuals, because at this stage each genotype corresponds to an individual deer as genotypes of replicate samples were removed from these analyses.

### *DNA EXTRACTION AND PROCESSING*

DNA was extracted and PCR amplified as described by Mitelberg (2010). Briefly, 10-12 scat

pellets from a sample were suspended in 1x PBS solution (pH 7.4) and vortexed vigorously to suspend deer epithelial cells from the surface of the pellets. The PBS suspension was then centrifuged at high speed and excess PBS was pipetted off, for a final volume of ~1 mL. DNA was extracted from this suspension using the DNeasy Blood and Tissue kit (Qiagen) according to the manufacturer's protocol. Two elutions were performed on every sample. All sixteen markers were amplified in a single 5 uL reaction following the protocol designed by Mitelberg (2010). Specifically, 1.5 ul DNA were added to 2.5 ul Qiagen Hotstart taq mastermix (Qiagen Multiplex Kits, Qiagen, USA), 0.365 ul primer mix, 0.635 ul H<sub>2</sub>O. Thermocycling conditions were as follows: Initial denaturation at 95 C for 15 minutes, followed by 37 cycles of 72 C for 90s, 59 C for 60s and a final extension at 68 C for 30 minutes. PCR products were run on an ABI prism spectral analyzer and visualized in GeneMapper v 2.7.

To ensure accurate genotyping, all samples were genotyped from a minimum of three separate PCR reactions. Heterozygote calls per locus were made only when both alleles were observed at least twice and at least once as a single genotype across the three reactions. Homozygote calls required that the single allele be observed three times across the three reactions. If spurious alleles were observed in any of the reactions, a fourth PCR reaction was run. In some instances, additional reactions were run using the second DNA elution or at single markers to fill in missing loci. Only samples that were typed at greater than sixty-five percent (10/15) of the loci were kept for further analysis (n =328). All markers had greater than seventy five percent genotyping success across all 328 samples.

## *ANALYSIS*

### *Mapping, recaptures, and null alleles*

Collection locations of sufficiently genotyped samples were mapped from GPS coordinates recorded in the field and assigned a location attribute according to the subregion in which they were found. Genotypes originating from the same individual but different samples were identified using Cervus v3.0.7. Genotypes that matched at a minimum of eight loci with no mismatches were assumed to be from the same individual deer. If samples with matching genotypes were collected on different days or were separated by more than 2 km, we considered them recapture events of the individual. Otherwise, samples yielding genotypes from the same individual were considered redundant and one of the genotypes was removed from the dataset. Because samples in these cases were typically close spatially, we selected the most complete genotype. If the number of loci was equal, we selected the sample that was collected first. In the case of recaptures, the genotype corresponding to the first sample collected was retained for further analyses. Distances between each recapture were calculated in ArcMAP v10.3.1 and tabulated along with the time (in days) between sampling. Microsatellite data were checked using MICROCHECKER, with 10000 randomizations implemented for each run. We ran the program iteratively with various population groupings to assess the presence of null alleles.

#### *Genetic Diversity, Effective Population Size, and Population Structure*

We calculated summary statistics for genetic diversity for each subregion using GenAlEx v. 6.502 (Peakall and Smouse 2012). We calculated global and pairwise genetic distances, measured as Jost's  $D$  ( $D_{est}$ ), between subregions using the MMOD package v 1.3.2 in R. Jost's  $D$  is suggested to perform better with highly polymorphic loci than traditional measures of genetic distance such as  $F_{st}$  and  $G_{st}$ . The latter two measures can give paradoxical results under conditions of strong differentiation or high diversity, as they strictly employ measures of heterozygosity and do not account for the identity and distribution of individual alleles (Jost

2008). We then used `hclust` from the `stats` package in R to generate a dendrogram from the pairwise genetic distance matrix. We estimated significance for each pairwise subregion comparison separately from 10,000 permutations of genotype and subregion. We estimated effective population size ( $N_e$ ) for each subregion using `NeEstimator v 2.1` (Do et al. 2014) with the linkage disequilibrium method. We used a critical value for the minimum allele frequency of 0.02 and omitted 2 loci with greater than 15% missing data (H and L) to get a numeric estimate of  $N_e$  for each subregion.

We used two complementary approaches to assess the distribution of genetic diversity in mule deer with respect to major highways. First, population subdivision across the study area was assessed using a Bayesian clustering algorithm implemented in the program `STRUCTURE v. 2.3.4` (Pritchard et al. 2003). We ran a total of 15 iterations per  $K$  value, where  $K$  represents the number of distinct genetic clusters, and assessed the data across a range of  $K = 1-10$ . Proportional assignments were made for each individual to each of  $K$  clusters. We used an admixture model, and ran each simulation for  $10^6$  iterations of the MCMC and  $2 \times 10^5$  burn in. We ran `STRUCTURE` results through `Structure Harvester` (Dent et al. 2005) to determine optimal values for  $K$  based on the Evano method (Evano et al. 2005).

Second, we applied discriminant function analysis of principal components (DAPC) using the `poppr` package v2.7.1 in R. This method applies a k-means clustering algorithm to multilocus genetic data that has been transformed using principal components analysis. The clustering is followed by a multivariate discriminant function analysis, which minimizes within group variance and maximizes between group variance in the PCA transformed data. This method is less restricted by `Structure` assumptions of Hardy-Weinberg equilibrium and linkage disequilibrium and is useful when weak structure is likely (Jombart et al. 2010). We retained the

first 45 principal components, which explained approximately 90% of the data. For both STRUCTURE and DAPC, we calculated the evenness of genetic clusters in each subregion using the Shannon diversity index as a means to rank relative admixture, and conversely genetic isolation, across subregions (Shannon and Weaver, 1949).

### *Individual Pairwise Relatedness*

We used inverse measures of relatedness between individuals ( $1/r$ ) to test the hypothesis that highways form a barrier to gene flow in mule deer. We first calculated individual pairwise genetic distance in GenAIEx v. 6.502, which is calculated as the inverse of the relatedness between two samples based on genetic congruity. For clarity, we refer throughout to this measure of genetic distance as relatedness, so as not to be confused with subregion level genetic distance as measured by  $D_{est}$ . We then compared mean pairwise relatedness for within- versus between-subregion comparisons. We expected lower relatedness for between-subregion comparisons. Significance was determined by bootstrapping a null distribution of differences in mean individual pairwise relatedness. We subtracted the means of 500 randomly sampled individual pairwise relatedness values from the mean of 500 different randomly sampled pairwise relatedness values that were drawn from the entire dataset (both with-in and between subregions combined) with replacement. We constrained the data to include only pairwise comparisons that fell within the overlapping range of Euclidean distances for pairs sampled within versus between subregions.

Second, we ran generalized linear models to identify significant predictors of relatedness between individual deer. Our predictors included Euclidean distance, a habitat based path distance (explained in Section 2.4.4), and a measure of the effect of highways on deer movement (also explained in Section 2.4.4). For both approaches, we limited our data to include only

pairwise comparisons between individuals sampled in geographically adjacent subregions.

### *Least Cost Path Analysis*

We developed a cost surface using a suite of candidate landscape covariates and a competing model framework, Akaike Information Criterion (AIC) (Burnham and Anderson 2002). Candidate explanatory variables of mule deer occurrence included topographic features, current land-uses, and vegetative characteristics (Table S1). Topographic variables included a terrain ruggedness measure termed unevenness, a terrain view-shed index known as openness (Yokoyama et al. 2002), steepness of slope, general topographic curvature, and site exposure index. Unevenness was calculated using ArcGIS 10.3.1's Spatial Analyst extension (Esri 2014) focal cell statistics tool to measure the variation, using standard deviation, of general curvature for a 150 m radius. General curvature was also calculated using ArcGIS 10.3.1's Spatial Analyst extension (Esri 2014) using a 30-meter resolution digital elevation model (DEM) (U.S. Geological Survey 2009) projected into the Universal Transverse Mercator, North American Datum of 1983 coordinate system. This DEM was also used to calculate slope in degrees and site exposure index, a measure of the effects of solar radiation and aspect, using the Surface Gradient and Geomorphometric Modeling toolbox (Evans et al. 2014) in ArcGIS (Esri 2014). Land-use and vegetation characteristics were represented using a road density metric and the LANDFIRE program's datasets for existing vegetation and height (LANDFIRE 2011; Rollins 2009). USGS transportation road segment data for California were obtained from the National Map (<https://viewer.nationalmap.gov/> Accessed June 15, 2017) and line density of all classes of roads were calculated using an analysis window of 120 m.

Existing vegetation types (LF EVT) was represented using the attribute values of red, green, and blue, which are a color map with values scaled between 0-1, that represent particular

classes of vegetation types using the Society of American Foresters classification system. High values of red (LF EVT red) represent barren, developed, and disturbed areas of introduced herbaceous and grassland vegetation types. High values of green (LF EVT green) are associated with native grasslands, woodlands, forests, and riparian vegetation types. High values of blue (LF EVT blue) are associated with developed areas such as agricultural fields and irrigated nonnative vegetation. LANDFIRE's existing vegetation height classes were used to create a continuous measure of vegetation height by taking the median value of a class, resulting in a range of vegetation height between 0-37.5 m for the study area.

We compared six models using combinations of the candidate variables and selected the best model with the lowest AIC value (Table S2). This model was used to calculate the inverse of the dependent variable (the probability of mule deer presence), to describe the cost of movement and habitat connectivity for mule deer across the study area. A high probability of modeled mule deer use of the landscape, assumed to represent high quality habitat, is therefore assumed to have low cost of movement. In contrast, modeled low quality habitat is estimated to have a high cost of movement. Pairwise least cost paths, both the geographic distance and the accumulated cost of the least cost path, were calculated using a python tool (<https://www.arcgis.com/home/item.html?id=bbc7ae14015747318e06dda0f6c5bddf> Accessed July 12, 2017) for use in ArcGIS 10.1 (Esri 2012). We calculated the least cost path for individual pairwise comparisons that were analyzed for genetic distances, resulting in 33,930 path calculations. We measured the Euclidean distance (m), the distance of the least cost path (m), and the accumulated cost of the path (Etherington and Penelope Holland 2013).

To explore whether or not high traffic volume, multilane freeway systems are a feature on the landscape that are costly to mule deer movement, we created a second cost surface. Using 2014



Caltrans data on annual traffic volumes (<http://www.dot.ca.gov/hq/tsip/gis/datalibrary/> Accessed August 10, 2017), we scaled the observed 0-377,000 Ahead Annual Average Daily Traffic (AADT) volume between 0-1, by dividing by the maximum value. Using a spatial join to attribute the AADT point values to the Caltrans freeway line segments, we then created a cost raster based on the rescaled AADT, and added it to the habitat based cost surface. This resulted in a second cost surface, ranging in cost values 0-2, that results in the possibility of different least cost paths and higher accumulated cost paths for pairwise comparisons that are separated spatially by one or more freeway systems.

We used the difference between the freeway cost surface and the habitat cost surface to define a “freeway effect” which we subsequently used in a multivariate regression analysis (explained in Section 2.4.3)

## RESULTS

### *Mapping, recaptures, and null alleles*

Cervus identified a total of 265 unique genotypes representing individual deer. For 40 individual deer, up to five samples were collected. For most of these individuals (32 of 40), the additional samples were considered redundant because they were collected in close spatial proximity, on the same day, or both. This resulted in removal of 54 genotypes that were redundant. For the other 8 individuals, there was at least one additional sample designated as a recapture event, resulting in the removal of 9 genotypes. Of these recaptures, 2 were samples of the same individual collected on opposite sides of a highway: across CA-71 (between CH and PB) and across I-405 (between HH and SMM). Another recapture from CH was a sample found in a CA-71 underpass, thereby providing at least two instances of movement between Prado and CH. Direct evidence of movement between Prado and CH through genetic analysis and camera-

trap data (Alonso et al. 2014), as well as high relatedness to CH deer (7/9 deer sampled in Prado showed first order relationships with deer sampled in CH) prompted us to include Prado samples with CH in subsequent analysis as a single subregion. The average Euclidean distance between samples for the 8 recaptured individuals was 1.84 km (s.d. = 0.96 km; max = 3.02 km), while the average Euclidean distance between 54 redundant genotypes for 32 individuals was 0.094 km (s.d.= 0.16 km; max = 0.75 km).

Null allele analysis showed locus B to have a very high null allele frequency, as observed in previous studies of mule deer genetics in southern California (Pease et al. 2008; Mittelberg 2010), and was thus removed from the dataset for subsequent analyses. Several other loci exhibited evidence of null alleles depending on how subregions were grouped (data not shown), likely indicating genetic structure and not necessarily the presence of true null alleles. We therefore proceeded in the analysis with the fourteen remaining loci.

#### *Genetic diversity, effective population size, and population structure*

Observed heterozygosity averaged across all loci for each subregion ranged from  $0.49 \pm \text{SE}: 0.046 - 0.69 \pm \text{SE}: 0.072$  (Table 1). The lowest observed heterozygosity was in SMM followed by SIMI. All loci were polymorphic in all populations except for SJH for which locus L was monomorphic. The fixation index was lowest in SAM (0.012, SE 0.032) with the exceptions of SJH and VM, where observed heterozygosity exceeded expected heterozygosity and hence the fixation indices in these subregions were negative. The fixation index was highest in SIMI (0.135, SE 0.047). The largest effective population sizes ( $N_e$ ) were observed in SAM ( $N_e = 548.2$ ; 95% CI = 89.1-inf) followed by VM ( $N_e = 84$ ; 95% CI = 6.6-inf). The smallest effective population size was observed in SJH ( $N_e = 16.8$ ; 95% CI = 10.5-30.8) followed by HH (21.4; 95% CI 14.1-36) (Table 1).

Global  $D_{est}$  was 0.072 (95 % CI = 0.057 - 0.092). Measures of pairwise  $D_{est}$  were significant at  $p \leq 0.005$  after permutation between all subregions, and ranged from 0.017, between SMM and SIMI, to 0.138, between SJH and SMM (Table 2). The highest average pairwise  $D_{est}$  among subregions, 0.11, was observed in SJH, followed by HH; the lowest average  $D_{est}$  of 0.05 was observed in SAM. Hierarchical clustering of subregion pairwise  $D_{est}$  showed VM clustering as sister group to CH/SAM, with all three subregions clustering as sister to the LA Region, and SJH forming an outgroup. Within the LA Region, SIMI and SAM cluster together with HH as an outgroup (Figure 2).

STRUCTURE analysis on all unique individuals ( $n = 265$ ) indicated that  $K = 5$  was the optimal number of genetic clusters (Figure 2) while DAPC analysis suggested that  $K = 6$  was optimal. Admixture was present in all subregions in both analyses; however, average proportional assignments to each cluster varied by subregion. The highest posterior assignments to a single cluster ranged from 32-65 percent and from 27-64 percent, in STRUCTURE and DAPC, respectively (Table 3). In both analyses, the highest assignment to a single cluster occurred in SJH. Evenness of cluster assignments also varied by subregion and by analysis. In both analyses, SJH showed the lowest evenness.

#### Individual pairwise relatedness within and between subregions

The mean inverse of individual pairwise relatedness between adjacent subregions was 16.54 (95% CI = 16.18-16.83) and within subregions was 15.93 (95% CI = 15.59-16.22), for a small yet significant difference of 0.608 ( $p = 0.007$ ) across comparable Euclidean distances, suggesting that highway barriers do contribute to increased differentiation. The best fit model for predicting pairwise relatedness ( $\Delta AIC = 202$ ) relative to the null model included the distance of the least cost path based on habitat alone and a binary variable indicating whether the samples

were collected across a major roadway or highway (Table 4). Additionally, when controlling for Euclidean distance, pairwise genetic distance was positively and significantly correlated with the accumulated cost of traversing the habitat along the least cost path ( $F = 5$ ;  $p = 0.045$ ; Figure 3).

### *Least Cost Path Analysis*

Several topographic features, vegetative, and anthropogenic factors were found to be associated with the likelihood mule deer are found on the landscape and were used to create a resistance surface (Figure 4). Terrain unevenness and openness both had strong quadratic relationships suggesting a preference for mid-range values within the modeled region. LANDFIRE's green attribute associated with several native vegetation types had a positive relationship, while steep slopes, high road densities, and non-native vegetation (LANDFIRES's red and blue values) resulted in a negative response (Figure 5A). Some responses were modified by an interaction term (Figure 5B). The response became negative to site exposure index (SEI) on steeper slopes (high values of SEI are southern aspects receiving more solar input), and to LANDFIRE's red values in areas of higher road densities. Though the response to LANDFIRE's green metric was positive, the response was even stronger at higher road densities.

## DISCUSSION

Roads and urban development can pose a major dispersal barrier for a variety of species, particularly large and highly mobile species, including ungulates. Desert bighorn sheep in California, for example, exhibited drastic reductions in genetic diversity and gene flow over a short time period, due largely to the impact of roads (Epps et al., 2005). While deer are comparatively well-adapted to human development, deer are nonetheless shown to avoid human development (Nicholson et al., 1997), suggesting that urban development may impose barriers to

movement. The aim of this study was to determine if major highways and the surrounding urban matrix act as significant dispersal barriers for mule deer in southern California.

Our resource selection models showed a strong negative response of mule deer presence with road density and developed areas. Accordingly, we found some evidence of genetic structure among subregions as well as a subtle but apparent effect of highways on individual pairwise genetic distance. Interestingly, however, our resource selection models also show an interaction between road density and landcover, such that the positive response to high quality vegetation becomes stronger with higher road density, suggesting that deer respond differently to roads depending on abutting habitat. Specifically, we found higher genetic distances within and between subregions that had high associated levels of habitat, mostly due to urban development, when controlling for distance. Therefore, not all highways and landscape configurations are equal in the context of wildlife movement. Our results highlight the need to account for both behavioral differences in focal species and the specific features of natural habitat, and highway and urban infrastructure barriers when planning for habitat connectivity in fragmented landscapes.

Broadly, mule deer in California partition into five distinct genetic clusters based primarily on ecological factors related to climate and elevation (Pease et al., 2010). This same study suggested that deer within our study area belong to a single genetic cluster, yet our results reveal more subtle patterns of genetic structure at both regional and local scales. Regionally, mule deer in our study area appear to cluster into three main groups: 1) all the LA Region (SIMI, SMM, and HH); 2) CH, SAM, and VM; and 3) only SJH (Figure 2). However, in both k-means clustering approaches, no single cluster was exclusive to any single region or subregion; and all clusters were represented in all or nearly all subregions (Table 3). The latter evidence supports

high levels of historic connectivity between subregions likely facilitated by the geography of the area (i.e. movement along mountainous corridors) where the resulting distribution of genetic diversity was driven largely by isolation by distance. This contrasts with our measures of genetic differentiation between subregions, all of which were statistically significant and substantially higher than has been observed in other ungulate populations, including white tailed deer (*Odocoileus virginianus*), across far greater distances exceeding 1000 km (Cullingham et al., 2011; Mager et al., 2013).

At more local scales, several interesting patterns emerged. First, although VM is geographically more proximate to the LA Region and to HH specifically (Figure 1), both pairwise  $D_{est}$  and STRUCTURE results suggested that deer sampled in VM were more genetically similar to OC Region deer (Figure 2; Table 2), specifically CH and SAM. Further, although represented by only 8 individuals, VM had the second highest estimated  $N_e$  and the highest observed heterozygosity, suggesting connectivity with a larger area of suitable deer habitat. In this case the connectivity was likely with the San Gabriel Mountains which are substantially larger than SAM or SMM and for which there is a large underpass across CA-210 that is well buffered by natural vegetation and limited human development. In contrast, the matrix between VM and HH is highly developed and requires traversing a wide intersection of two major highways (CA-134 and I-5). Future work in VM that includes sampling deer in the San Gabriel Mountains and more data on the historical connection between them might show the connectivity requirements for a relatively small mountain range to support such a high  $N_e$ .

Our results also highlight an important management unit for mule deer in Southern California. Deer from SJH showed the highest genetic differentiation from other subregions, as well as the lowest effective population size. Specifically, average pairwise  $D_{est}$  between SJH and

all other subregions was over 60 percent greater than the next highest average  $D_{est}$  (observed in HH), and is comparable to values observed for populations of white-tailed deer separated by the Rocky Mountains in Canada (Cullingham et al. 2011). Further, in both STRUCTURE and DAPC analyses, SJH had the highest incidence of assignment to a single cluster and hence the lowest evenness in genetic diversity of all subregions considered (Table 3). A vast urban matrix and major highway (I-5) separate SJH and SAM subregions, and similar genetic results for this area have been found in bobcats (Lee et al. 2012, Ruell et al. 2012). Mountain lions had existed in the area historically, but once isolated by the freeways, soon suffered extinction, which is caution to the effects of small population sizes for large species in the SJH.

The pattern for SJH in the OC Region is paralleled to a lesser magnitude by HH in the LA Region, with HH having the second highest average  $D_{est}$  and the third lowest evenness in both STRUCTURE and DAPC analyses (Table 3). HH is separated from SMM by I-405, one of the busiest highways in the country that spans 12 lanes between these subregions. Ongoing camera monitoring of four potential crossings along this highway segment indeed demonstrated that deer are less likely to utilize crossings than other species, although some movement of deer under I-405 was observed at a single underpass (NPS- *personal communication*).

The lowest divergence was observed between CH and SAM and SMM and SIMI in the OC and LA Regions, respectively, reflecting either higher rates of gene flow between the subregions or slower rates of genetic drift due to population size. Although CH and SAM showed low levels of genetic distance ( $D_{est}$ ) across CA-91, the presence of highways and intervening development may later show genetic impacts. The expansion of CA-91 is relatively recent (27 % increase in ADDT between 1993 to 2014; Table S3), but monitoring of several underpasses along CA-91 by remotely-triggered cameras showed only limited use by deer of a

single underpass connecting CH to SAM from (Boydston- *unpublished data*). Low differentiation between SIMI and SMM may also result from higher effective population sizes as well as the presence of at least one potential movement corridor located at Liberty Canyon in Calabasas, CA and low relative traffic volumes along US-101. The Liberty Canyon underpass has dimensions adequate for deer to use and is characterized by high levels of adjacent natural habitat, as has been shown to be preferred by deer (Ng et al. 2004). It is also the proposed location for a wildlife crossing as part of the CalTrans initiative to improve habitat connectivity for mountain lions and other wildlife in this study area. Similarly, CA-71 does not appear to inhibit deer movements, given that several recaptured individuals were identified directly within underpasses and on either side of this highway. This highway has several large underpasses, some built specifically as wildlife crossings (Alonso et al., 2014), thus highlighting the benefits of planning for wildlife connectivity during urban infrastructure expansion.

Collectively, our results suggest that I-405 and I-5 and the associated urban matrix typical of major highway systems pose the greatest barrier to gene flow for mule deer. Although we did not detect reduced gene flow across CA-91 or CA-101, the patterns of increasing volume of traffic and expanding development occurring in these systems suggests these highways may become problematic for genetic exchange in mule deer in the future.

## CONCLUSION

As mule deer are not territorial, individuals that disperse successfully across highways crossing may be more likely to contribute genetically to the adjoining population. However, as human populations continue to expand in urban areas with associated increase in transportation needs and infrastructure, effective migration may decrease. Our findings underscore the continued relevancy of wildlife crossings and connectivity across urban matrices to land and



wildlife managers in areas where connectivity is increasingly limited by continued urbanization. Additionally, our study highlights the paucity of data available for understanding and evaluating mule deer movements across these landscapes. Results of this study suggest that future work should address seasonal movements, survival and reproductive success linked to habitat quality and urban development for mule deer and other highly mobile species for which urban associated barriers may impose direct costs in terms of demographic and genetic viability.

TABLE AND FIGURES

**Table 2.1.** Annual Average Daily Traffic volumes (cars per day) in 1993 and 2014 for 5 major highways intersecting subregions of natural habitat in the study area

Route	AADT (1993)	AADT (2014)	% increase
CA-71	34437	82900	1.41
CA-91	202166	256114	0.27
US-101	132653	155192	0.17
I-405	272200	276200	0.01
I-5	196647	282944	0.44

**Table 2.2.** Logistic regression model structure for estimating mule deer habitat quality. The inverse of this model was used to create a cost surface for comparing pair-wise least cost paths and accumulated cost paths to pairwise genetic distance.

Type	Variable	DF	Adj. Deviance	Coefficient	SE	Chi-Square	P-Value
Topographic	Constant	14	382.20	-20.2900	8.570	382.20	<0.001
	Unevenness	1	68.61	3.5470	0.443	68.61	<0.001
	Unevenness <sup>2</sup>	1	43.48	-1.1600	0.179	43.48	<0.001
	Openness	1	4.96	0.4700	0.213	4.96	0.026
	Openness <sup>2</sup>	1	4.90	-0.0029	0.001	4.90	0.027
	Site Exposure Index	1	10.28	0.0405	0.013	10.28	0.001
	Slope (degrees)	1	0.07	0.0071	0.026	0.07	0.785
	Slope <sup>2</sup>	1	12.34	-0.0025	0.001	12.34	<0.001
	Site Exposure Index x Slope	1	10.15	-0.0017	0.001	10.15	0.001
	Anthropogenic & Vegetative	Road Density	1	1.38	0.0513	0.044	1.38
LF EVT Green		1	0.80	0.3070	0.344	0.80	0.372
LF EVT Red		1	0.80	0.2700	0.302	0.80	0.370
LF EVT Blue		1	7.58	-0.8040	0.294	7.58	0.006
Road Density x LF EVT Green		1	31.19	0.2106	0.040	31.19	<0.001
Road Density x LF EVT Red		1	23.23	-0.2674	0.058	23.23	<0.001
Road Density x LF EVT Blue		1	23.23	-0.2674	0.058	23.23	<0.001

x LANDFIRE  
EVT Red

Error	1643	1916.27
Total	1657	2298.48

**Table 2.3.** Competing model results using Akaike Information Criterion (AIC) and two model fit statistics, adjusted  $R^2$ , and Area under the Receiver Operating Curve (AUC).

Model Description <sup>a</sup>	Deviance	k	AIC	$\Delta$ AIC	$R^2_{adj}$	AUC
Unevenness <sup>2</sup> , Openness <sup>2</sup> , Slope <sup>2</sup> , Site Exposure Index x Slope, Road Density x LF EVT Green, Road Density x LF EVT Red, LF EVT Blue	1916.27	15	1946.27	0.00	16.02%	75.2
Unevenness <sup>2</sup> , Openness <sup>2</sup> , Slope <sup>2</sup> , Site Exposure Index x Slope, Road Density x LF EVT Green, Road Density x LF EVT Red, LF EVT Blue x LF EVT Height	1937.12	16	1969.12	22.85	15.07%	74.4
Unevenness <sup>2</sup> , Openness <sup>2</sup> , Slope <sup>2</sup> , Site Exposure Index x Slope, Road Density x LF EVT Green, Road Density x LF EVT Red, LF EVT Blue, LF EVT Height <sup>2</sup>	1937.83	16	1969.83	23.56	15.04%	74.4
Unevenness <sup>2</sup> , Openness <sup>2</sup> , Slope <sup>2</sup> , Site Exposure Index x Slope, Road Density, LF EVT Green, LF EVT Red, LF EVT Blue, LF EVT Height	1951.20	14	1979.20	32.93	14.54%	74.2
Unevenness <sup>2</sup> , Openness <sup>2</sup> , Slope <sup>2</sup> , Curvature <sup>2</sup> , Site Exposure Index <sup>2</sup> , Road Density, LF EVT Green, LF EVT Red, LF EVT Blue, LF EVT Height	1955.95	16	1987.95	41.68	14.25%	74.2
Unevenness, Openness, Slope, Curvature, Site Exposure Index, Road Density, LF EVT Green, LF EVT Red, LF EVT Blue, LF EVT Height	2110.76	11	2132.76	186.49	7.73%	69.5

**Table 2.4.** Effective population size, observed heterozygosity and expected heterozygosity across 14 loci for each subregion.

<b>Subregion (N)</b>	<b>Ne (95% CI)</b>	<b>Ho (SE)</b>	<b>He (SE)</b>
CH (73)	69.6 (48-112.6)	0.51 (0.06)	0.06 (0.52)
SAM (45)	inf (235.9-inf)	0.55 (0.06)	0.06 (0.55)
SJH (24)	16.6 (10.4-29.9)	0.55 (0.06)	0.06 (0.54)
VM (8)	79 (6.9-inf)	0.69 (0.07)	0.07 (0.55)
HH (30)	22.9 (15.2-38.8)	0.54 (0.05)	0.05 (0.58)
SMM (52)	63.9 (40.5-124.8)	0.49 (0.05)	0.05 (0.55)
SIMI (33)	32.9 (20.9-62.3)	0.5 (0.06)	0.06 (0.56)

\* Ne = Effective population size; Ho = observed heterozygosity; He = expected heterozygosity

**Table 2.5.** Pairwise and average genetic distances ( $D_{est}$ ) between 7 mountainous subregions separated by major highways in Southern California.

<b>Subregion</b>	<b>CH</b>	<b>SAM</b>	<b>SJH</b>	<b>VM</b>	<b>HH</b>	<b>SMM</b>	<b>SIMI</b>	<b>AVERAGE</b>
<b>CH</b>	-	0.0001	***	0.0028	***	***	***	0.065
<b>SAM</b>	0.02	-	***	0.0008	***	***	***	0.05
<b>SJH</b>	0.13	0.07	-	0.0005	***	***	***	0.11
<b>VM</b>	0.05	0.05	0.09	-	0.0004	0.0001	0.0061	0.067
<b>HH</b>	0.07	0.05	0.13	0.07	-	***	***	0.072
<b>SMM</b>	0.06	0.06	0.14	0.08	0.05	-	0.005	0.068
<b>SIMI</b>	0.06	0.05	0.12	0.06	0.06	0.02	-	0.062

£ Below diagonal: Genetic distance ( $D_{est}$ ); Above diagonal: p-value

\*\*\* Indicates  $p < 0.0001$  after 10000 bootstrap iterations

**Table 2.6.** Average proportional assignment of individuals to K clusters and relative evenness across clusters by subregion for both STRUCTURE (A) and DAPC (B)

A. <u>STRUCTURE (K = 5)</u>							
	Clust 1	Clust 2	Clust 3	Clust 4	Clust 5	-	Rank H'/H <sub>max</sub>
CH	<b>0.41</b>	0.09	0.36	0.06	0.07	-	4
SAM	0.21	0.24	<b>0.32</b>	0.08	0.15	-	2
SJH	0.07	<b>0.65</b>	0.12	0.08	0.07	-	7
VM	0.13	0.21	<b>0.33</b>	0.18	0.15	-	1
HH	0.09	0.08	0.12	0.15	<b>0.55</b>	-	5
SMM	0.11	0.09	0.10	<b>0.44</b>	0.26	-	3
SIMI	0.11	0.07	0.07	<b>0.58</b>	0.17	-	6

B. <u>DAPC (K = 6)</u>							
	Clust 1	Clust 2	Clust 3	Clust 4	Clust 5	Clust 6	Rank H'/H <sub>max</sub>
CH	<b>0.36</b>	0.20	0.02	0.06	0.28	0.08	3
SAM	0.23	<b>0.27</b>	0.11	0.10	0.23	0.07	1
SJH	0.03	0.02	<b>0.64</b>	0.23	0.05	0.03	7
VM	0.17	0.03	0.12	<b>0.60</b>	0.04	0.04	6
HH	0.09	0.03	0.00	<b>0.51</b>	0.15	0.22	5
SMM	0.04	0.04	0.02	0.16	0.33	<b>0.41</b>	4
SIMI	0.06	0.11	0.07	0.18	0.24	<b>0.33</b>	2

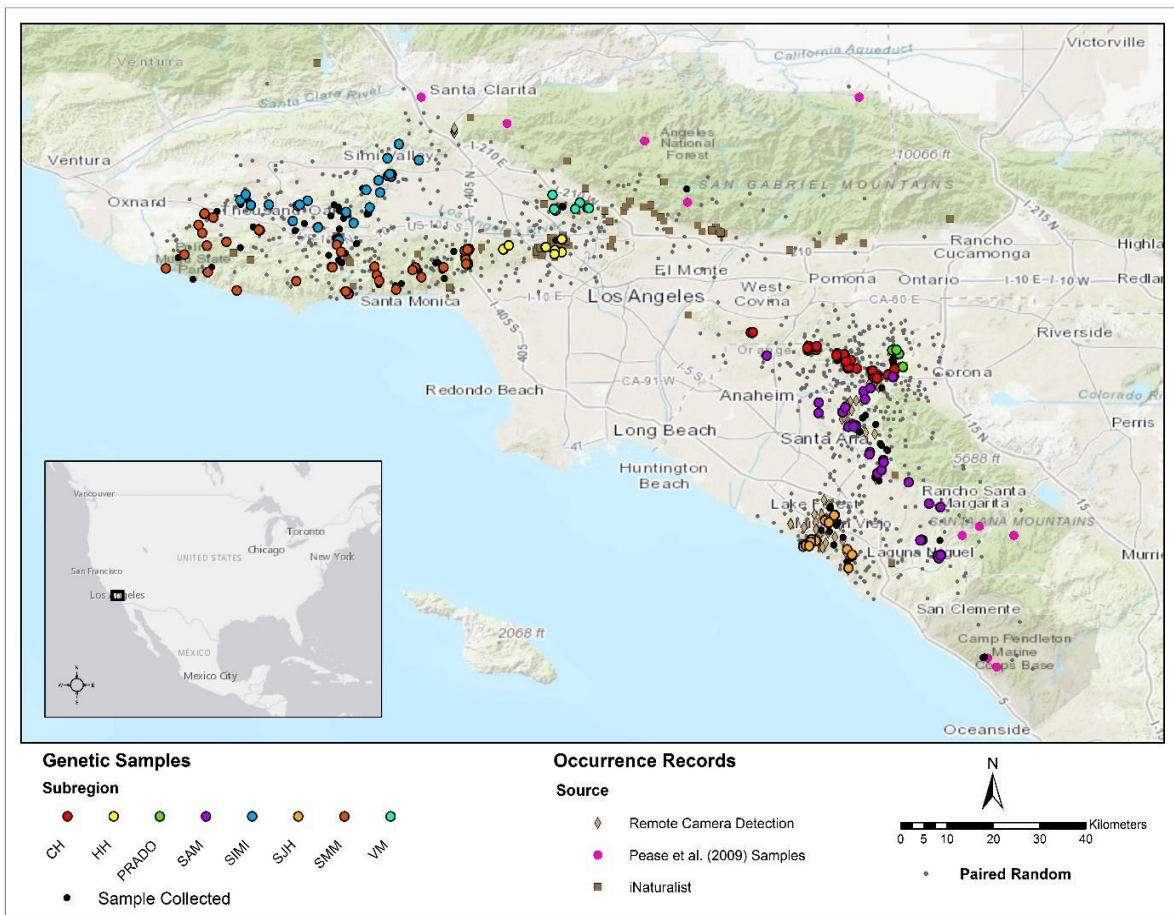
**Table 2.7.** Generalized linear models for predictors of individual pairwise relatedness ( $1/r$ ) between deer sampled in adjacent subregions

<b>Model</b>	<b><math>\beta_{\text{dist}}</math></b>	<b><math>\beta_{\text{additional}}</math></b>	<b><math>\Delta\text{AIC}</math></b>
GD <sup>1</sup> ~ 1	-	-	202
GD ~ Euclidean	0.5338	-	52
GD ~ HLCP <sup>2</sup>	0.5367	-	50
GD ~ FLCP <sup>3</sup>	0.5370	-	50
GD ~ HLCP + Hwy <sup>4</sup>	0.3813	0.8523	0

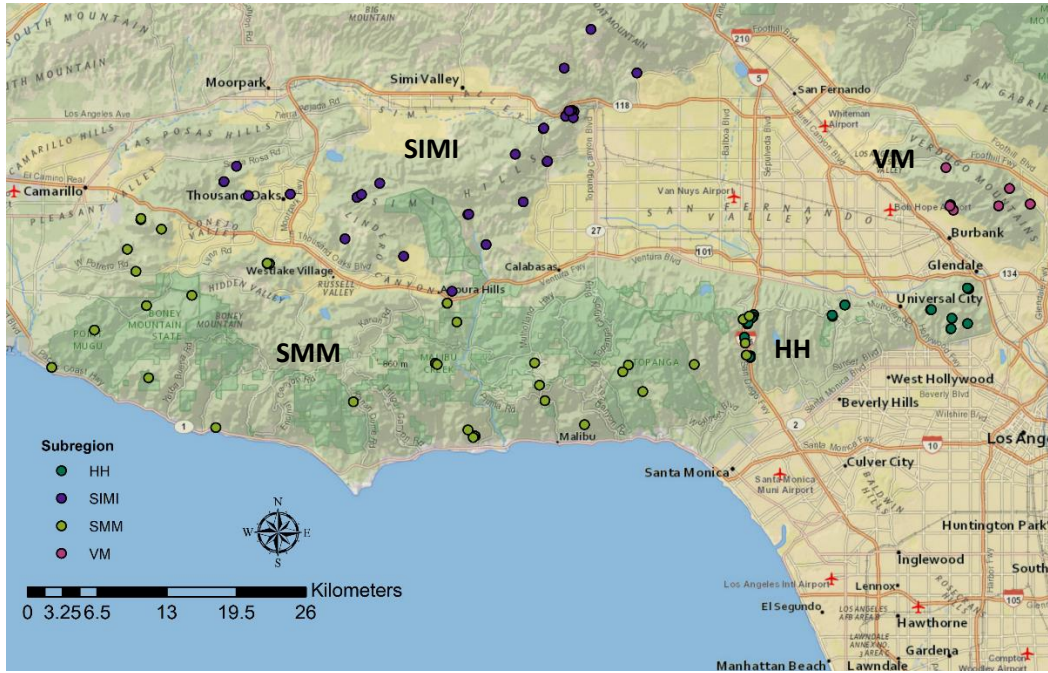
<sup>1</sup> Genetic Distance ( $1/r$ ); <sup>2</sup> Habitat Least Cost Path; <sup>3</sup> Freeway Least Cost Path; <sup>4</sup> Binary indication of whether samples were collected across a highway (1) or not (0)

**Figure 2.1.** Study area map showing the location of genetic samples gathered across the sub-regions and the other occurrence records used to estimate selection of habitat features by mule deer for the whole study area (a), and sample locations for the LA (b) and OC regions (c). We used a paired random sampling approach to sample the range of conditions found in the areas where samples and occurrence data were collected.

A)



B)



C)





**Figure 2.2.** Posterior assignments for individual deer to each of 5 genetic clusters identified in STRUCTURE. Subregions are arranged and grouped according to the pairwise genetic distance ( $D_{est}$ ) matrix as shown by the dendrogram.

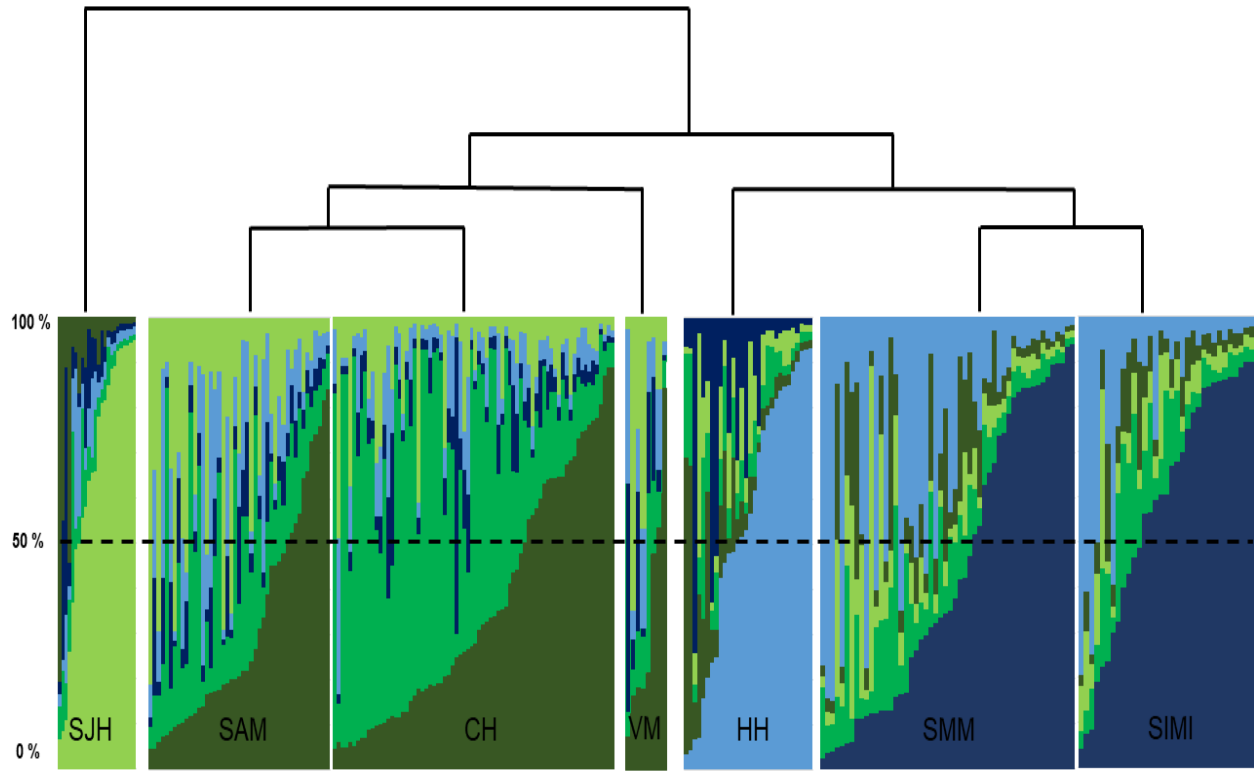


**Figure 2.3.** Mean pairwise genetic distance as a function of the accumulated cost along the least cost path divided by the Euclidean distance between samples collected within all subregions (squares) and between adjacent subregions (circles). The correlation was significant (adj.  $R^2 = 0.24$ ,  $F_{\text{stat}} = 5$ ,  $p\text{-value} = 0.045$ ).

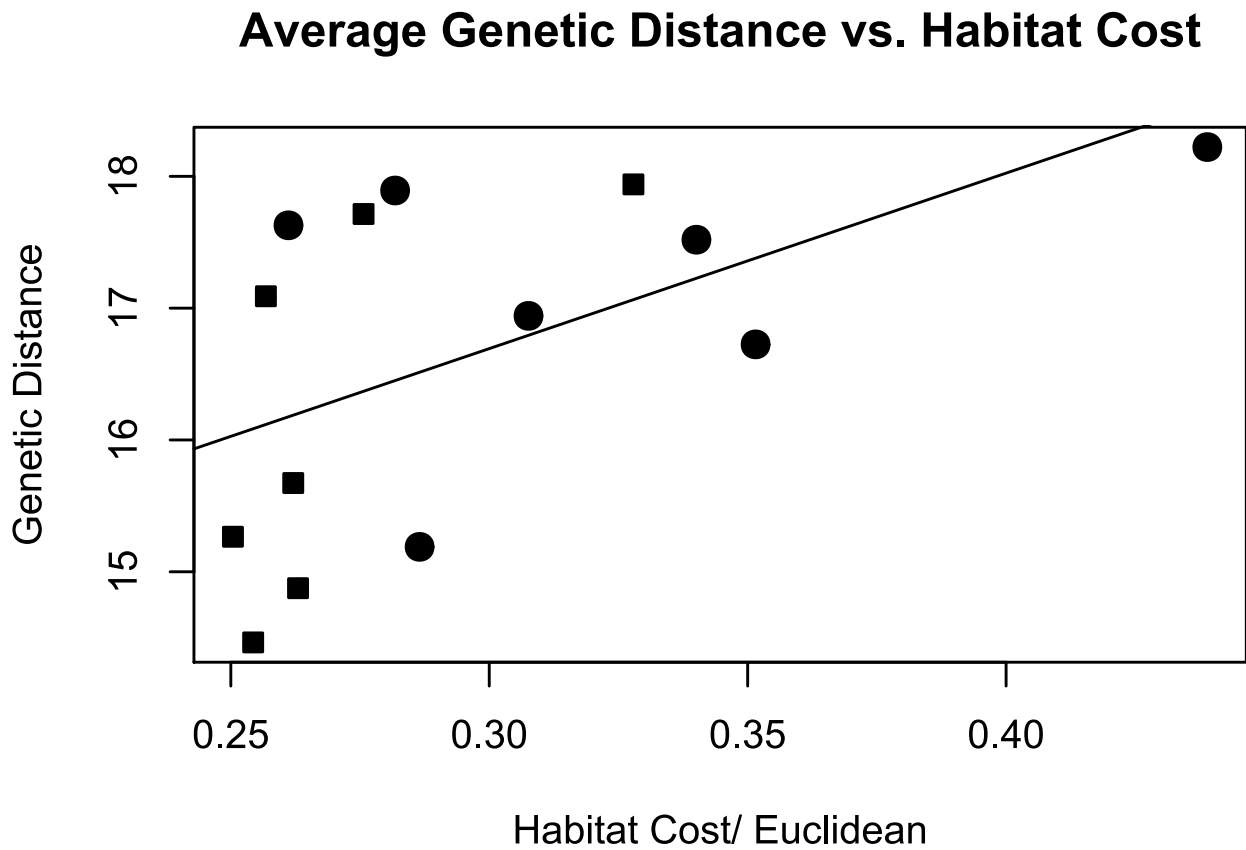
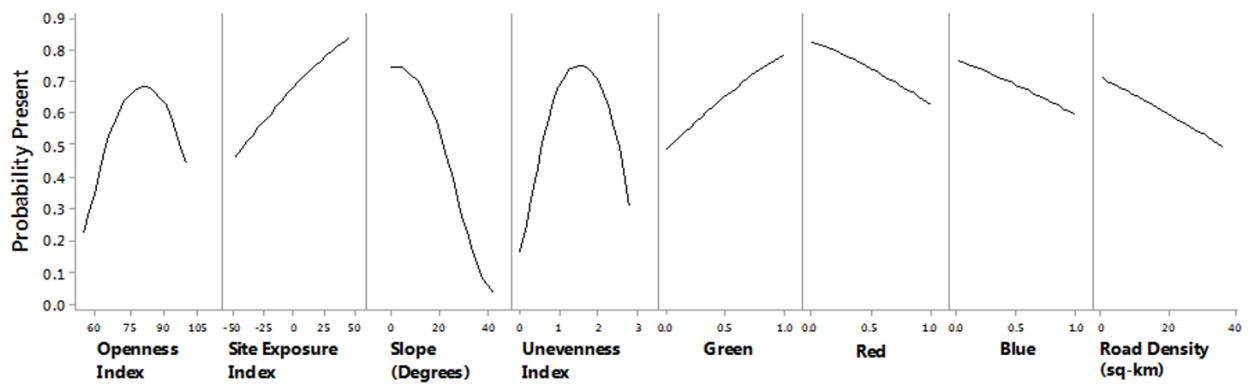


**Figure 2.4.** Response curves for mule deer occurrence data versus an equal number of randomly stratified locations. Factors exhibiting direct responses (quadratic and linear) include terrain unevenness and openness, and 4 LANDFIRE attributes (A). Factors modified by an interaction term include site exposure index (SEI) x slope, and 2 LANDFIRE attributes (red and green) x road density (B).

**A.**



**B.**

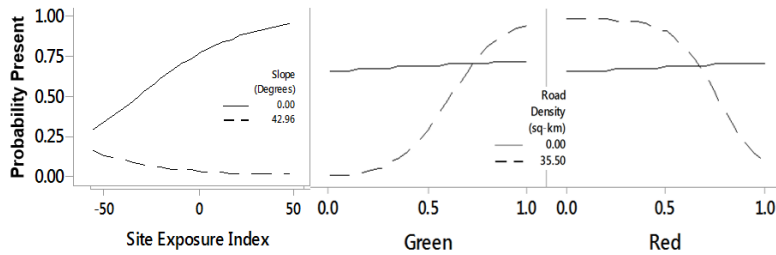
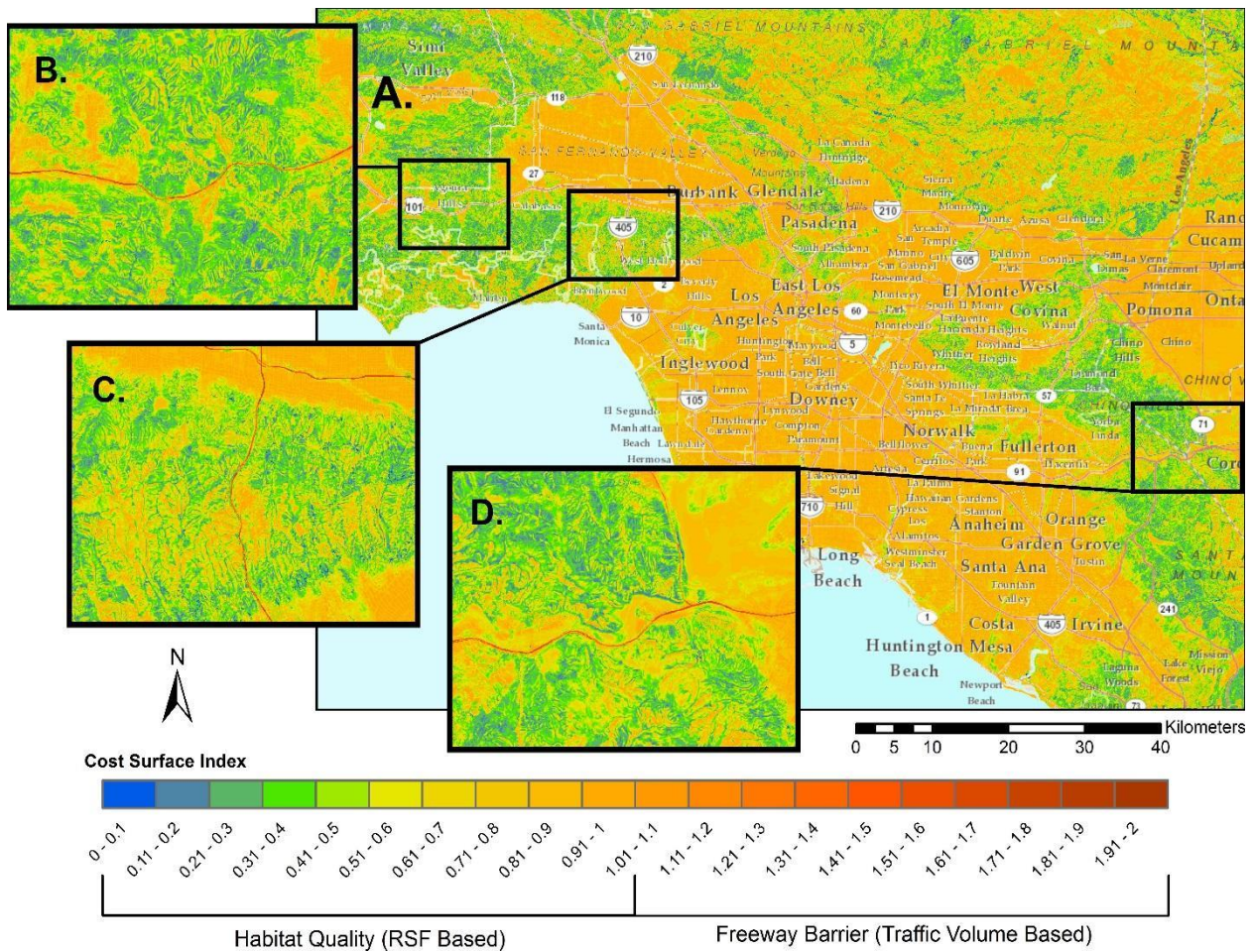


**Figure 2.5.** Cost surface used to estimate mule deer habitat connectivity for the study area (A.). Using a resource selection function (RSF) approach, we estimated high quality habitat would have little cost for movement for mule deer in the region and landscape features where mule deer were not observed to use, as having a high cost of movement on a scale of 0-1 (the inverse probability of mule deer presence). To explore whether or not high traffic volume freeways may pose a movement barrier, we added additional costs to the locations of freeway systems based on the Ahead Annual Average Daily Traffic (ADDT) volume rescaled to values between 0-1 and added it to the habitat based cost surface. These areas of increased cost to transverse are shown for a portion of the US-101 (B.), the I-405 (C.), and the CA-91 and CA-71 intersection (D.).



## REFERENCES

1. Alonso, R. S., Lyren, L. M., Boydston, E. E., Haas, C. D. & Crooks, K. R. (2014). An evaluation of a road expansion and wildlife connectivity mitigation project on a southern California freeway. *Southwestern Naturalist* 59: 181-187
2. Barr, K. R., Kus, B. E., Preston, K. L., Howell, S., Perkins, E., & Vandergast, A. G. (2015). Habitat fragmentation in coastal southern California disrupts genetic connectivity in the cactus wren (*Campylorhynchus brunneicapillus*). *Molecular Ecology*, 24(10), 2349-2363
3. Benson, J. F., Mahoney, P. J., Sikich, J. A., Serieys, L. E., Pollinger, J. P., Ernest, H. B., & Riley, S. P. (2016, August). Interactions between demography, genetics, and landscape connectivity increase extinction probability for a small population of large carnivores in a major metropolitan area. In *Proc. R. Soc. B* (Vol. 283, No. 1837, p. 20160957). The Royal Society.
4. Benson, John F., Jeff A. Sikich, and Seth PD Riley. "Individual and population level resource selection patterns of mountain lions preying on mule deer along an urban-wildland gradient." *PloS one* 11.7 (2016): e0158006.
5. Blanchong, J. A., Sorin, A. B. and Scribner, K. T. (2013), Genetic diversity and population structure in urban white-tailed deer. *The Journal of Wildlife Management*, 77: 855–862. doi:10.1002/jwmg.521
6. Bouzat, J. L., Cheng, H. H., Lewin, H. A., Westemeier, R. L., Brawn, J. D., & Paige, K. N. (1998). Genetic evaluation of a demographic bottleneck in the greater prairie chicken. *Conservation Biology*, 12(4), 836-843.
7. Boydston E.E., Crooks K.R. (2013). Movement Patterns of Bobcats and Coyotes after Widening of CA-71 near CA-91 in Southern California: Final Report In. U.S. Geological Survey, Sacramento, CA, pp 194
8. Brook, B. W., Sodhi, N. S., & Bradshaw, C. J. (2008). Synergies among extinction drivers under global change. *Trends in Ecology & Evolution*, 23(8), 453-460.
9. Cincotta, Richard P., Jennifer Wisnewski, and Robert Engelman. "Human population in the biodiversity hotspots." *Nature* 404.6781 (2000): 990.
10. Coulon, A., Cosson, J.F., Angibault, J.M., Cargnelutti, B., Galan, M., Morellet, N., Petit, E., Aulagnier, S. and Hewison, A.J.M. (2004). Landscape connectivity influences gene flow in a roe deer population inhabiting a fragmented landscape: an individual-based approach. *Molecular Ecology*, 13(9), pp.2841-2850.
11. Cullingham, C. I., Merrill, E. H., Pybus, M. J., Bollinger, T. K., Wilson, G. A., & Coltman, D. W. (2011). Broad and fine-scale genetic analysis of white-tailed deer populations: estimating the relative risk of chronic wasting disease spread. *Evolutionary*

*Applications*, 4(1), 116-131.

12. Burnham, K. P., Anderson, D. R., 2002. Model Selection and Multimodel Inference: A Practical Information-Theoretic Approach (2nd ed.). Springer-Verlag, ISBN 0-387-95364-7.
13. Do, C., Waples, R. S., Peel, D., Macbeth, G. M., Tillett, B. J., & Ovenden, J. R. (2014). NeEstimator v2: re-implementation of software for the estimation of contemporary effective population size (Ne) from genetic data. *Molecular Ecology Resources*, 14(1), 209-214.
14. Epps, C. W., Palsbøll, P. J., Wehausen, J. D., Roderick, G. K., Ramey, R. R., & McCullough, D. R. (2005). Highways block gene flow and cause a rapid decline in genetic diversity of desert bighorn sheep. *Ecology Letters*, 8(10), 1029-1038.
15. Ernest, H. B., Vickers, T. W., Morrison, S. A., Buchalski, M. R., & Boyce, W. M. (2014). Fractured genetic connectivity threatens a southern California puma (*Puma concolor*) population. *PloS one*, 9(10), e107985.
16. Esri, 2012. ArcGIS Desktop Release 10.1. Environmental Systems Resource Institute, <http://www.esri.com/>, Redlands.
17. Esri, 2014. ArcGIS Desktop Release 10.3. Environmental Systems Resource Institute, <http://www.esri.com/>, Redlands.
18. Etherington, T.R., Penelope Holland, E., 2013. Least-cost path length versus accumulated-cost as connectivity measures. *Landscape Ecology* 28, 1223-1229.
19. Evanno, G., S. Regnaut, and J. Goudet. 2005. Detecting the number of clusters of individuals using the software STRUCTURE: a simulation study. *Molecular Ecology* 14.8: 2611-2620.
20. Evans, J., Oakleaf, J., Cushman, S., Theobald, D., 2014. An ArcGIS toolbox for surface gradient and geomorphometric modeling, version 2.0-0, Laramie, WY, <http://evansmurphywix.com/evansspatial>.
21. Frantz, A. C., et al. "Comparative landscape genetic analyses show a Belgian motorway to be a gene flow barrier for red deer (*Cervus elaphus*), but not wild boars (*Sus scrofa*)."  
*Molecular Ecology* 21.14 (2012): 3445-3457.
22. Gagnon, J. W., Theimer, T. C., Dodd, N. L., Boe, S., & Schweinsburg, R. E. 2007. Traffic volume alters elk distribution and highway crossings in Arizona. *Journal of Wildlife Management* 71(7), 2318-2323.
23. Harveson, Patricia M., et al. "Impacts of urbanization on Florida Key deer behavior and population dynamics." *Biological Conservation* 134.3 (2007): 321-331.

24. Herkert, J.R. (1994). The effects of habitat fragmentation on midwestern grassland bird communities. *Ecological Applications* 4.3: 461-471.
25. Hobbs, N.T. (1996). Modification of ecosystems by ungulates. *The Journal of Wildlife Management*: 695-713.
26. Holderegger, Rolf, and Manuela Di Giulio. "The genetic effects of roads: a review of empirical evidence." *Basic and Applied Ecology* 11.6 (2010): 522-531.
27. Ito, T. Y., Lhagvasuren, B., Tsunekawa, A., Shinoda, M., Takatsuki, S., Buuveibaatar, B., and Chimeddorj, B. (2013). Fragmentation of the habitat of wild ungulates by anthropogenic barriers in Mongolia. *PLoS One*, 8(2), e56995.
28. Johnson, W.E., Onorato, D.P., Roelke, M.E., Land, E.D., Cunningham, M., Belden, R.C., McBride, R., Jansen, D., Lotz, M., Shindle, D. and Howard, J. (2010). Genetic restoration of the Florida panther. *Science*, 329(5999), pp.1641-1645.
29. Jombart, T., Devillard, S., & Balloux, F. (2010). Discriminant analysis of principal components: a new method for the analysis of genetically structured populations. *BMC genetics*, 11(1), 94.
30. Jost, L. (2008). GST and its relatives do not measure differentiation. *Molecular Ecology*, 17 (18), 4015-4026.
31. Kalinowski ST, AP Wagner, ML Taper (2006). ML-Relate: a computer program for maximum likelihood estimation of relatedness and relationship. *Molecular Ecology Notes* 6:576-579
32. Kalinowski, S.T., Taper, M.L. & Marshall, T.C. (2007). Revising how the computer program CERVUS accommodates genotyping error increases success in paternity assignment. *Molecular Ecology* 16: 1099-1106. <http://dx.doi.org/10.1111/j.1365-294x.2007.03089.x>
33. Keller, I., and C.R. Largiader. (2003). Recent habitat fragmentation caused by major roads leads to reduction of gene flow and loss of genetic variability in ground beetles." *Proceedings of the Royal Society of London B: Biological Sciences* 270.1513.
34. LANDFIRE, 2011. LANDFIRE 1.1.0--Existing vegetation height and type layers, ed. LANDFIRE. U.S. Department of Agriculture and U.S. Department of the Interior.
35. Lee, Justin S., et al. "Gene flow and pathogen transmission among bobcats (*Lynx rufus*) in a fragmented urban landscape." *Molecular ecology* 21.7 (2012): 1617-1631.
36. Mager, K. H., Colson, K. E., & Hundertmark, K. J. (2013). High genetic connectivity and introgression from domestic reindeer characterize northern Alaska caribou herds.

*Conservation genetics*, 14(6), 1111-1123.

37. McClure, M. L., Dickson, B. G., & Nicholson, K. L. (2017). Modeling connectivity to identify current and future anthropogenic barriers to movement of large carnivores: A case study in the American Southwest. *Ecology and evolution*, 7(11), 3762-3772
38. Mitelberg, A. (2010). Social structure and genetic connectivity in the San Diego southern mule deer. Master's thesis, San Diego State University. San Diego, California.
39. Mitelberg, A., & Vandergast, A. G. (2016). Non-Invasive Genetic Sampling of Southern Mule Deer (*Odocoileus hemionus fuliginatus*) Reveals Limited Movement Across California State Route 67 in San Diego County. *Western Wildlife*, 3, 8-18.
40. Mora, C., and Sale, P. F. (2011). Ongoing global biodiversity loss and the need to move beyond protected areas: a review of the technical and practical shortcomings of protected areas on land and sea. *Marine ecology progress series*, 434, 251-266.
41. Munshi-South, J., and Kharchenko, K. (2010). Rapid, pervasive genetic differentiation of urban white-footed mouse (*Peromyscus leucopus*) populations in New York City. *Molecular Ecology*, 19(19), 4242-4254.
42. Newman, B. J., Ladd, P., Brundrett, M., and K.W. Dixon. (2013). Effects of habitat fragmentation on plant reproductive success and population viability at the landscape and habitat scale. *Biological Conservation*, 159, 16-23.
43. Nicholson, M. C., Bowyer, R. T., & Kie, J. G. (1997). Habitat selection and survival of mule deer: tradeoffs associated with migration. *Journal of Mammalogy*, 78(2), 483-504.
44. Peakall, R. O. D., & Smouse, P. E. (2006). GENALEX 6: genetic analysis in Excel. Population genetic software for teaching and research. *Molecular ecology notes*, 6(1), 288-295.
45. Riley, S. P., Pollinger, J. P., Sauvajot, R. M., York, E. C., Bromley, C., Fuller, T. K., & Wayne, R. K. (2006). FAST-TRACK: A southern California freeway is a physical and social barrier to gene flow in carnivores. *Molecular Ecology*, 15(7), 1733-1741.
46. Riley, S. P., Serieys, L. E., Pollinger, J. P., Sikich, J. A., Dalbeck, L., Wayne, R. K., & Ernest, H. B. (2014). Individual behaviors dominate the dynamics of an urban mountain lion population isolated by roads. *Current Biology*, 24(17), 1989-1994.
47. Rollins, M.G., 2009. LANDFIRE: a nationally consistent vegetation, wildland fire, and fuel assessment. *International Journal of Wildland Fire* 18, 235-249.
48. Rooney, T.P., and D.M. Waller. (2003). Direct and indirect effects of white-tailed deer in forest ecosystems. *Forest Ecology and Management* 181.1: 165-176.



49. Sato, J. J., Kawakami, T., Tasaka, Y., Tamenishi, M., & Yamaguchi, Y. (2014). A few decades of habitat fragmentation has reduced population genetic diversity: A case study of landscape genetics of the large Japanese field mouse, *Apodemus speciosus*. *Mammal Study*, 39(1), 1-10.
50. Shannon, C. E., & Weaver, W. (1949). The mathematical theory of communication. Urbana, Ill. *Univ. Illinois Press*, 1, 17.
51. Spencer, W., P. Beier, K. Penrod, Winters, Paulman, Rustigian-Romsos, J. Strittholt, M. Parisi, and A. Pettler. (2010). California Essential Habitat Connectivity Project: A Strategy for Conserving a Connected California. Prepared for California Department of Transportation, California Department of Fish and Game, and Federal Highways Administration.
52. U.S. Geological Survey, 2009. National Elevation Dataset (NED)--Raster digital data, ed. U.S. Geological Survey. The National Map, Sioux Falls.
53. Wang, M., and A. Schreiber. (2001). The impact of habitat fragmentation and social structure on the population genetics of roe deer (*Capreolus capreolus L.*) in Central Europe." *Heredity* 86.6: 703-715.
54. Wilson, G. A., & Rannala, B. (2003). Bayesian inference of recent migration rates using multilocus genotypes. *Genetics*, 163(3), 1177-1191.
55. Yokoyama, R., Shirasawa, M., Pike, R.J., 2002. Visualizing topography by openness: a new application of image processing to digital elevation models. *Photogrammetric engineering and remote sensing* 68, 257-266

## CHAPTER 3

### Dietary diversity and resource selection by big brown bats (*Eptesicus fuscus*) in agricultural landscapes exhibiting different levels of pesticide-use in California

#### ABSTRACT

Bats provide invaluable economic and environmental services in agriculture by consuming insects that damage crops and are otherwise controlled through the use of chemical pesticides. Quantifying these services is a major research focus, yet little is known about the dietary diversity or foraging behavior of bats in intensively managed agricultural landscapes. Further, few data are available for understanding the influence of pesticide-use on bat foraging, concomitantly negating our understanding of exposure risks for bats. We have implemented an RSF modeling approach to analyze telemetry data on ten female foraging big brown bats, in order to determine if these bats exhibit a preference for certain crop types over others and to test whether bats tend to avoid or select for areas with high pesticide use. We additionally have analyzed guano from 17 wild big brown bats and four additional individuals of three bat species captured in two locations which vary in landscape levels of pesticides applied. We demonstrate that brown bats exhibit selection and avoidance for specific crop types and that pesticides do exhibit an important influence on bat foraging decisions. We further show that dietary diversity is reduced in high-pesticide use areas, potentially resulting from reduced prey availability. Finally, we observed high foraging distances for big brown bats in these landscapes relative to previously observed foraging distances in non-agricultural landscapes, suggesting potential energy costs associated with low or unpredictable prey availability in intensively managed agriculture. Collectively, our results highlight the importance of understanding foraging

strategies for economically valuable species in altered landscapes and may provide a management framework for agricultural producers to promote bat predation on their lands.

## INTRODUCTION

Animals that occupy intensively managed agricultural landscapes must contend with a variety of challenges, including chemical pollutants and habitat degradation. In addition to the potential toxic effects of various pesticides (Clark and Rattner 1987), altered habitats are often highly degraded with respect to resource availability, which can have energetic costs for foraging animals (Bruun & Smith, 2003; Tremblay et al., 2005). Understanding these impacts is important for preserving biodiversity in agricultural systems, particularly for species that provide ecological services.

The Central Valley of California is one of the top U.S. agricultural export regions (University of California Agricultural Issues Center, <https://aic.ucdavis.edu/2015/06/09/2014-california-export-data>), with approximately 200 million pounds of the active ingredients (a.i.) in pesticides applied annually to support food production (<http://www.pesticideinfo.org>). Insecticides, in particular, are often highly toxic and harmful to both humans and wildlife (Wesienberger 1993, Davidson 2004), comprise approximately 2% of pesticides applied (<http://www.pesticideinfo.org>). The distribution of pesticide-use varies spatially and temporally, creating a mosaic of risk exposure across the landscape and providing a useful gradient for identifying and understanding the effects of agricultural management and pesticide-use on wildlife at the landscape scale.

Insectivorous bats foraging in agricultural areas are susceptible to chronic exposure to pesticides through their insect diets (Stahlschmidt and Brühl 2012). Impacts from such exposure can be direct (i.e. altering their survival, reproduction, behavior, physiology or immune function), or indirect (i.e. limiting food resources). Few data have been collected on the toxicological sensitivity of bats to pesticides, although two studies suggest that, despite lower sensitivity to death from organophosphate insecticides, bats are more susceptible to sub-lethal effects on neuromuscular control and orientation (Clark 1986; Clark and Rattner 1987), which can be fatal in the wild. Eidela and Whittaker (2007) discovered organophosphate residues in tissues from small sample sizes of both live-captured and recovered carcasses of Northern long eared and federally endangered Indiana bats and DDT has been discovered in guano deposits in New Mexico (Clark 2001), suggesting that bats are ingesting agricultural pesticides while foraging. Population level outcomes of exposure to insecticides are even less-well studied. Frick et al. (2007) observed declines in recruitment in populations of *Yuma myotis* following a large-scale pesticide spill, which they attribute largely to limitations on insect resources. Apart from these observations, little research has been published on assessing the risks and ecological outcomes for bats foraging in intensively managed agricultural landscapes.

Bats serve as an important model for understanding the effects of landscape level pesticide use in intensively managed agricultural systems given their insectivorous diets and their ability to forage widely across the landscape in a single evening (Shiel et al., 1999). Further, because bats provide critical biological pest control services, estimated to value upwards of 23 billion dollars annually across the United States (Boyles et al., 2011), they are of particular importance in developing strategies to mitigate pesticide-use and to provide incentive for farmers to employ alternative management methods that are less harmful to people and the environment.

To accurately assess exposure risk for bats to pesticides requires an adequate characterization of their foraging patterns in agricultural landscapes. We followed a two-pronged approach to assess how landscape-level pesticide-use influences bat foraging patterns and dietary diversity. First, we used radio-telemetry to track female big brown bats (*Eptesicus fuscus*) captured at two sites which differed in cumulative pesticide-inputs at the landscape scale. We calculated observed foraging extents (OFE), followed by implementation of a Resource Selection Function (RSF) to determine the features of the landscape bats actively select or avoid during foraging. We used a distance-based analysis, rather than site-occupancy models, as this method can reduce the selection estimate bias inherent in high error location estimates (Forester et al., 2009). Further, distance variables for various resources have been shown to improve predictions of bat occupancy (Rainho et al., 2011). We hypothesized that if bats actively avoid or select particular crop types or current pesticide sources, then their foraging locations would differ significantly from random with respect to these aspects of their environment.

Second, we used a metagenomics approach to assess dietary diversity for brown bats captured in two sites that varied considerably in the intensity of pesticide-inputs, as measured by the total weight of pesticide applied during the summer months when bats are actively foraging and reproducing. We hypothesized that higher insecticide inputs would limit resource availability for bats and therefore, dietary diversity would be lower in areas with higher annual pesticide inputs. We further hypothesized that if intensively managed agricultural landscapes are degraded with respect to prey availability for bats, then foraging ranges would be substantially large compared to previously observed foraging ranges of big brown bats in non-agricultural landscapes. Finally, we evaluated specific prey items to identify whether pest species are being consumed by bats.

## METHODS

### *STUDY AREA*

The study area consisted of two conventionally managed almond orchards located in Kern County, CA, USA (Figure 3.1) that differed with respect to pesticide-inputs at a landscape scale. Kern County comprises the southern border of the San Joaquin Valley, CA which is predominantly agricultural, with several towns and developed areas surrounded by a large matrix of variable agricultural commodity production. Almond orchards were selected based on patterns of landscape level pesticide-use surrounding the orchard. Specifically, we calculated the mean cumulative weight of pesticides applied across approximately 150 km<sup>2</sup>, or the extent 9 Public Land Survey System townships ([http://nationalmap.gov/small\\_scale/a\\_plss.html](http://nationalmap.gov/small_scale/a_plss.html)) directly surrounding and including the orchard from March – September (2011 – 2014), the period when bats are most actively foraging and reproducing. One orchard was located near the town of Arvin, CA (site: ARVIN), 24 km southeast of Bakersfield, CA, and the other near Shafter, CA (site: SHAFTER), 40 km northwest of Bakersfield, CA. The two orchards were similar in age and canopy structure, yet varied in landscape context. The ARVIN orchard, approximately 0.5 km<sup>2</sup> in area, was located approximately 2.5 km from the town of Arvin, and was bordered to the north by uncultivated fields and a walnut orchard, to the east by corn, to the south by cotton and to the west by a vineyard during our study period. At the landscape scale, this area is dominated by a combination of fruit and nut orchards, vineyards, and various field crops. Mean cumulative pesticide inputs for this landscape was 2,384,740 lbs. The SHAFTER orchard, approximately 1 km<sup>2</sup> in area and is located approximately 5 km from the town of Shafter. SHAFTER was bordered on all sides by almond orchards, which were managed by various growers. This landscape is heavily dominated by almond orchards, fruit orchards, cattle pastures, and

miscellaneous field crops. Pesticide inputs surrounding this orchard were 3,866,493 lbs. for the same time frame and spatial extent as locality ARVIN.

### *CAPTURE AND TELEMETRY*

Bats were captured using 8 mm mist nets (Avinet, Inc., USA) stacked at single, double and triple high configurations along roads and tree rows within almond orchards. Mist nets were opened at sunset and closed at 2 am each night, and each site was sampled for 10 nights from June to August 2015. Individuals were identified to species, aged (adult or juvenile), and assessed for reproductive condition (lactating, postlactating and non-reproductive). Guano deposited in the capture bag or during processing was collected and preserved in 96% ethanol and stored at -20° C until processing. Measurements were taken to confirm species identification and to assess body condition. Radio transmitters (Holohil, LLC, Canada) weighing less than 5% of body mass were affixed to adult and juvenile female big brown bats using a degradable epoxy adhesive. Bats were captured and processed in accordance with UCLA Animal Care and Use Committee requirements (ARC# 2012-004-03) under a California Department of Fish and Wildlife Scientific Collecting Permit (SCP #11920).

A total of 14 bats were fit with VHF radio transmitters (Holohil, LLC). Two transmitters failed before sufficient data could be collected. A third individual was never located following her release, while an additional individual was only located once briefly while foraging. Analyses were therefore performed on the remaining big brown bats (n = 10) for which sufficient data were collected (SHAFTER: n = 3; ARVIN: n = 7). The day following capture, active searches were performed to locate bats within roosts. Roosts for nine bats were located within a

few hours of searching, but the roost for one adult female, although successfully tracked during foraging, could not be located because it was on private property.

To track nightly foraging movements, two mobile teams assembled near the roosts and awaited emergence. Once a focal bat was active, foraging locations were collected at two-minute intervals using bi-angulation of telemetry signals and communication between teams through short-wave radios.

Bat locations were estimated from telemetry data in LOAS v. 4.0 (Ecological Software Solutions, LLC). Bearing errors were generated for each person performing telemetry from bearings taken on a known location. Bat location estimates were then imported into ArcMAP (ESRI) for visual inspection. Locations that were greater than 1 km from the locations immediately preceding and immediately following the location were removed. Locations were pruned to limit the dataset to no more than 5 locations taken within in the same 30 min time period to limit spatial autocorrelation. Home ranges were calculated for each bat as minimum convex polygons (MCP) in GME (Spatial Ecology, LLC).

Crop data for 2015 were obtained through the Kern County Agricultural Commission (<http://www.kernag.com/caap/crop-reports/crop-reports.asp>). Crop categories were consolidated into 8 categories: 1) field crops such as grains and corn; 2) fruit orchards which were predominantly citrus but also included stone fruits, apples, and pomegranate; 3) miscellaneous vegetable crops; 4) developed areas such as towns and cities; 5) pastures including cattle stock yards and grazing; 6) uncultivated fields; 7) nut orchards; and 8) vineyards. Pesticide data was obtained from California Department of Pesticide Regulation (<http://calpip.cdpr.ca.gov>) and was implemented as a ninth variable. Only crop and pesticide data corresponding to the days for which each bat was tracked were included in individual bat datasets. Spatial information for both



crop and pesticide data were recorded as meridian townships and sections according to the Public Land Survey System. The PLSS layer was joined with the crop and pesticide data and converted to separate rasters for each feature. Available points for each crop type and pesticide input were computed from a raster with cell resolution of 30 m across Kern County. This raster was intersected in GME with each bat MCP to generate a dataset of available points for each landscape feature for each bat. Distance to each used and available point was calculated in GME.

### *DNA PROCESSING*

We sequenced DNA from guano collected from 17 brown bats (SHAFTER: n = 10; ARVIN: n = 7). In addition, we sequenced DNA from guano from 2 Yuma myotis (*M. yumanensis*), a pallid bat (*Antrozous pallidus*), and a Brazilian free-tailed bat (*Tadarida brasiliensis*). DNA was extracted from guano using the Qiagen DNA Stool Extraction Kit (Qiagen, USA) with modifications as described in Zeale et al. (2010). We custom ordered hybrid primers designed to target ~ 130 bp sequence of the 16S region of the mitochondrial genome that has been shown to be useful for distinguishing insects in animal diets (Kartzinal et al., 2015), as well as a 33 bp Nextera transposase sequence (Illumina, San Diego, California;

<https://support.illumina.com/content/dam/illumina->

[support/documents/documentation/chemistry\\_documentation/experiment-design/illumina-](https://support.illumina.com/content/dam/illumina-support/documents/documentation/chemistry_documentation/experiment-design/illumina-)

[adapter-sequences-1000000002694-03.pdf](https://support.illumina.com/content/dam/illumina-support/documents/documentation/chemistry_documentation/experiment-design/illumina-adapter-sequences-1000000002694-03.pdf)). Each PCR was run in triplicate using the QIAGEN

Multiplex PCR Kit (Qiagen, Valencia, CA) and pooled in equal concentration. PCR

thermocycling conditions were as follows: initial denaturation at 95 °C for 10 min, followed by

35 cycles of denaturing at 95 °C for 30 s, annealing at 50 °C for 30 s and extension at 72 °C for

30s, with a final extension at 72 °C for 2 min. Following PCR, we performed a bead clean up with

Sera-Mag SpeedBeads (GE Healthcare, Life Sciences, Marlborough, MA). Concentration was quantified on a Victor3 multilable plate reader (PerkinElmer, Waltham, MA) using the Qubit® dsDNA BR Assay Kits (Invitrogen, Molecular Probes). Fluorescence was measured at 485/530 nm. We added a unique Nextera XT index (Nextera XT Index Kit v2, Illumina, San Diego, CA) to each sample library in a second PCR. We used the KAPA HiFi HotStart Ready Mix PCR Kit (Kappa Biosystems, Wilmington, Massachusetts) starting with 10 ng input DNA. PCR thermocycling conditions for this step were as follows: Initial denaturation at 95°C for 5 min, followed by 5 cycles of denaturing at 98°C for 20 secs, annealing at 56°C for 30 secs, and extension at 72°C for 3 min; an extension at 72°C for 5 min and a final extension at 8°C for 10 cycles. We conducted a final bead clean up and quantified as previously described. We then pooled equal copy numbers to 10nM. Copy number was calculated by dividing the product of DNA molarity and sampling concentration (ng) by the product of amplicon length and the molar concentration of DNA (<http://cels.uri.edu/gsc/cndna.html>). Libraries were sequenced as 150 bp paired-end reads on the HiSeq 4000 sequencing platform (Illumina, San Diego, CA).

## *ANALYSIS*

### *Resource Selection Function*

To assess how big brown bats navigate agricultural landscapes during foraging, we implemented a RSF model to assess bat preference or avoidance for 8 main crop categories and local pesticide inputs. RSFs are a viable strategy for characterizing habitat and resource use in wild populations (Johnson et al., 2006) especially when mixed effects are incorporated to account for hierarchical structure in natural populations (i.e. individuals in colonies; Gillies et al., 2006). We implemented both animal and site as nested random effects, hence allowing each animal to have its own coefficient of selection, and each site an independent intercept. This has

been shown to improve model performance, particularly with unbalanced sample designs and variability in individual animal preferences (Gillies et al., 2006).

Distance to used and available points for each bat were then input as variables in a RSF to identify which crop types bats select or avoid, with a binary response variable indicating whether a location was used (1) or available but not used (0). General linear mixed effects models were run using the R package lme4 (Bates et al., 2015), with individual and site implemented as nested random effects. We compared several models which included 1) random effects and all crop types but excluding pesticides; 2) random effects and all crop types and including pesticides; and 3) random effects plus all crop types interacting with pesticides. Our null model included only random effects. We selected the best model with the lowest AIC value.

### *Dietary Diversity*

All reads were pre-processed using the Anacapa toolkit (<https://github.com/limey-bean/Anacapa>). Briefly, we trimmed sequencing adapters from the 5' end and adapters and primer sequence from the 3' end of each read using cutadapt (Martin, 2011). Reads with a quality score < 35 or reads with < 100 bp after trimming were removed with the Fastxtoolkit (Gordon and Hannon, 2010). Cutadapt was then used to sort all reads by their index and primer sequence and to trim additional basepairs from the end of reads to increase quality. We sorted out unpaired forward and reverse reads into separate files from the paired reads, and used dada2 to identify amplicon sequence variants (ASV) to denoise, dereplicate, merge paired reads (where applicable) and detect any chimera sequences.

In order to assign sequence reads to a taxonomic group, we first generated a custom reference library using CRUX ([https://github.com/limey-bean/CRUX\\_Creating-Reference-libraries-Using-eXisting-tools](https://github.com/limey-bean/CRUX_Creating-Reference-libraries-Using-eXisting-tools)). This pipeline first performs an *in silico* PCR against the EMBL

standard nucleotide sequence database (Stoesser et al., 2002) to generate a seed library of reads with unique taxon identifiers. Library reads are then checked to confirm that they contain the primer regions, which are subsequently trimmed using cutadapt. The seed library is then BLASTed (Camacho et al., 2009) against the NCBI nr nt database (<ftp://ftp.ncbi.nlm.nih.gov/blast/>). BLAST results are dereplicated by accession number and converted to FASTA format. We used entrez\_qiime ([https://github.com/bakerccm/entrez\\_qiime](https://github.com/bakerccm/entrez_qiime)) to produce a taxonomy file from the blast output and then generated an indexed reference library using Bowtie2 (Langmead et al., 2009). We then used Bowtie2 to get the best hits between our sample reads and our reference library. We used a global read matching algorithm and a local setting for any leftover reads. Confidence intervals for our taxonomic assignments were generated from the resulting SAM output from Bowtie 2 using a Bayesian Least Common Ancestor algorithm that was adapted from Gao et al., 2017.

We used the observed number of species and Shannon entropy to measure and compare alpha diversity (Caporaso et al. 2010) in bat diets between the two sites. We took the average of ten replicated rarefactions at increments ranging from 1,000 – 10,000 reads per sample (Rodrigues et al. 2013). Although saturation across samples was reached at approximately 2,000 reads, as a conservative means to ensure that we captured the diversity in bat diets, we ran each rarefaction up to 4,000 reads. We ran paired t-tests to determine whether dietary diversity was significantly different between the two sites. We additionally used a nonmetric multivariate dimensional scaling (NMDS) analysis to visualize community composition and ran a PERMANOVA and a test of multivariate homogeneity of group dispersions (adonis and betadist functions in r library vegan (Dixon 2003, Oksanen et al. 2007)) to measure dispersion and assess the relative heterogeneity of bat diets between the two sites.

## RESULTS

### *CAPTURE AND TELEMETRY*

A total of 10 female brown bats were tracked via radio-telemetry while foraging from June – August 2015. Acquired foraging locations for each bat ranged from 33 – 156 points after manual removal of points with high autocorrelation or error (Table 3.1). Mean OFE was 70.1 km<sup>2</sup> (16.4 – 118 km<sup>2</sup>) for adult females and 101.55 km<sup>2</sup> (47 -151.2 km<sup>2</sup>) for juvenile females. OFEs did not differ significantly between sites ( $t = 0.039$ ,  $p = 0.97$ ). Average distance between foraging locations and day roost was  $5.54 \pm 2.94$  km for adults, and  $5.07 \pm 2.25$  km for juveniles.

### *RESOURCE SELECTION FUNCTION*

The best fitting general linearized mixed-effects model suggested that brown bats selected for fruit orchards and field crops and avoided developed areas and uncultivated agricultural plots (Table 3.2). Additionally, there were several significant interactions between pesticide input and certain crops. Specifically, bats were observed foraging closer to fruit orchards and vegetable crops that had higher pesticide inputs. Conversely, bats were observed farther than expected by chance from field crops and vineyards that had high pesticide inputs (Table 3.2). The next best fit model ( $\Delta AIC = 26.6$ ), which assessed pesticide input as an independent factor and not as an interaction variable, showed significant avoidance of pesticides, as well as developed areas and uncultivated agricultural plots. The null had the poorest fit ( $\Delta AIC = 378$ )

### *DIETARY DIVERSITY*

A total of 116 unique arthropod taxonomic assignments were made based on 16S sequences in bat guano from all four bat species and 88 assignments from big brown bats alone

(Figure 3.2). Rarefaction curves showed higher rates of prey sequence accumulation in Brazilian free-tailed bats, followed by Yuma myotis, and then by brown bats and pallid bats (Figure 3.3). Alpha diversity was not significantly different between sites, whether measured by relative abundance of observed species ( $t = 1.3479$ ,  $p = 0.21$ ; Figure 3.4a) or by a Shannon Entropy measure ( $t = 0.99654$ ,  $p = 0.38$ ; Figure 3.4b). However, beta diversity of prey items differed significantly by site (PERMANOVA;  $p = 0.007$ ; Figure 3.4c). Further, measures of dispersion in NMDS analysis showed a significant difference in prey item heterogeneity between sites based on species presence in guano. ( $k = 3$ , stress = 0.074,  $p = 0.005$ , Figure 3.4d).

Several important agricultural pest species were identified as primary prey items in the diets of brown bats (Figure 3.2) including members of the family of Melolothini beetles (also known as May beetles and June bugs), the southern house mosquito (*Culex quinquefasciatus*), and several cutworms including the large yellow underwing (*Noctua pronuba*) and the Western bean cutworm (*Striacosta albicosta*). This analysis shows that bat guano can be an effective source not only for prey information in wild bats, but also informative of arthropod diversity at landscape scales. This is particularly important with regards to agricultural pests. Our results also suggest that pesticide use may not affect species alpha diversity but can potentially reduce beta diversity, supporting previous observations (Hendrickx et al., 2007; Eekros et al., 2010).

## DISCUSSION

Overall, the results of this research suggest pesticides and intensive agricultural management may impact bat utilization of the landscape as well as the diversity of bat prey. Many acoustic studies have shown bats to be impacted by the structure and composition of landscape features in agricultural areas (Lentini et al., 2012; Kalda et al., 2015; Kelly et al.,

2016). Relatively few studies have assessed the impacts of pesticides on bats foraging in agricultural systems, although differences in bat foraging activity between conventional and organic farms suggest that pesticides likely limit resource availability for bats (Wickramasinghe et al., 2003; Wickramasinghe et al., 2004).

We assessed whether pesticides and crop types influence foraging behavior, and if landscape level pesticide-use has an important effect on dietary diversity for big brown bats. Observed foraging areas were substantially large, suggesting that resource limitation in agricultural landscapes may be driving higher foraging energy costs. Pesticide inputs were significantly selected against and showed the greatest positive correlation with distance to observed locations compared to all other variables. However, interaction terms in our model suggested that certain crop types (fruit orchards and vegetable crops) are more likely to be utilized with increasing pesticide inputs. We found dietary beta diversity was significantly lower in the high pesticide-use area (SHAFTER) and critically, that bats consume economically important pests. Each of these observations suggest that agricultural landscapes, and particularly pesticides, may impose substantial energy costs to bats. Such costs may in turn impact pest control services provided by foraging bats.

In general, animals in human dominated landscapes tend to occupy larger territories than individuals in non-modified landscapes (Nicholson et al., 1997; Riley et al., 2003). Big brown bats in this study were observed foraging across greater distances than previously observed in non-agricultural landscapes (Brigham, 1991), possibly due to lower total prey availability or lower predictability in the distribution and abundance of prey across a mosaic landscape. Nocturnal insect diversity has been shown to be lower in conventionally managed farms relative to organic farms, suggesting that resource availability is affected by pesticide-use in agricultural

systems (Wickramasinghe et al., 2003; Wickramasinghe et al., 2004). Similarly, both prey availability and foraging activity of pallid bats was shown to be higher in natural habitat compared to vineyards (Rambaldini and Brigham, 2004). In big brown bats, foraging activity was shown to be significantly impacted by the availability of remnant vegetation surrounding vineyards in Northern California (Kelly, et al., 2016). Large foraging distances for brown bats in agricultural landscapes may have potential fitness costs due to the high energetic demands associated with flight (Thomas et al., 1972). In conjunction with potential exposure to pesticides and reduced resource availability, populations in these areas may be more stressed energetically. Interestingly, the individual with the smallest home range and shortest commute distances was the only lactating female monitored, likely reflecting the high metabolic costs of caring for young (Henry et al., 2002).

Our resource selection functions showed that bats exhibit variable preferences for different crop types at the individual level, but collectively avoid pesticides in general. Interestingly, however, interactions between pesticide-use and fruit orchards and vegetable crops suggest that bats select for high pesticide-use in these crop types. This has implications for the exposure risk for bats in these crop types, as they are more likely to encounter toxins in their diet by selecting for these areas. Further research should focus on assessing bat activity in these crop types during spray events to assess whether bat-use directly overlaps temporally with the application of potentially harmful chemicals.

Beta diversity of brown bat diets was shown to be lower in the high pesticide-use site (SHAFTER), suggesting greater dietary heterogeneity in the diets of bats from a low pesticide-use site (ARVIN). Although alpha diversity was not significantly different between sites, the power to detect a significant difference was low given small sample size. In fact, the overall



pattern clearly suggests lower diversity in the diets of bats sampled in SHAFTER (Figure 3.2). Further, although we did not include replicates of other bat species (except for *M. yumanensis*,  $n = 2$ ), our rarefaction analysis showed much faster rates of accumulation of prey sequences for Yuma myotis and Brazilian free-tailed bats compared to brown and pallid bats (Figure 3.3), and thus, these bat species appear to have more diverse diets. Given that sympatric bats species are known to partition prey (Razgour et al., 2011; Emrich et al., 2014) and big brown bats are known to specialize on Coleoptera spp. (Clare et al., 2014) as we detected, we infer that a landscape that supports a greater number of bat species is also likely to promote stronger pest control. We never encountered any other species at SHAFTER besides big brown bats, and although this is less likely a direct result of lower pesticide-use in the ARVIN site rather than other elements of landscape heterogeneity or roost availability not measured in this study, it does suggest that spatial variation in the presence of bat species in agricultural landscapes may contribute to variation in the magnitude of ecosystem services bats provide. Therefore, bats should be a focal management focus for growers, including creating amenable habitat features and reducing pesticide-use.

TABLES AND FIGURES

**Table 3.1.** Telemetry location numbers, observed foraging extent (OFE), mean foraging distance from roost locations (Avg. Dist) and the furthest location from roost locations (Max Dist.) for each radio-tracked bat (n = 10).

<b>Animal</b>	<b>Age</b>	<b>Site</b>	<b># Locs.</b>	<b>OFE* (km<sup>2</sup>)</b>	<b>Avg. Dist (km)</b>	<b>Max. Dist (km)</b>
<b>B76</b>	A	AV	33	45	6.60 ± 5.72	16.36
<b>B83</b>	A	AV	55	33.4	3.51 ± 1.64	11.44
<b>B91</b>	A	AV	60	105	10.08 ± 6.05	18.96
<b>B63<sup>1</sup></b>	A	AV	99	118	NA <sup>1</sup>	NA <sup>1</sup>
<b>B10</b>	J	AV	132	47	3.22 ± 1.46	9.63
<b>B47</b>	J	AV	156	127	4.47 ± 4.63	18.88
<b>B67</b>	J	AV	105	81	4.22 ± 4.01	15.71
<b>B22</b>	A	SH	114	65.9	4.79 ± 2.81	9.21
<b>B51</b>	A	SH	59	16.4	2.68 ± 1.55	5.52
<b>B43</b>	J	SH	124	151.2	8.33 ± 7.50	25.30

<sup>1</sup>Roost was never located for B63

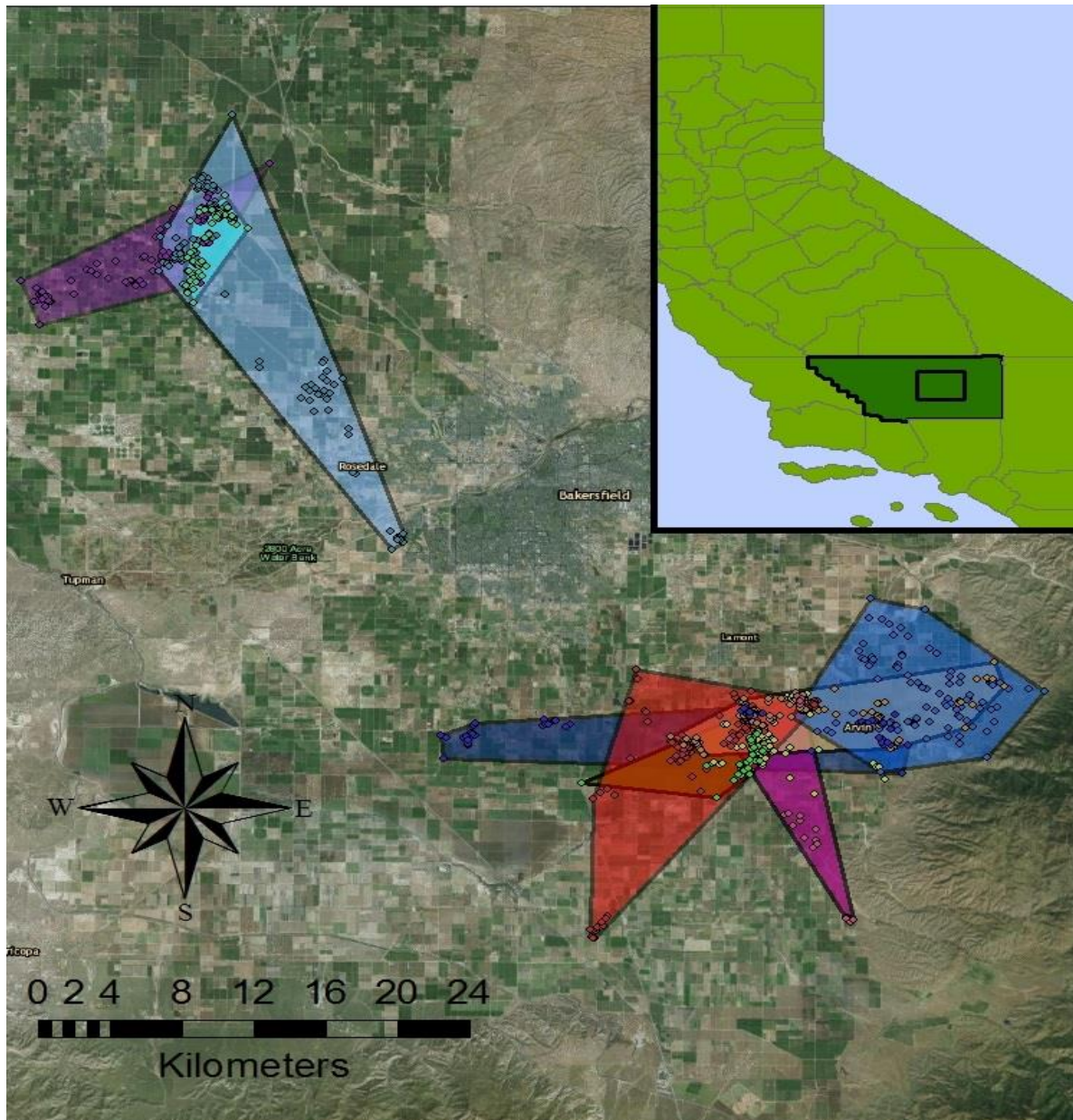
**Table 3.2.** Mixed effects model components, ΔAIC (calculated against null model), and significantly (p < 0.05) selected (S) and avoided (A) land features with and without the interaction of pesticide inputs (lbs).

<u>MODEL STRUCTURE</u>	<u>ΔAIC</u>	<u>S</u>	<u>A</u>	<u>Lbs*S</u>	<u>Lbs*A</u>
Y~1+(1+animal roost) (NULL)	378	NA	NA	NA	NA
Y~crop types + (1+animal roost)	263.4	Fruit	D <sup>1</sup> , UC <sup>2</sup>	NA	NA
Y~crop types+LBs+(1+animal roost)	26.6	Field Fruit	D, UC, LBs <sup>3</sup> .	NA	NA
Y~ crop types * LBs + (1+animal roost)	0	Field Fruit	D, UC	Fruit Veg	Field Vine

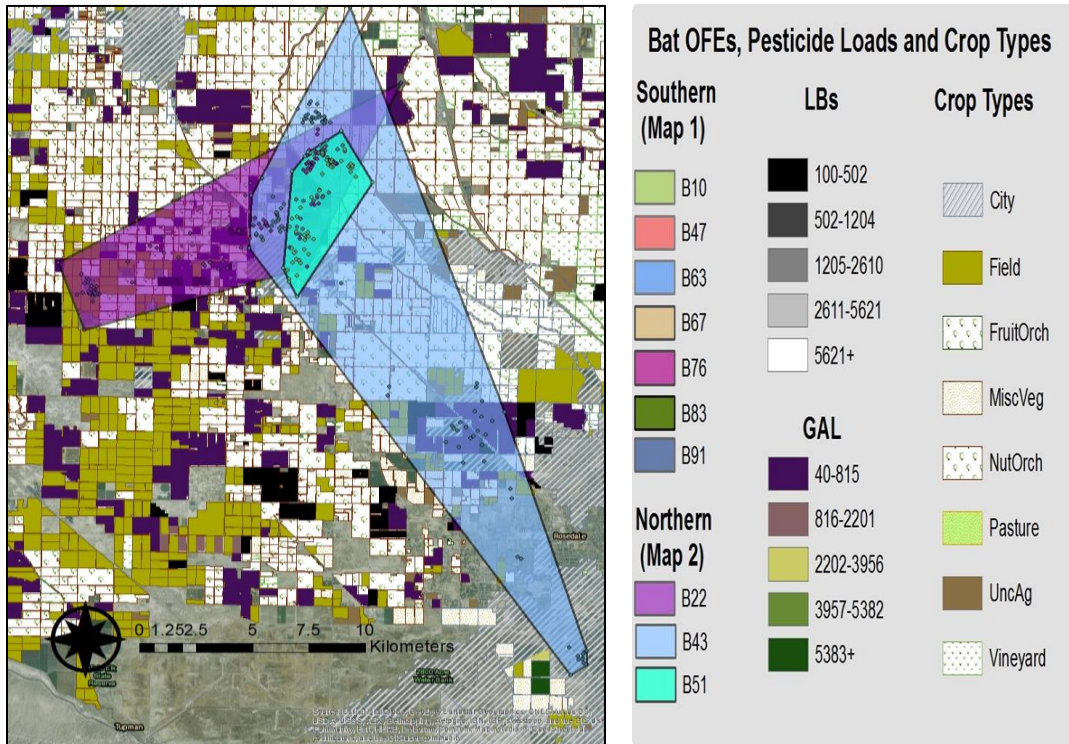
<sup>1</sup> Developed areas; <sup>2</sup> Uncultivated agricultural fields; <sup>3</sup> Summed pesticides (lbs.)

**Figure 3.1.** Study area map with relative position of both sites (A), as well as observed foraging extents (colored polygons), distribution of crop types and pesticide inputs for SH (B) and AV (C).

A)



B)



C)

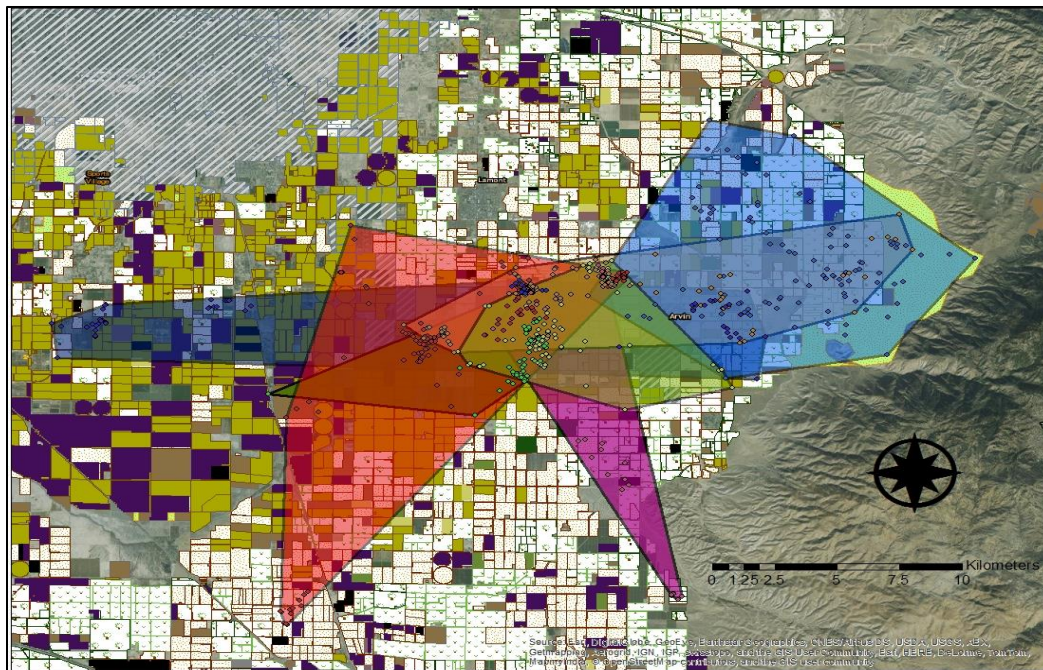


**Figure 3.2.** Relative abundance of prey types detected in guano from 17 brown bats captured in a low pesticide-use area (ARVIN- left) and high pesticide-use area (SHAFTER- right). For readability, only the first 20 most abundant prey types are listed in the legend.

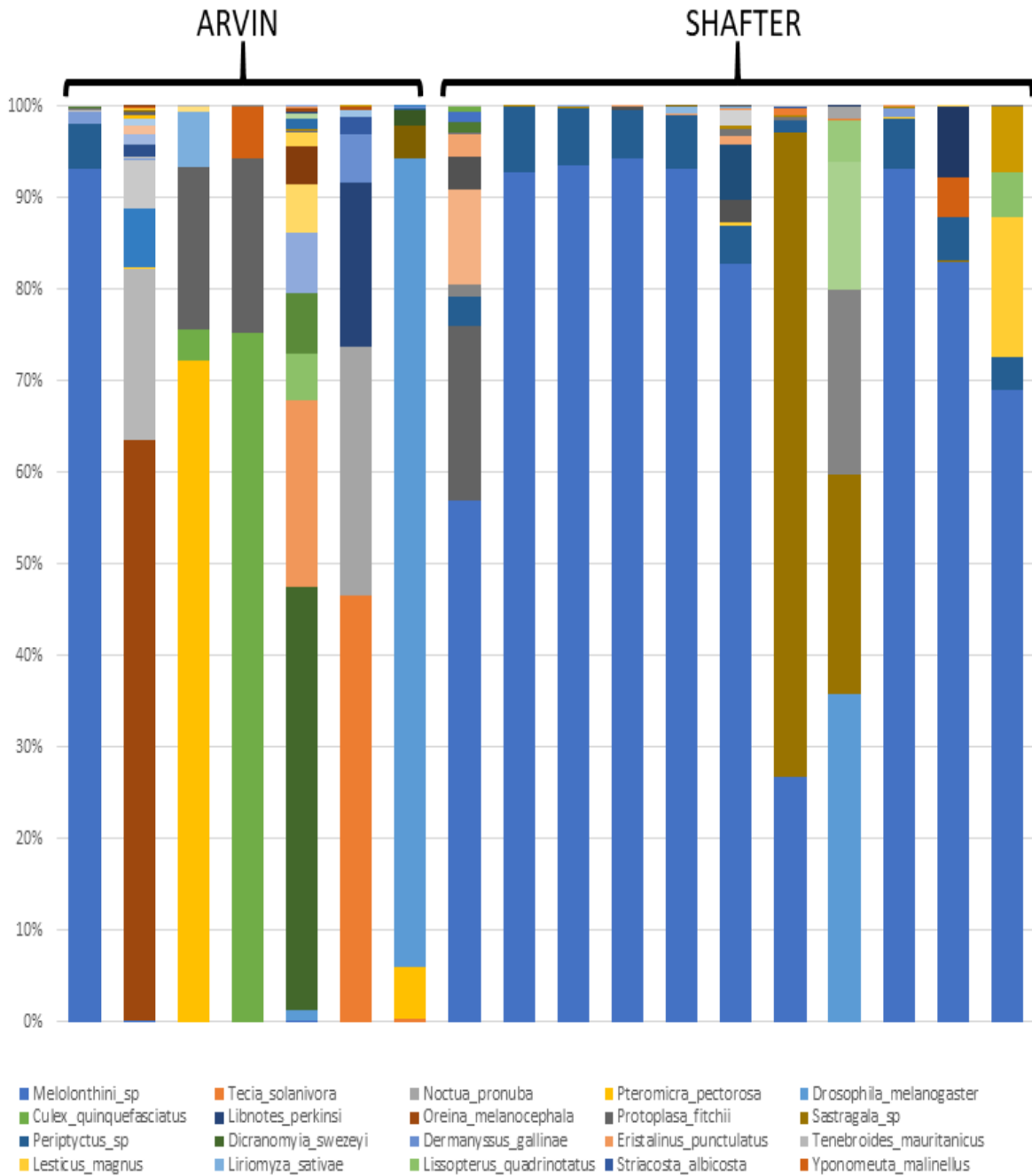


**Figure 3.3.** Average accumulation of prey sequences across sampling intervals ranging from 1000 – 10,000. Rarefaction results are presented as the average accumulation across 10 replicate runs. Error bars are shown for brown bats captured at the Arvin site (blue) and the Shafter site (purple). Other bat species include Yuma myotis (green), pallid bat (red), and free-tailed bat (orange).

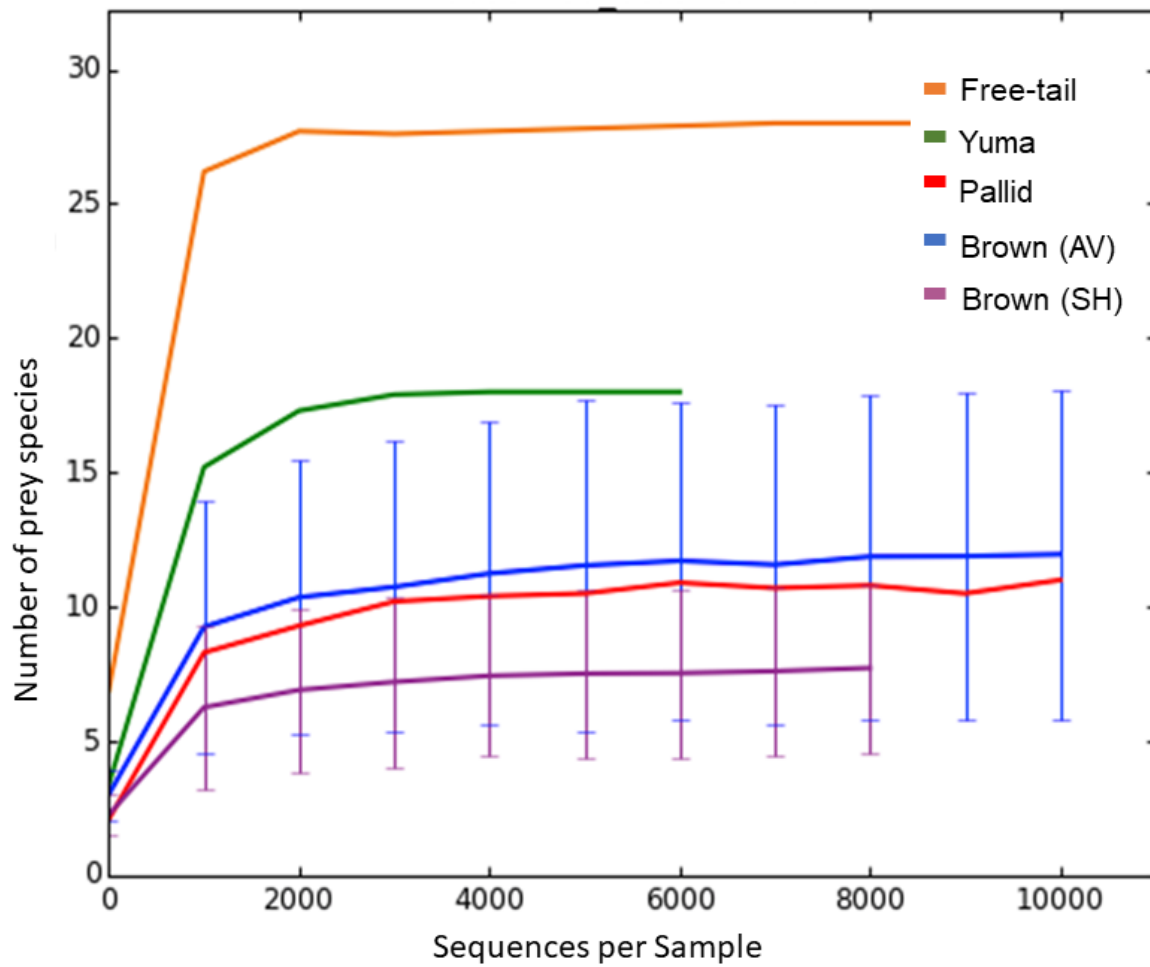
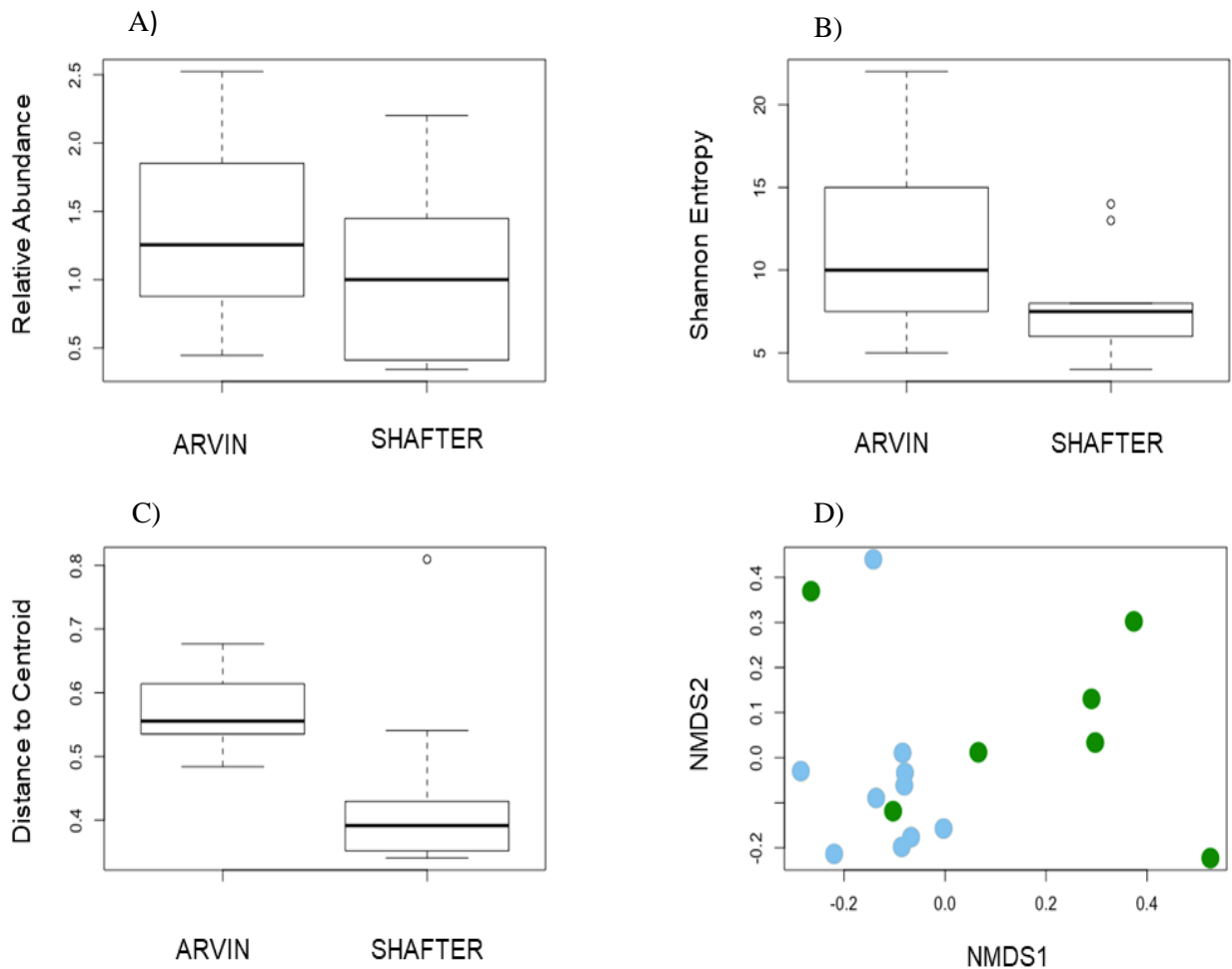


**Figure 3.4.** Comparison of alpha (top panels) and beta (bottom panels) diversity of prey types detected in guano of 17 brown bats captured in a low (ARVIN) and high (SHAFTER) pesticide-use area. Alpha diversity was not significantly different between sites whether measured by the relative abundance of observed prey sequences (A;  $t = 0.99$ ;  $p = 0.38$ ) or Shannon Entropy (B;  $t = 1.34$ ,  $p = 0.21$ ). Beta diversity of prey types as calculated using the Bray-Curtis dissimilarity measure implemented in a PERMANOVA test was significantly different between the two sites (C;  $F = 2.54$ ;  $R^2 = 0.145$ ;  $p = 0.007$ ); and by a nonmetric multidimensional scaling analysis (D;  $k = 3$ ; stress = 0.074;  $p = 0.005$ ). The figure shows a two-dimensional representation of dietary similarity between the bats captured at ARVIN (green circles) and SHAFTER (blue diamonds).



## REFERENCES

1. Bates, D., Maechler, M., Bolker, B., and Walker, S. (2015). Fitting Linear Mixed-Effects Models Using lme4. *Journal of Statistical Software*, 67(1), 1-48.<[doi:10.18637/jss.v067.i01](https://doi.org/10.18637/jss.v067.i01)>.
2. Boyles, J. G., Cryan, P. M., McCracken, G. F., & Kunz, T. H. (2011). Economic importance of bats in agriculture. *Science*, 332(6025), 41-42.
3. Brigham, R. M. (1991). Flexibility in foraging and roosting behaviour by the big brown bat (*Eptesicus fuscus*). *Canadian Journal of Zoology*, 69(1), 117-121.
4. Bruun, M., & Smith, H. G. (2003). Landscape composition affects habitat use and foraging flight distances in breeding European starlings. *Biological Conservation*, 114(2), 179-187.
5. Camacho, C., Coulouris, G., Avagyan, V., Ma, N., Papadopoulos, J., Bealer, K. and Madden, T.L., 2009. BLAST+: architecture and applications. *BMC bioinformatics*, 10(1), p.421.
6. Caporaso, J. G., Lauber, C. L., Walters, W. A., Berg-Lyons, D., Huntley, J., Fierer, N., ... & Gormley, N. (2012). Ultra-high-throughput microbial community analysis on the Illumina HiSeq and MiSeq platforms. *The ISME journal*, 6(8), 1621-1624.
7. Clare, E. L., Symondson, W. O., & Fenton, M. B. (2014). An inordinate fondness for beetles? Variation in seasonal dietary preferences of night-roosting big brown bats (*Eptesicus fuscus*). *Molecular Ecology*, 23(15), 3633-3647.
8. Clark, D. R. (1986). Toxicity of methyl parathion to bats: mortality and coordination loss. *Environmental toxicology and chemistry*, 5(2), 191-195.
9. Clark Jr, D. R. (2001). DDT and the decline of free-tailed bats (*Tadarida brasiliensis*) at Carlsbad Cavern, New Mexico. *Archives of environmental contamination and toxicology*, 40(4), 537-543.
10. Clark, D. R., & Rattner, B. A. (1987). Orthene® toxicity to little brown bats (*Myotis lucifugus*): acetylcholinesterase inhibition, coordination loss, and mortality. *Environmental toxicology and chemistry*, 6(9), 705-708.
11. Davidson, C. (2004). Declining downwind: amphibian population declines in California and historical pesticide use. *Ecological Applications*, 14(6), 1892-1902.
12. Dixon, P. (2003). VEGAN, a package of R functions for community ecology. *Journal of Vegetation Science*, 14(6), 927-930.



13. Ekroos, J., Heliölä, J., & Kuussaari, M. (2010). Homogenization of lepidopteran communities in intensively cultivated agricultural landscapes. *Journal of Applied Ecology*, 47(2), 459-467.
14. Eidels, R. R., Whitaker Jr, J. O., & Sparks, D. W. (2007, January). Insecticide residues in bats and guano from Indiana. In *Proceedings of the Indiana Academy of Science* (Vol. 116, No. 1, pp. 50-57).
15. Emrich, M. A., Clare, E. L., Symondson, W. O., Koenig, S. E., & Fenton, M. B. (2014). Resource partitioning by insectivorous bats in Jamaica. *Molecular Ecology*, 23(15), 3648-3656.
16. Forester, J. D., Im, H. K., & Rathouz, P. J. (2009). Accounting for animal movement in estimation of resource selection functions: sampling and data analysis. *Ecology*, 90(12), 3554-3565.
17. Frick, W. F., Rainey, W. E., & Pierson, E. D. (2007). Potential effects of environmental contamination on Yuma myotis demography and population growth. *Ecological Applications*, 17(4), 1213-1222.
18. Gao, X., Lin, H., Revanna, K., & Dong, Q. (2017). A Bayesian taxonomic classification method for 16S rRNA gene sequences with improved species-level accuracy. *BMC bioinformatics*, 18(1), 247.
19. Gordon, A. and Hannon, G.J., 2010. Fastx-toolkit. FASTQ/A short-reads preprocessing tools (unpublished) [http://hannonlab.cshl.edu/fastx\\_toolkit](http://hannonlab.cshl.edu/fastx_toolkit), 5.
20. Gillies, C. S., Hebblewhite, M., Nielsen, S. E., Krawchuk, M. A., Aldridge, C. L., Frair, J. L., ... & Jerde, C. L. (2006). Application of random effects to the study of resource selection by animals. *Journal of Animal Ecology*, 75(4), 887-898.
21. Hendrickx, F., MAELFAIT, J. P., Van Wingerden, W., Schweiger, O., Speelmans, M., Aviron, S., ... & Burel, F. (2007). How landscape structure, land-use intensity and habitat diversity affect components of total arthropod diversity in agricultural landscapes. *Journal of Applied Ecology*, 44(2), 340-351.
22. Henry, M., Thomas, D. W., Vaudry, R., & Carrier, M. (2002). Foraging distances and home range of pregnant and lactating little brown bats (*Myotis lucifugus*). *Journal of Mammalogy*, 83(3), 767-774.
23. Johnson, C. J., Nielsen, S. E., Merrill, E. H., McDonald, T. L., & Boyce, M. S. (2006). Resource selection functions based on use-availability data: theoretical motivation and evaluation methods. *Journal of wildlife Management*, 70(2), 347-357.

24. Kalda, O., Kalda, R., & Liira, J. (2015). Multi-scale ecology of insectivorous bats in agricultural landscapes. *Agriculture, Ecosystems & Environment*, 199, 105-113.
25. Kartzinel, T. R., & Pringle, R. M. (2015). Molecular detection of invertebrate prey in vertebrate diets: trophic ecology of Caribbean island lizards. *Molecular ecology resources*, 15(4), 903-914.
26. Kelly, R. M., Kitzes, J., Wilson, H., & Merenlender, A. (2016). Habitat diversity promotes bat activity in a vineyard landscape. *Agriculture, Ecosystems & Environment*, 223, 175-181.
27. Kern County Dep. Agriculture Crop Mapping Data <http://www.kernag.com/gis/gis-data.asp>
28. Kern County Dep. Agriculture Pesticide Use Reports <http://www.kernag.com/ep/permit-use/permit-use.asp>
29. Langmead, B., Trapnell, C., Pop, M. and Salzberg, S.L., 2009. Ultrafast and memory-efficient alignment of short DNA sequences to the human genome. *Genome biology*, 10(3), p.R25
30. Lentini PE, Gibbons P, Fischer J, Law B, Hanspach J, Martin TG (2012) Bats in a Farming Landscape Benefit from Linear Remnants and Unimproved Pastures. *PLoS ONE* 7(11): e48201. <https://doi.org/10.1371/journal.pone.0048201>
31. Martin, M. (2011). Cutadapt removes adapter sequences from high-throughput sequencing reads. *EMBnet. journal*, 17(1), pp-10.
32. Nicholson, M. C., Bowyer, R. T., & Kie, J. G. (1997). Habitat selection and survival of mule deer: tradeoffs associated with migration. *Journal of Mammalogy*, 78(2), 483-504.
33. Oksanen, J., Kindt, R., Legendre, P., O'Hara, B., Stevens, M. H. H., Oksanen, M. J., & Suggests, M. A. S. S. (2007). The vegan package. *Community ecology package*, 10, 631-637.
34. Rainho, A., & Palmeirim, J. M. (2011). The importance of distance to resources in the spatial modelling of bat foraging habitat. *PLoS One*, 6(4), e19227.
35. Rambaldini, D. A., & Brigham, R. M. (2011). Pallid bat (*Antrozous pallidus*) foraging over native and vineyard habitats in British Columbia, Canada. *Canadian Journal of Zoology*, 89(9), 816-822.
36. Razgour, O., Clare, E. L., Zeale, M. R., Hanmer, J., Schnell, I. B., Rasmussen, M., ... & Jones, G. (2011). High-throughput sequencing offers insight into mechanisms of resource partitioning in cryptic bat species. *Ecology and Evolution*, 1(4), 556-570.

37. Rodrigues, J. L., Pellizari, V. H., Mueller, R., Baek, K., Jesus, E. D. C., Paula, F. S., ... & Tiedje, J. M. (2013). Conversion of the Amazon rainforest to agriculture results in biotic homogenization of soil bacterial communities. *Proceedings of the National Academy of Sciences*, *110*(3), 988-993.
38. Riley, S. P., Sauvajot, R. M., Fuller, T. K., York, E. C., Kamradt, D. A., Bromley, C., & Wayne, R. K. (2003). Effects of urbanization and habitat fragmentation on bobcats and coyotes in southern California. *Conservation Biology*, *17*(2), 566-576.
39. Shiel, C. B., Shiel, R. E., & Fairley, J. S. (1999). Seasonal changes in the foraging behaviour of Leisler's bats (*Nyctalus leisleri*) in Ireland as revealed by radio-telemetry. *Journal of Zoology*, *249*(3), 347-358.
40. Stahlschmidt, P., & Brühl, C. A. (2012). Bats at risk? Bat activity and insecticide residue analysis of food items in an apple orchard. *Environmental toxicology and chemistry*, *31*(7), 1556-1563.
41. Stoesser, G., Baker, W., van den Broek, A., Camon, E., Garcia-Pastor, M., Kanz, C., Kulikova, T., Leinonen, R., Lin, Q., Lombard, V. and Lopez, R., 2002. The EMBL nucleotide sequence database. *Nucleic acids research*, *30*(1), pp.21-26.
42. Thomas, S. P., & SUTHERS, R. A. (1972). The physiology and energetics of bat flight. *Journal of Experimental Biology*, *57*(2), 317-335.
43. Tremblay, I., Thomas, D., Blondel, J., Perret, P., & Lambrechts, M. M. (2005). The effect of habitat quality on foraging patterns, provisioning rate and nestling growth in Corsican Blue Tits *Parus caeruleus*. *Ibis*, *147*(1), 17-24.
44. Weisenburger, D. D. (1993). Human health effects of agrichemical use. *Human pathology*, *24*(6), 571-576.
45. Wickramasinghe, L. P., Harris, S., Jones, G., & Vaughan Jennings, N. (2004). Abundance and species richness of nocturnal insects on organic and conventional farms: effects of agricultural intensification on bat foraging. *Conservation Biology*, *18*(5), 1283-1292.
46. Zeale, M. R., Butlin, R. K., Barker, G. L., Lees, D. C., & Jones, G. (2011). Taxon-specific PCR for DNA barcoding arthropod prey in bat faeces. *Molecular ecology resources*, *11*(2), 236-244.